THESIS

COMPARATIVE PHYSIOLOGY OF *MYCOBACTERIUM ABSCESSUS* IN SYNTHETIC LABORATORY MEDIUM AND CYSTIC FIBROSIS SPUTUM

Submitted by

Crystal J. Wiersma

Department of Microbiology, Immunology, and Pathology

In partial fulfillment of the requirements

For the Degree of Master of Science

Colorado State University

Fort Collins, Colorado

Fall 2019

Master's Committee:

Advisor: Mary Jackson

Bradley Borlee
Courtney Jahn

ABSTRACT

COMPARATIVE PHYSIOLOGY OF *MYCOBACTERIUM ABSCESSUS* IN SYNTHETIC LABORATORY MEDIUM AND CYSTIC FIBROSIS SPUTUM

Mycobacterium abscessus complex is a group of rapid-growing nontuberculous mycobacteria that are multidrug resistant and that cause chronic pulmonary infections in individuals with cystic fibrosis (CF) and other pre-disposing conditions. Research progress is challenged by the lack of laboratory models that mimic the lung environment, a nutritionally complex environment not well represented by current laboratory medium. In this study, the growth characteristics and gene expression profile of a diverse panel of *M. abscessus* isolates were characterized and compared when grown in 7H9 Middlebrook medium (a synthetic *Mycobacterium* laboratory culture medium); Synthetic Cystic Fibrosis Medium 2 (SCFM2), a medium which mimics the composition of CF sputum; and actual patient CF sputum. Tests were also performed measuring the antibiotic susceptibility and characterizing the cell envelope composition of the *M. abscessus* isolates in these media. Although the medium composition did not affect the antibiotic susceptibility or growth of the isolates, it caused changes in fatty acid and outer membrane lipid compositions which may account, at least in part, for observed differences in the subsequent infectivity of the isolates inside macrophages and epithelial cells. The gene expression profiles showed similar upregulation of pathways related to carbon metabolism for *Mycobacterium abscessus* grown in SCFM2 and grown in CF sputum while reaffirming the complexity of CF sputum and the many metabolic and structural adaptations that *M. abscessus* undergoes during growth in varied environments.

ACKNOWLEDGEMENTS

I would like to acknowledge our collaborators throughout this project. Without their assistance, this project would not have been possible. We worked with Dr. Andres Floto and lab at the University of Cambridge; Dr. Julian Parkhill and lab at the Sanger Sequencing Center; and Drs. Rebecca Davidson and Michael Strong and labs at National Jewish Health. Thank you for providing research materials and clinical samples, advice, and assistance with completing experiments. Thank you to Drs. Rebecca Davidson and Jeanne Benoit for guiding me through RNAseq data analysis. At CSU, thank you to Dr. Michael McNeil for your enthusiastic help with the cell envelope analysis and to Dr. Diane Ordway and lab for completing the cell infection studies.

I would like to thank my advisor, Dr. Mary Jackson for sharing your scientific knowledge and guiding me through this project. Thank you for your support and abundant patience.

Thank you to my committee members Drs. Brad Borlee and Courtney Jahn for your recommendations and guidance.

Thank you to all the past and present members of the Jackson lab who freely gave advice, encouragement, and friendship. A special thank you to Dr. Juan Belardinelli for all the training in the lab and willingly answering my countless questions. Also, thank you to Dr. Charlotte Avanzi for all of your help with the RNAseq experiments.

Finally, thank you to my family, friends, teachers, and classmates for supporting me and providing direction in my academic pursuits to date. Thank you to my parents for encouraging me to stick with it. Thank you to my husband, Steve, for constantly encouraging me, cheering me up, and keeping me fed.

TABLE OF CONTENTS

Introduction

The *Mycobacterium abscessus* complex (*Mabsc*) includes *M. abscessus* subspecies (subsp.) *abscessus* (*Mabs*), *M. abscessus* subsp*. massiliense* (*Mmas*)*, and M. abscessus* subsp. *bolletii. Mabsc* can be readily found in the environment - for example in municipal water colonizing water fixtures, and inhabiting the soil (Claeys et al. 2018; Covert et al. 1999; Prevots et al. 2016; Thomson et al. 2013a; Thomson et al. 2013b). These rapidly growing nontuberculous mycobacteria can cause chronic pulmonary infections in individuals with predisposing lung diseases such as cystic fibrosis (CF), bronchiectasis, and other inflammatory lung diseases (Floto et al. 2015; Thomson 2010). Several recent studies have revealed that the prevalence of *Mabsc* infections is increasing globally in CF patients (Pierre-Audigier et al. 2005; Prevots et al. 2010; Prevots et al. 2016; Thomson 2010). It has also been shown by a global whole genome sequencing study that there are globally circulating *Mabsc* and *Mmas* clones isolated at CF centers across the globe (also referred to as "clustered" isolates) (Bryant et al. 2016; Hasan et al. 2019). These strains are overrepresented, which may point to an adaptive advantage of these strains in the CF lungs.

Mabsc is intrinsically resistant to most chemotherapeutic agents, including most of the antibiotics used to treat *M. tuberculosis* infection. *Mabsc* (along with other mycobacteria) displays a number of natural resistance mechanisms including a waxy and impermeable cell wall, drug export systems, antibiotic modifying/inactivating enzymes and genetic polymorphism of target genes (Maurer et al. 2014; Nessar et al. 2012; van Ingen et al. 2014). For these reasons, *Mabsc* infections in CF patients frequently have poor outcomes, with very long and often ineffective treatments that last at least 18-24 months with several antibiotics (Floto et al. 2016; Griffith et al. 2019). In addition to this, *in vitro* studies of *Mabsc* antibiotic susceptibility rarely correlate with *in vivo* treatment results. *In vitro* testing only consistently correlates in tests of macrolide resistance (van Ingen et al. 2014).

This lack of correlation may be due to a number of factors, including the ability of *Mabsc* to form microaggregates or biofilms *in vivo* and differences between the physiology of the bacterium in the infected human lung and in laboratory settings. To this day, the physiology of the bacteria at the site of infection has not been characterized, as clinical samples with a high enough titer for analysis are difficult to obtain. Animal models are useful, but must be severely immunocompromised in order to be infected, and they can also be very expensive and unsuitable for analyses requiring gram quantities of bacteria, such as some cell wall composition analyses. As a result, the correlation between metabolism and gene expression levels of bacteria grown *in vitro* in the common *Mycobacterium* medium Middlebrook 7H9-ADC-Tween 80 with the profile of bacteria growing in the CF lung is currently unknown.

These challenges led us to seek a medium that could be used routinely in the lab, would be more accessible and more suitable for high-throughput experiments than animal and/or whole cell models; and that is more representative of the CF lung conditions while lacking the patient-to-patient variability.

CF disease is a genetic disease which impairs the epithelial immunity of the lung and causes the accumulation of large amounts of sputum in the lungs (Taylor Sitarik et al. 2012). The CF transmembrane conductance regulator (CFTR) protein is a chloride channel that balances the chloride concentration in the cell and influences epithelial immunity. In CF, varied deleterious gene mutations cause the CFTR protein to be dysfunctional, to not be produced, or to be produced at reduced levels. CFTR mutations affect the movement of water across epithelial barriers and inhibit the lungs epithelial immunity. The thickened sputum impairs ciliary movement decreasing airway clearance and trapping bacteria in the lungs, increasing the risk of infection. For bacteria infecting a CF host's lung, this sputum is a rich source of salts, amino acids, lipids, extracellular DNA and other host-derived factors (Turner et al. 2015). Sputum composition can vary between patients due to infection status- bacterial titer and species in the sputum, treatment status – whether antibiotics

are present in the sputum due to ongoing treatment, and patient variability – salts and nutrient concentrations due to the genotype of CF and severity of lung decline. Besides these variations in composition, sputum is difficult to collect in the large quantities required for laboratory work. In order to address the unique conditions in the CF lung, a synthetic cystic fibrosis sputum (SCFM2) was developed as a nutritionally defined medium for bacterial growth. Its composition is based on the average concentrations of ions, free amino acids, glucose and lactate in CF sputum (Palmer et al. 2007). Mucin, DNA, N-acetyl glucosamine, and dioleoylphosphatidylcholine (DOPC) -a lipid mimicking the lung's surfactant - were also included in this medium at levels similar to those seen in CF sputum (Turner et al. 2015).

This medium was first developed to study another common CF lung pathogen, *Pseudomonas aeruginosa*. It was validated through transposon sequencing (TN-seq) studies comparing the nutritionally controlled genes of *P. aeruginosa* grown in CF sputum to *P. aeruginosa* grown in SCFM2 (Turner et al. 2015). The studies found that the essential genome and the nutritionally controlled genes in SCFM2 were similar to the genes in CF sputum. Less than 0.7% of genes were differentially essential between the media - meaning they were essential in one medium, but not the other.

During infection, *Mabsc* must adapt to the unique conditions in the CF lung, adaptations that may lead to changes in gene expression levels, virulence and cell envelope composition among others. Thus, we chose to use SCFM2 to genetically and biochemically characterize *Mabsc* and to confirm if this medium was a better approximation of the CF lung physiology than the standard 7H9-ADC-Tween 80. We hypothesized that the lung environment can be more accurately replicated with SCFM2 than 7H9-ADC-Tween 80. Using this model, we assessed growth, antibiotic susceptibility, cell envelope composition, and RNA expression levels of clinical *Mabsc* (clustered and non-clustered *Mabs* and *Mmas*) isolates.

To test these hypotheses, we measured antibiotic susceptibility to test if SCFM2 would be a more relevant medium for antibiotic testing than cation-adjusted Mueller-Hinton II (MHII), the Clinical and Laboratory Standards Institute (CLSI) recommended medium for minimum inhibitory concentration (MIC) testing of *Mabsc*. Further, we determined the composition of the cell envelope including the total lipids, fatty acids, mycolic acids and sugars. We chose to evaluate the cell envelope composition of *Mabsc* as the waxy hydrophobic cell envelope unique to *Mycobacterium* contributes to the persistence, immunopathogenicity and antibiotic resistance of this genus (Falkinham, 2018). The cell envelope is composed of many complex lipids and glycoconjugates including mycolic acids, arabinogalactan, peptidoglycan, glycopeptidolipids (GPLs), lipoglycans such as lipoarabinomannan (LAM), lipomannan (LM), and more (Daffe et al. 2014). Alterations in cell envelope composition are known to affect the virulence of *Mycobacterium*. *Mabsc* can display a smooth or a rough phenotype characterized, at least in part, by the presence or absence, respectively, of cell envelope glycopeptidolipids (GPLs) (Pawlik et al. 2013). Rough phenotypes have been associated with hypervirulence and poorer disease outcome (Howard et al. 2006; Pawlik et al. 2013). Overall, the *Mabsc* cell envelope has not been as comprehensively characterized as *M. tuberculosis.* Characterization of the *Mabsc* cell envelope may lead to the discovery of new pathways that can serve as drug targets, as effective anti-mycobacterial drugs frequently target cell envelope synthesis.

Finally, we chose to use RNA sequencing (RNAseq) to characterize the gene expression profile of isolates grown in SCFM, 7H9-ADC-Tween 80, and 20% CF sputum in M63 medium. These comparisons allowed us to evaluate how similar the gene expression profile of bacteria grown in 7H9-ADC-Tween 80 or SCFM2 is to bacteria grown in CF sputum. These data will indicate if SCFM2 is a model system that more closely mimics the lung physiology and causes similar physiological adaptation as is activated by bacterial growth in CF sputum.

Materials and Methods

Bacterial strains

Reference strains *M. abscessus* subsp. *abscessus* ATCC 19977 and *M. abscessus* subsp. *massiliense* CIP 108297 were obtained from the ATCC.

M. abscessus subsp. *abscessus* 1091 a rough clustered isolate; *M. abscessus* subsp. *abscessus* 184 a smooth non-clustered isolate; and *M. abscessus* subsp. *massiliense* 1239 a smooth clustered isolate were collected from patients in the United Kingdom. *M. abscessus* subsp. *massiliense* 604 a smooth non-clustered isolate was collected from a patient in Denmark. All isolates were characterized by whole genome sequencing in the genome wide association study completed by Bryant et al. in 2013.

M. abscessus subsp. *abscessus* clinical isolates 1334, OM128, OM200, OM91, and 1339; and *M. abscessus* subsp. *massiliense* clinical isolates 1335, 1337, OM194, OM130, and OM69 (2016 study) were collected from CF patients at Papworth University Hospital in Cambridge, UK. *M. abscessus* subsp. *abscessus* strains OM128 and OM200 were rough morphotypes which do not produce GPLs and have been shown to be more virulent. The rest of the isolates were smooth morphotypes. All patients had American Thoracic Society defined disease except for the patient infected with *M. abscessus* subsp. *massiliense* OM69. Patients cleared the infections from *M. abscessus* subsp. *abscessus* OM91, *M. abscessus* subsp. *abscessus* 1339, and *M. abscessus* subsp. *massiliense* OM69. The patient infected with *M. abscessus* subsp. *massiliense* OM130 was less than six months into treatment at time of data collection. The remaining infections were persistent at time of data collection (positive sputum cultures still present after six or more months of treatment). These clinical isolates were obtained from the University of Cambridge, UK (Prof. A. Floto).

Media preparation

Mabsc cultures were grown in Middlebrook 7H9 (BD) supplemented with 0.5% glycerol, 10% albumin-dextrose-catalase (ADC), and 0.05% Tween-80; on Middlebrook 7H10 agar supplemented with 10% ADC; in SCFM2 (Turner et al., 2014), in minimal M63 medium (2g/L $(NH_4)_2SO_4$, 13.6 g/L KH_2PO_4 (monobasic), 0.5 mg/L $FeSO_4 \bullet 7H_2O$, pH to 7.0 with KOH, autoclaved to sterilize) supplemented with 1mM $MgSO_4$, 0.05% Tyloxapol, and 0.2% glucose; or in M63 medium supplemented with 1mM $MgSO_4$, 0.05% Tyloxapol, and 10% or 20% CF sputum. BBL Mueller Hinton II Broth, cation-adjusted (BD) was used for MIC testing.

SCFM2 was prepared as described in Turner et al (2014) with the following modifications to ensure sterile medium. eDNA was dissolved at a concentration of 15 mg/ml in diH_2O and autoclaved to sterilize. Bovine submaxillary mucin (Alfa Aeser) was sterilized by γ-irradiation delivering a dose of 2.5 megarads.

CF sputum was collected from CF patients receiving treatment at Papworth University Hospital in Cambridge, UK, or at National Jewish Health in Denver, CO. The sputum was γ-irradiated with a dose of 2.5 megarads. Samples from National Jewish Health patients or Papworth University Hospital patients were pooled and then centrifuged (10 min, 3000g) to pellet debris. The supernatant was collected (approximately 80% of the total volume) and diluted to a concentration of 10% vol/vol or 20% vol/vol in MM63 buffer. It was then filtered through a 0.45µm filter to remove insoluble material. Sputum and prepared media were stored at -80 °C.

Growth Curves

Starter cultures were grown in 7H9-ADC-Tween 80. Cells were pelleted, resuspended in an equal volume of SCFM2 buffered base, and allowed to adapt overnight at 37 °C with shaking at 130 rpm. 50 ml cultures were inoculated at 0.005 OD_{600} in 7H9-ADC-Tween 80, SCFM2, SCFM2 without DNA, SCFM2 without mucin, or SCFM2 without DOPC from the adapted pre-culture and grown at 37 °C with shaking at 130 rpm. A portion of each culture was removed, diluted, and plated on 7H10-

ADC for CFU counts at inoculation and every 12 hours until day 5. Plates were incubated at 37 °C in a stationary incubator for 3 days before counting CFU.

Minimum Inhibitory Concentration Testing

The minimum inhibitory concentration (MIC) of selected antibiotics was tested in 96-well microtiter plates in cation-adjusted MHII and SCFM2 without DNA and without mucin. Antibiotics tested were amikacin, apramycin, azithromycin, clarithromycin, erythromycin, kanamycin, ethambutol, rifampicin, streptomycin, cefoxitin, tobramycin, linezolid, tetracycline, imipenem, and ciprofloxacin. The antibiotics were tested in a two-fold dilution series. Bacteria were added to a concentration of 0.001 OD_{600} to medium containing antibiotic. Plates were incubated stationary at 37 °C. MIC was measured at day 10 by reading the well with the lowest concentration of antibiotic showing no visible growth.

Cell envelope analyses

Starter cultures were grown in 7H9-ADC-Tween 80; the cells were pelleted, resuspended in SCFM2 buffered base, and adapted to the medium overnight. 250 mL cultures were inoculated at a concentration of 0.005 OD_{600} and grown to early exponential phase. Cells were pelleted (10 min, 3000g) and washed twice with PBS. Cell pellets were stored at –80 °C until analysis. During cell envelope extractions all centrifugation was for five minutes at 2000xg unless otherwise noted. N_2 was used for all drying steps.

- **Lipid and fatty acid extraction**

Total lipids from cell pellets were extracted using a chloroform:methanol extraction. First, 6mL $CHCl_3$:CH_3OH (1:2) was added to each pellet, and samples were spun on an angled rotary shaker at room temperature (RT) overnight (O/N). After centrifugation, the organic phase was collected and dried. Next, 6 mL $CHCl_3$:CH_3OH (2:1) was added to the pellet, spun O/N at room temperature (RT), centrifuged, and organic phase collected and pooled with previous organic

extraction. This was repeated one more time for three total extractions. The dried organic phase was washed with $CHCl_3$:CH_3OH:NaCL (0.9%, 4:2:1). After centrifugation, the organic phase, containing the extractable lipids, was transferred to a new weighed tube. This was dried and resuspended in $CHCl_3$:CH_3OH (2:1) at 10 mg/mL. The lipids were analyzed with thin-layer chromatography (TLC) and liquid chromatography/mass spectrometry (LC/MS). For TLC visualization, lipids (0.1mg) were spotted on a 10 cm TLC silica plate, 1 cm from base, with 0.5 cm separating samples. The TLCs were run in solvent systems consisting of 90:10:1 $CHCl_3$:CH_3OH:H_2O (by vol.) or 20:4:0.5 $CHCl_3$:CH_3OH:H_2O (by vol.). The TLCs were run till the solvent front was approximately 1 cm from the top of the plate. The plate was removed, and dried completely. It was developed with α-naphthol and a heat gun on low temperature.

Lipids resuspended in $CHCl_3$:CH_3OH (2:1) were analyzed in positive and negative mode by LC/MS following the method described in Sartain et al. (2011) on a high-resolution Agilent 6220 TOF mass spectrometer interfaced to a LC (Grzegorzewicz et al. 2012b).

To quantify extractable lipids, 225 mL triplicate cultures were grown in 7H9-ADC-Tween 80 and in SCFM2 without mucin to early exponential phase. Then lipids were extracted as above. Lipids and the cell pellet were dried completely and dry lipid weight was compared to the combined weight of the lipids and dry cell pellet.

To analyze short chain fatty acids by GC/MS, fatty acid methyl esters were prepared from lipid extracts. To this end, 100 µL of 3M HCl in methanol was added to dry lipid extracts and the mixture was incubated at 80 °C overnight. Then, 1 mL of H_2O and 1 mL of hexane were added to cooled samples. Samples were vortexed and centrifuged. The top organic layer was transferred to a new tube, and dried gently under N_2. Finally, samples were resuspended in hexane for GC/MS analysis as described by Davidson et al. (2017).

Preparation of cell wall core-derived monosaccharides and mycolic acids from delipidated cells

The delipidated cell pellet consisting of the mycobacterial cell wall core (a macromolecular complex consisting of covalently-linked peptidoglycan, arabinogalactan and mycolic acids) was partitioned into aqueous and organic phases through acid hydrolysis with trifluoroacetic acid (TFA, Sigma). First, 10 µg 3-*O*-methylglucose was added as an internal standard. Then, the samples were hydrolyzed with 500µl 2M TFA for 2 hours at 120 °C. After cooling to RT, the pellet was twice extracted with 1 mL $CHCl_3$. The organic phase was collected for mycolic acid analysis and the aqueous phase was collected for sugar analysis.

- **Mycolic acid analysis**

The mycolic acid-containing organic phase was dried then base-hydrolyzed. To this end, 1M KOH:CH_3OH was added and incubated for 2 hours at 80° C. After cooling to RT, the reaction mixture was neutralized to pH 5 with HCl and twice extracted with diethyl ether. The ether fractions were collected, pooled, and dried under nitrogen flow. They were then dissolved in $CHCl_3$:CH_3OH (2:1) for LC/MS analysis of mycolic acid composition. 5 µM 1,2-dioleoyl-*sn*-glycerol-3-phosphoethanolamine-*N*-nonadecanoyl was added as an internal standard. The mycolic acids were analyzed with LC/MS as described by Grzegorzewicz et al. (2012a).

For visualization by TLC, mycolic acid methyl esters were prepared from the cell wall core material. The cell pellet left after lipid extraction was resuspended in 2 mL of 15% tetrabutylammonium hydroxide (Sigma) and was saponified overnight at 100 °C. After cooling to RT, 2 mL of water, 3 mL of dichloromethane, and 300 µL of iodomethane (Sigma) were added to the mixture. This was shaken on an angled rotary shaker for 4 hours to methylate the mycolic acids. Next, the mixture was centrifuged for 7 minutes at 2000 rpm, the lower organic layer was transferred to a new tube and washed 3 times with 6 mL of water (centrifuging for 7 minutes at 2000 rpm). After washing the organic layer was dried with nitrogen, then extracted with 4 mL of

diethyl ether and sonicated for 5 minutes (Branson 2510 sonicator). Finally, the reaction mixture was centrifuged for 10 minutes at 2000rpm, and the ethereal extract containing mycolic acid methyl esters was transferred to a new tube and dried. The dried product was stored at -20 °C or resuspended in 300µL of dichloromethane and stored at 4 °C until TLC analysis. For TLC visualization, mycolic acids were spotted on a 10 cm TLC silica plate, 1cm from base, with 0.5 cm separating samples. The TLCs were run in the solvent system 95:5 hexane: diethyl ether (by vol.) three times, allowing the plates to dry between runs. The plates were run till the solvent front was approximately 1 cm from the top of the plate. The plate was removed, and dried completely. They were developed with $CuSO_4$ and a heat gun on low temperature.

- **Alditol acetate derivatization of cell wall core, extractable lipids, and whole cell sugars**

Monosaccharides from whole cells, extractable lipids, and cell wall core were prepared from the aqueous phase of the TFA hydrolysis as described in Bhamidi, et al. (2012). Briefly, dried extracts were reduced with 100 µL of 10 mg/mL sodium borodeuteride dissolved in 1:1 1M NH_4OH:EtOH for 4 hours. The reactions were quenched with 100 µL glacial acetic acid. Then methanol was added, and the samples were dried under N_2. The dried samples were per-*O*-acetylated with acetic anhydride for one hour at 100 °C to produce alditol acetates of the glycosyl residues. Next, the samples were gently dried – as the derivatized products are volatile. The dried samples were twice extracted with 1:1 H_2O:$CHCl_3$. The pooled organic phases containing glycosyl residues were gently dried and analyzed with GC/MS. GC/MS conditions and data analysis were as described in Palcekova et al. (2019).

Cell infection protocol

A549 cells, adenocarcinomic human alveolar basal epithelial cells, and THP-1 cells, acute monocytic leukemia monocytes, were infected with *Mabsc* to model virulence through cellular

uptake and intracellular replication. A549 cells and THP-1 cells were maintained in complete RPMI medium. THP-1 cells were differentiated to macrophages by incubating for 3 days with 100nM Phorbol 12-myristate 13-acetate (PMA). $1x10^5$ THP-1 or A549 cells were infected at a multiplicity of infection (MOI) of 10 with one of the following: *M. abscessus* subsp*. abscessus* 184 or *M. abscessus* subsp*. massiliense* 1239 grown in 7H9, SCFM2, or SCFM2 without mucin. Infected cells were incubated at 37 °C in a 5-6% CO2 incubator for two hours, then washed 3x with PBS to remove extracellular bacteria. Bacteria cells were quantified at T_0 (after removing extracellular bacteria), day 1, and day 2. To count intracellular CFUs, the medium was removed from the cell cultures and replaced with a sterile lysis buffer of 0.05% Tween-80 in ddH_2O and incubated at 37 °C for 20 minutes. The plate wells were then scraped and the solution was removed, diluted, and plated. After 3-4 days incubation CFUs were counted and the original bacterial load of the cells was calculated.

RNA sequencing and analysis

- **RNAseq culture preparation**

Starter cultures were grown in 7H9-ADC-Tween 80. For SCFM2 and 20% sputum grown cultures, OD_{600} was measured, cells pelleted, resuspended in SCFM2 buffered base or M63 base. They were adapted to the medium overnight by incubating at 37 °C with shaking at 135rpm. 50 ml (SCFM2 and 7H9-ADC-Tween 80) or 25 mL (20% sputum and MM63-$MgSO_4$-glucose) cultures for RNA sequencing were then diluted and inoculated to an OD_{600} of 0.005. Cultures were grown at 37 °C with shaking at 135 rpm.

Cultures were collected during early exponential phase as measured by optical density (0.2-0.35 OD_{600}) in 7H9-ADC-Tween 80, M63-$MgSO_4$-glucose, and 20% CF sputum in M63-$MgSO_4$ or with CFU counts of 10^7 - 10^8/mL in SCFM2. Cells were centrifuged for 10 minutes at 3000xg. Supernatant was discarded, and cells were resuspended in 3 mL of RNA*later* (Invitrogen) and split into triplicate

samples. Cells were stored at 4 °C for 48 hours then stored at -80 °C until RNA isolation and sequencing.

- **RNA extraction**

Cultures stored in RNAlater were thawed on ice, and then centrifuged for 3 minutes at 3000xg. Cultures grown in SCFM2 with mucin or CF sputum were diluted in water 1:2 and centrifuged for 5 minutes at 3000xg. The supernatant was removed by pipetting. The cell pellet was resuspended in 600 µL of Tri-reagent from the Zymo Direct-zol RNA minikit. Cells were broken by bead beating 2x60sx6m/s (MP FastPrep 24) with a five minute rest on ice between cycles. Samples were centrifuged 30s at 12000xg to pellet beads and supernatant was transferred by pipetting to Qiagen MaXtract High Density Tubes. (Matrix in column was first pelleted by centrifuging 30s at 14,000g). Then 100 µL chloroform (or 150 µL for diluted samples) was added to column and gently mixed by inverting. Tubes were centrifuged for 5 minutes at 12000xg at 4 °C. The clear aqueous phase was collected and transferred to a fresh tube. Next, the RNA was purified using Zymo Direct-Zol RNA minikit with no modifications to the published purification protocol. The recommended on-column treatment with DNAse1 was performed. Samples were eluted in 50 µl of nuclease free water. An additional DNAse treatment with Turbo DNA-free kit (Invitrogen) was completed using the routine DNAse treatment protocol. The samples were incubated in the Turbo DNAse for 30 minutes at 37 °C on a tube shaker at 400 rpm.

- **RNA quality and integrity checks**

The RNA was checked for DNA contamination using qPCR with SYBR Green Master Mix (Sigma-Aldrich) using manufacturer's recommended cycling conditions. The expression of *sigA*, a constitutively expressed gene in *Mabsc,* was measured using 5-10 ng RNA as a template. The primers used were *sigA* forward (5'-CGTTCCTGGACCTGATTCAG-3') and *sigA* reverse (5'-GTACGTCGAGAACTTGTAACCC-3') *M. abscessus subs. abscessus* ATCC 19977 genomic DNA was

used as a positive control, and nuclease free water was used as a negative control. Only one sample had a threshold cycle (C_t) of less than 34, indicating successful removal of contaminating DNA for all other samples. The sample with a C_t of less than 34 was retreated with Turbo DNAse; and the success of the treatment confirmed with qPCR. Qubit HS RNA (Thermo Fisher) was used to calculate an accurate RNA concentration, according to the manufacturer's recommendations.

RNA quality was assessed using an Agilent High Sensitive RNA Screentape on an Agilent Tapestation, according to the manufacturer's recommendations. All RNA had an RNA Integrity Number (RIN) of greater than 6, indicating sufficient RNA quality for sequencing.

- **RNA library prep**

Between 500 ng and 5 µg of RNA was subjected to rRNA depletion using the Illumina Ribo-Zero rRNA Removal Kit (gram positive Bacteria) followed by bead clean-up (AMPure RNA) according to the manufacturers' protocols.

Initial concentration of depleted RNA was assessed based on an estimated 90% depletion after the Ribo-zero kit. Following rRNA depletion, the cDNA libraries was constructed using the KAPA RNA Hyperprep kit (Roche) according to the manufacturer instructions. Briefly, depleted RNA was fragmented for 6 minutes at 85 °C to yield 300-400 bp fragments. Dual indexed Kapa adapters were used to barcode the library and were diluted according to Kapa's recommendation and the starting RNA concentration. Amplification was performed based on Kapa's recommendation and the starting RNA concentration. After the final amplification step, libraries were quantified using Qubit dsDNA BR Assay Kit (Thermo Fisher Sc., USA, MA) and the fragment size was assessed on an Agilent Tapestation using the D1000 Screen tape.

Libraries were diluted at 10 nM and multiplexed in three sequencing runs at equimolar concentrations. Libraries were then sequenced using single-end or pair-end reads on an Illumina NextSeq instrument using the high-output 75 cycles or mid-output 150 cycles.

- **RNAseq data analysis**

After demultiplexing, the quality of the reads was assessed using FastQC (https://www.bioinformatics.babraham.ac.uk/projects/fastqc/). Reads were trimmed for quality score of greater than 20 and length greater than 50 using Skewer (Jiang et al. 2014) followed by a final quality check with FastQC. Reads were mapped to *M. abscessus* subsp*. abscessus* ATCC 19977 NC_010397.1 using Bowtie 2 (Langmead et al. 2012). Count tables were constructed using HTSeq-count set to intersection_nonempty using the gff3 file for NC_010397.1 counting reads on gene_id. Gene expression and differential expression analysis was completed using DESeq2. A significant change in expression was defined as a *p*-adj value of <0.05 and a log fold change of >2.

Fastq files from the Miranda-CasoLuengo et al. (2016) study of *M. abscessus* ATCC 19977 grown in 7H9-ADC-Tween 80 and SCFM2 were retrieved from the NCBI gene expression omnibus (GEO) (Barrett et al. 2013) under accession numbers GSE78787 and GSE72996. SRR files were converted to Fastq files using the SRA toolkit version 2.10.0. (http://ncbi.github.io/sra-tools/). The files were then taken through the above analysis pipeline in order to ensure consistency of data analysis for comparisons.

See supplementary material for code and complete options used in each program.

KO categories were assigned with KEGG Mapper, using organism mab.

A summary of the analysis including reads, mapping, and alignment rates is included in the supplementary material.

Venn diagrams were constructed using http://bioinformatics.psb.ugent.be/webtools/Venn/.

cDNA synthesis

cDNA was prepared using Superscript IV First-Strand Synthesis System (Thermo Fisher). Random hexamers were annealed to the template RNA. All RNA not used for RNA sequencing was synthesized to cDNA for more stable storage.

qRT-PCR

cDNA was diluted to 2-10 ng/uL for RT-PCR. Gene expression of selected genes was analyzed for SCFM2 and SCFM2 without DOPC. cDNA from two RNA extractions for each condition was used, and each sample was run in triplicate. RNA was first tested with qPCR for DNA contamination. *sigA* expression was used for normalization. The following primers were used: MAB_4008c_for (5'-RCAGCAGTTCTTCCGTGAAA-3'), MAB_4008c_rev (5'-CAAGCTTCTCGATGTCCTCTAC-3'), MAB_3881_for (5'-TCACGAGTCCGGTTCATCTA-3'), MAB_3881_rev (5'- GTGATGACGAGTGATGTGGAA-3'), MJSM_0304_for (5'-CCGTCGCAGGGTATTTCATT-3'), MMASJSM_0304_rev (5'-AGCCCGACGTTCTGTATCT-3'), MMASJSM_0305_for (5'- TTCTGGAGATGGACATCCTGAC-3'), MMASJSM_0305_rev (5'-GTGCCGTATGAGTTGGGAAATC-3'). All primers were supplied by Integrated DNA Technologies. PCR products were visualized on a 2% agarose gel stained with SYBR Safe (Invitrogen). All amplicons were of expected size, which ranged from 100-125 bp. Primers were checked for compatibility by PCR (25 µL reaction, TaKaRa PrimeSTAR HS DNA Polymerase) with the following conditions: 95 °C for 20 sec; and 30 cycles of 95 °C for 20s, 50-60 °C 10s, and 72 °C 20s with a final extension of 72 °C 5 minutes. Amplicons were checked by loading 10µL sample on a 2% agarose gel electrophoresis stained with SYBR safe (Invitrogen). A gradient of annealing temperatures from 50 °C to 60 °C was used to check compatibility of *sigA* primers and find the ideal annealing temperature. SYBR Green PCR Master Mix (Sigma-Aldrich) was used for qPCR with the following conditions: 95 °C for 30s, 40 cycles of 95 °C for 10s, elongation temp 30s, plate read. The elongation temperature was set to 50 °C for MAB_4008c and MAB_3881 and to 56 °C for MJSM_0304 and MJSM_0305. Melt curve analysis showed one peak, indicating one amplicon. Expression levels were normalized to *sigA* and SCFM2 sample 1 was set as the control.

Experiment Summary

Table 1: Description of bacterial strains used in study and a summary of the media and bacterial strains used for each experiment

Strains		**Origin**
M. abscessus subsp. *massiliense* 1239, *M. abscessus* subsp. *abscessus* 1091 (rough morphotype), *M. abscessus* subsp. *abscessus* 184,		United Kingdom patients
M. abscessus subsp. *massiliense 604*		Denmark patient
M. abscessus subsp. *abscessus* 1334, OM128 (rough morphotype), and OM200 (rough morphotype); *M. abscessus* subsp. *massiliense* 1335, 1337, OM194, and OM130		Cystic fibrosis patients at Papworth University Hospital; persistent infections
M. abscessus subsp. *abscessus* OM91, 1339, and *M. abscessus* subsp. *massiliense* OM69		Cystic fibrosis patients at Papworth University Hospital; cleared infections
M. abscessus subsp. *massiliense* OM130		Cystic fibrosis patients at Papworth University Hospital; less than six months of treatment
Experiment	**Media used**	**Strains used**
Growth curves	7H9, SCFM2, SCFM2 without DNA, SCFM2 without mucin, SCFM2 without DOPC	1239, 604, 1091, 184
MIC testing	MHII, SCFM2 without DNA and without mucin	1239, 604, 1091, 184, and *M. abscessus* subsp. *abscessus* 1334, OM128, OM200, OM91, and 1339; and *M. abscessus* subsp. *massiliense* 1335, 1337, OM194, OM130, and OM69
Cell envelope analyses	7H9, SCFM2,	1239, 604, 1091, 184
Cell envelope analyses, subset	CF sputum, M63 glucose, SCFM2 without mucin	1239
TBSA investigation	7H9 ADC TW-80, 7H9 OADC TW-80, 7H9 ADC DOPC, SCFM2, SCFM2 without DOPC	1239
Cell infections	7H9, SCFM2, SCFM2 without mucin	1239, 184
RNA sequencing	7H9, SCFM2	1239, 604, 1091, 184
RNA sequencing, subset	CF sputum, M63 glucose	1239
qRT-PCR for TBSA analysis	SCFM2, SCFM2 without DOPC	1239

Results

Strain selection

Four *Mabsc* strains were chosen for characterization in our studies. *M. abscessus* subsp. *abscessus* and subsp. *massiliense* are closely related, but they are distinct in antibiotic resistance (Kim et al. 2010) and clinical response to treatment making identification necessary for proper treatment. Most subsp. *abscessus* isolates have an erythromycin ribosome methylation (*erm*) gene that confers macrolide resistance which subsp. *massiliense* does not possess (Choi et al. 2012; Kim et al, 2010). In a Genome Wide Association Study (GWAS), Bryant et al. (2016) characterized clinical isolates from CF treatment centers in the United Kingdom, Ireland, Netherlands, Denmark, Sweden, Australia, and the USA. They found that 74% of isolates fell into genetically related clusters. Clusters were groups of five or more isolates that had an average SNP variance across the entire genome of 20 SNPs (range of 1-200). Bryant et al. (2016) proposed that these clustered isolates are transmissible strains of *Mabsc* due to their genetic relatedness and because the isolates were collected at geographically distant CF centers. Non-clustered isolates were strains found in their study that did not show genetic relatedness to other clinical isolates. We wanted to characterize a clustered and non-clustered isolate, from both *M. abscessus* subsp. *abscessus* and *M. abscessus* subsp. *massiliense*. We chose *M. abscessus* subsp. *abscessus* 184 and *M. abscessus* subsp. *massiliense* 604 as non-clustered isolates, *M. abscessus* subsp. *abscessus* 1091 and *M. abscessus* subsp. *massiliense* 1239 as clustered isolates. Further, 1091 is a rough morphotype strain, while all other strains are smooth. Rough isolates generally lack glycopeptidolipids (GPLs) a major outer membrane component, and are associated with poorer clinical outcome than smooth strains (Howard et al. 2006; Pawlik et al. 2013).

Growth curves

As SCFM2 was developed and tested with *P. aeruginosa,* our very first tests were to see if *Mabsc* would grow in this medium. Further, we wanted to assess if growth was restricted in rate or final titer and if growth was restricted or promoted by some of the unusual components of the medium – mucin, DNA, and DOPC. To test this, we grew 1239, 604, 184, and 1091 in complete SCFM2, SCFM2 without DNA, SCFM2 without mucin, and SCFM2 without DOPC compared to growth in 7H9-ADC-Tween 80. Due to the turbidity of the medium when mucin or DOPC are present, bacterial growth in the medium could not be monitored by OD_{600}. Thus, we assessed bacterial growth by CFU counts upon plating on 7H10-ADC. We found that all *Mabsc* isolates grew at a similar rate and to a similar titer in 7H9-ADC-Tween 80 and all variants of SCFM2. All isolates growth was measured in all media variants. However, only representative growth curves are shown in figure 1.

M. abscessus subsp. *abscessus* 1091 is a rough isolate, which causes it to tightly clump in liquid medium resulting in inconsistencies in OD600 readings and CFU counts. While looking at the overall trend convinced us there was no growth difference of 1091 based on media, the growth curves are not regular. In all media, there was an initial lag phase, followed by exponential growth between hours 12-48, followed by a stationary phase lasting till the end of the growth curve at 5 days (120 hours). Bacteria reached a final titer between log 9-10.6 CFU/mL. A secondary goal of measuring growth was to determine a time point during exponential growth to collect the cells for cell envelope extractions and RNA sequencing. Based on all growth curves, we collected the isolates at day 1.5, after inoculation of 0.005 OD_{600}.

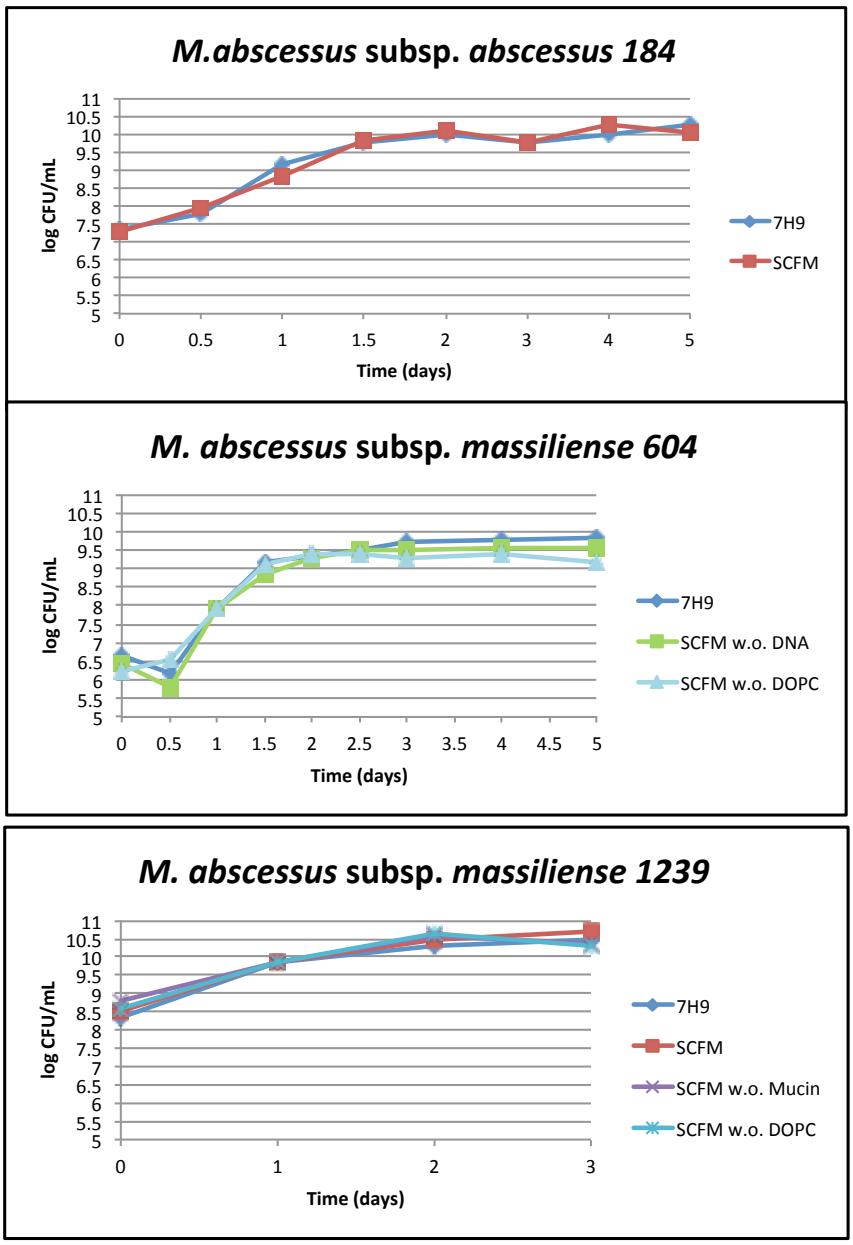

Figure 1: Growth curves showing varying isolates in SCFM2 media variations compared to 7H9.

Antibiotic susceptibility testing

Mabsc is intrinsically resistant to many antibiotics through mechanisms related to its waxy cell envelope, adherence to surfaces, the presence of efflux pumps, and resistance genes such as the *erm* gene (Choi et al. 2012; Falkingham 2018; Kim et al 2010; Nessar et al. 2012; van Ingen et al. 2014). The *erm* gene confers resistance to macrolides in more than half of *M. abscessus* subsp

abscessus isolates. A current obstacle to the informed treatment of *Mabsc* infections is the lack of correlation between *in vivo* susceptibility and *in vitro* antibiotic susceptibility for most antibiotics with the exception of macrolide resistance (Kim et al. 2010). This limitation has prompted a search for growth conditions more reflective of the microenvironment and physical conditions under which *Mabsc* thrives in the infected host. We thus sought to determine if susceptibility of strains grown in SCFM2 was the same as the susceptibility of strains grown in cation-adjusted MHII, the standard medium used for antibiotic susceptibility testing in nontuberculous mycobacteria. We tested a panel of fifteen antibiotics against fifteen reference strains and clinical isolates from the *Mabsc*. *Mabsc* pulmonary infections are treated with combination drug therapy typically including an aminoglycoside, macrolide, and a beta-lactam (Floto et al. 2016). We used this to guide our selection of antibiotics and chose aminoglycosides – amikacin, apramycin, kanamycin, streptomycin, and tobramycin; macrolides - azithromycin, clarithromycin, and erythromycin; and beta-lactams – imipenem and cefoxitin. We also chose the antimycobacterial drugs ethambutol and rifampicin which can be incorporated in *Mabsc* treatment regimens. Linezolid was chosen because it is the common drug used to treat multi-drug resistant infections. Finally, we also tested tetracycline and ciprofloxacin as they sometimes display activity against *Mabsc*. We found expected high levels of antibiotic resistance in many of the clinical isolates tested. Overall, there were very few instances of altered antibiotic susceptibility between SCFM2 (prepared here without DNA and without mucin) and cation-adjusted MHII, which was defined as greater than 2-fold difference in susceptibility. As this was not a trend in the data, rather isolated instances of varied susceptibility, we concluded that *Mabsc* MIC values in SCFM2 without mucin and without DNA will not correlate with *in vivo* drug efficacy more than *Mabsc* MIC values in cation-adjusted MHII. MIC values for the isolates characterized in this study are shown in Table 2 while values for the other 11 clinical isolates screened are shown in the supplementary material. All clinical isolates screened showed expected high levels of resistance characteristic of *Mabsc.*

Table 2: MIC values (µg/ml) of selected antibiotics tested against the four characterized isolates. Green fill indicates no or less than 2-fold difference in susceptibility, blue fill indicates that the isolate was greater than 2-fold more susceptible in MHII than SCFM2.

	M. abscessus subsp. *massiliense* 1239		*M. abscessus* subsp. *massiliense* 604		*M. abscessus* subsp. *abscessus* 1091		*M. abscessus* subsp. *abscessus* 184	
	MHII	SCFM	MHII	SCFM	MHII	SCFM	MHII	SCFM
Amikacin	32	64	128	64	32	16	256	>256
Apramycin	2	1	2	1	4	2	2	1
Azithromycin	>160	>160	1.25	2.5	>160	>160	2.5	2.5
Clarithromycin	>160	>160	0.156	0.3125	80	40	0.156	0.3125
Erythromycin	>256	>256	2	8	>256	>256	8	4
Kanamycin	16	8	32	64	32	32	16	32
Ethambutol	320	320	320	320	160	320	160	320
Rifampicin	>320	>320	>320	>320	>320	>320	>320	>320
Streptomycin	32	64	256	128	128	128	>256	>256
Cefoxitin	50	100	25	100	100	100	25	50
Tobramycin	128	64	>256	>256	64	64	>256	256
Linezolid	4	4	8	16	8	16	8	16
Tetracycline	10	20	>160	>160	>160	>160	>160	>160
Imipinem	64	128	Inconsistent results		256	>256	32	64
Ciprofloxacin	64	128	64	64	64	64	32	64

M. abscessus subsp*. abscessus* is known to be inducibly resistant to macrolides through increased expression of the *erm(41)* gene. ERM41 methylates the 23S rRNA between A_{2057} and A_{2059} (*E. coli* numbering) in the peptidyl transferase center of the ribosome. This prevents macrolides from binding and induces resistance with varying levels of resistance depending on the macrolide (Choi et al, 2012). *M. abscessus* subsp*. massiliense's erm(41)* has two deletions and a frame shift mutation which render it inactive, and thus *M. abscessus massiliense* has no inducible macrolide resistance. However, some *M. abscessus* subsp. *massiliense* isolates have been shown to be resistant to macrolides. These resistant isolates have a point mutation at $A_{2058}G$, $A_{2058}C$, or $A_{2059}G$ of the 23S rRNA gene. As a final variation, a small portion (6/46 as reported by Kim *et al.*) of *M. abscessus* subsp. *abscessus* can be susceptible to macrolides due to a point mutation $T_{28}C$ in the *erm(41)* gene. A key clinical difference is that while *M. abscessus* subsp. *abscessus* has inducible resistance to macrolides, isolates of *M. abscessus* subsp. *massiliense* isolates with one of these point mutations are highly resistant with no previous macrolide exposure. Considering these varying mechanisms of resistance, it appears that all may be at play in our tested isolates. The clustered isolates *M.*

abscessus subsp. *abscessus* 1091 and *M. abscessus* subsp. *massiliense* 1239 both showed macrolide resistance while the non-clustered isolates *M. abscessus* subsp. *abscessus* 184 and *M. abscessus massiliense* 604 did not.

Cell envelope analyses

- **Total extractable lipid content**

Fatty acids, lipids, mycolic acids, lipoglycans, and sugars were extracted and analyzed by TLC, SDS-PAGE, GC/MS, and LC/MS. The extractable lipids were between 11.5-15.9% of the total cell dry weight (Error! Reference source not found.)**.** There was no significant difference in lipid eight between 7H9-ADC-Tween 80 and SCFM2 (without mucin) grown bacteria. *M. abscessus* subsp. *abscessus* 1091 was grown and extracted in a different experiment which may explain the slightly higher percent lipids. SCFM2 without mucin was used in this experiment as mucin is not completely removed during the extraction process and would bias weights.

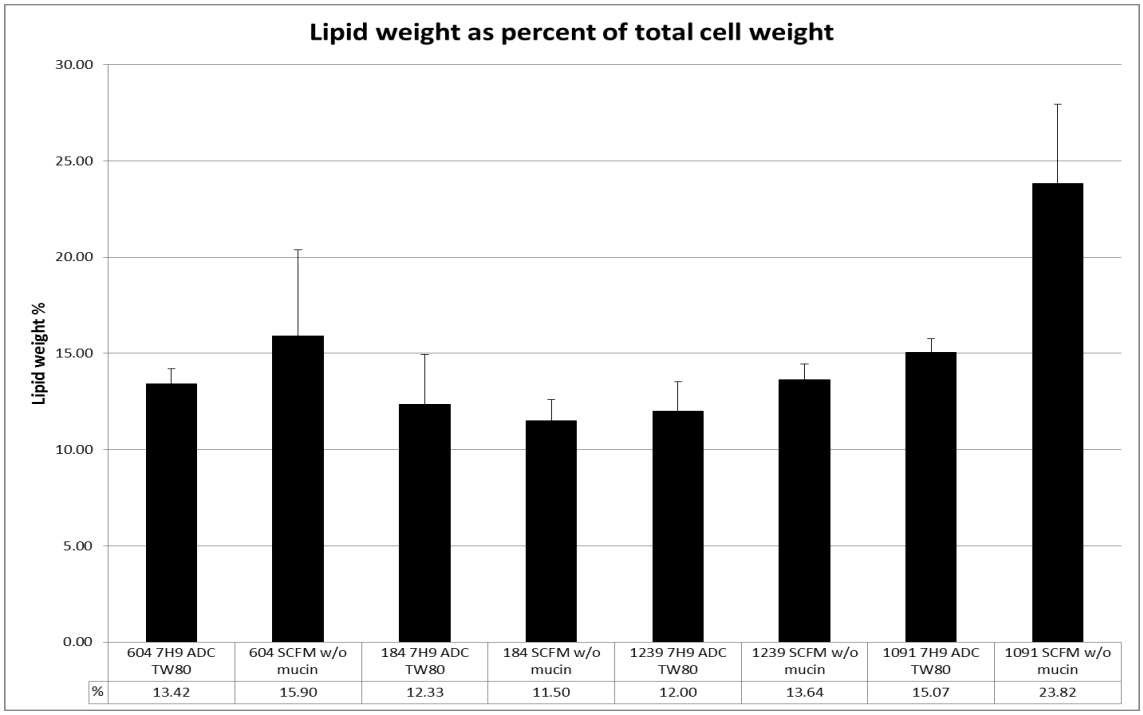

Figure 2: Extractable lipids weight of strains in 7H9-ADC-Tween 80 and SCFM2 without mucin.

- **Fatty acid composition**

The major forms of chain fatty acids in *Mabsc* are palmitoleic acid (C16:1), palmitic acid (C16:0), oleic acid (C18:1), stearic acid (C18), and tuberculostearic acid (C19:0; TBSA). These fatty acids are components of glycerophospholipids such phosphatidylethanolamine (PE), phosphatidylinositol (PI), mannosylated forms of phosphatidylinositol (PIMs), mono-, di- and tri-glycerides and other cell envelope lipids and lipoglycans. The fatty acid composition of the strains was determined by GC/MS and relative percent abundance of the major forms was calculated. The fatty acid composition of all strains grown in 7H9-ADC-Tween 80 and 10% CF sputum M63 was typical of *Mabsc*. However, when the strains were grown in SCFM2 and SCFM2 w/o mucin, all strains accumulated oleic acid (C18:1) and there was significantly less tuberculostearic acid (TBSA, C19:0) present (Table 3).

Table 2: Fatty acid composition by percent of total of the isolates grown in varying media. C18:1 (oleic acid) and C19 (tuberculostearic acid) are bolded. Oleic acid increases, and tuberculostearic acid decreases in SCFM2 with and without mucin. There was a technical error leading to the exclusion of *M. abscessus* subsp*. massiliense* 604 SCFM from the results.

Fatty acid	*M. abscessus* subsp. *massiliense* 1239			*M. abscessus* subsp. *massiliense* 604			*M. abscessus* subsp. *abscessus* 184			*M. abscessus* subsp. *abscessus* 1091		
	ADC-Tween-80	SCFM2	SCFM2 w/o mucin	ADC-Tween-80	SCFM2	SCFM2 w/o mucin	ADC-Tween-80	SCFM2	SCFM2 w/o mucin	ADC-Tween-80	SCFM2	SCFM2 w/o mucin
$C_{14:0}$	2.31	1.7	1.82	2.81	-	1.03	3.72	0.13	1.07	4.92	1.94	1.25
$C_{15:0}$	5.59	1.86	4.6	0.35	-	0.18	0.56	0.27	0.43	1.25	0.35	0.22
$C_{16:1}$	4.53	1.28	2.27	5.75	-	2.78	7.68	2.71	5.72	12.22	2.21	1.82
$C_{16:0}$	30.04	21.38	35.44	44.65	-	42.76	28.99	32.33	20.26	25.22	20.65	31.46
$C_{18:1}$	**30.25**	**45.96**	**37.58**	**33.49**	**-**	**44.29**	**33.95**	**40.3**	**51.85**	**31.63**	**49.47**	**50.04**
$C_{18:0}$	5.5	17.4	11.42	2.53	-	3.28	6.41	10.12	17.53	5.56	16	6.96
$C_{19:0}$	**11.34**	**0.83**	**2.18**	**3.94**	**-**	**0.51**	**6.76**	**0.44**	**0.49**	**7.8**	**0.8**	**1.84**
$C_{20:0}$	7.12	8.34	2.65	4.82	-	4.31	9.69	13.02	1.86	7.7	7.27	4.01
$C_{24:0}$	3.32	1.25	2.05	1.66	-	0.87	2.24	0.69	0.8	3.71	1.3	2.4

We confirmed this decrease in TBSA in a repeat experiment with 1239 so we explored the effect further. TBSA is a short chain methyl branched fatty acid only known to be biosynthesized by *Mycobacterium* and a few closely related genera. Oleic acid, C18:1, is the metabolic precursor to

TBSA. The biosynthetic pathway, first proposed by Akamatsu et al (1970a, 1970b) is that TBSA is synthesized from C18:1 esterified in a phospholipid. It is first methylated and then reduced at the C10 position to C19 (Figure 3).

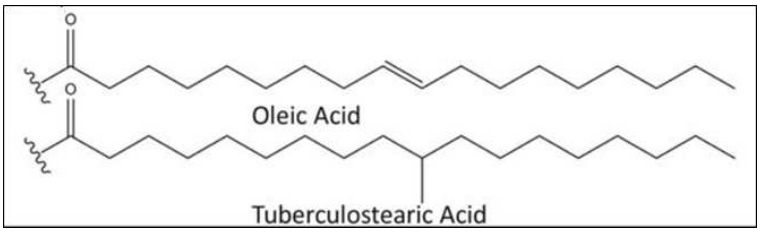

Figure 3: Structure of oleic acid (C18:1) and tuberculostearic acid (C19)

The only reported way to induce this change in fatty acid abundance in *Mycobacterium* is to change the growth temperature (Suutari et al. 1993; Taneja et al. 1979). When temperature is decreased, the percent abundance of TBSA decreases concomitantly with an increase in all unsaturated fatty acids. However, this will not decrease the levels of TBSA at the magnitude we observed. DOPC is added to SCFM2 and we hypothesized that this could be a potential source of oleic acid for the bacteria that is somehow altering the biosynthesis of tuberculostearic acid. To test this hypothesis, we grew *M. massiliense* 1239 in SCFM2 without mucin, and SCFM2 without DOPC and without mucin. We found that when DOPC was removed from SCFM2, levels of oleic acid and tuberculostearic acid returned to 7H9-ADC Tween 80 levels.

To verify that the tuberculostearic acid content of the cells was specifically decreased relative to other fatty acids, we calculated percent change in fatty acid abundance. The fatty acids C15, palmitic acid, and stearic acid did decrease in abundance with percent decreases of 20-60% in SCFM2 with DOPC relative to 7H9-ADC-Tween 80. We presume this is due to an increase in oleic acid abundance, which increased by about 40%. However, tuberculostearic acid levels decreased approximately 90% in SCFM2 with DOPC indicating that they were disproportionately decreasing compared to the other fatty acids. (Figure 4). These trends reflected in the fatty acid composition of two major mycobacterial glycerophospholipids, phosphatidylinositol dimannoside (PIM2) (not

shown) and phosphatidylethanolamine (PE), by LC/MS indicating that this decrease in tuberculostearic acid did not specifically affect one lipid species (Figure 5).

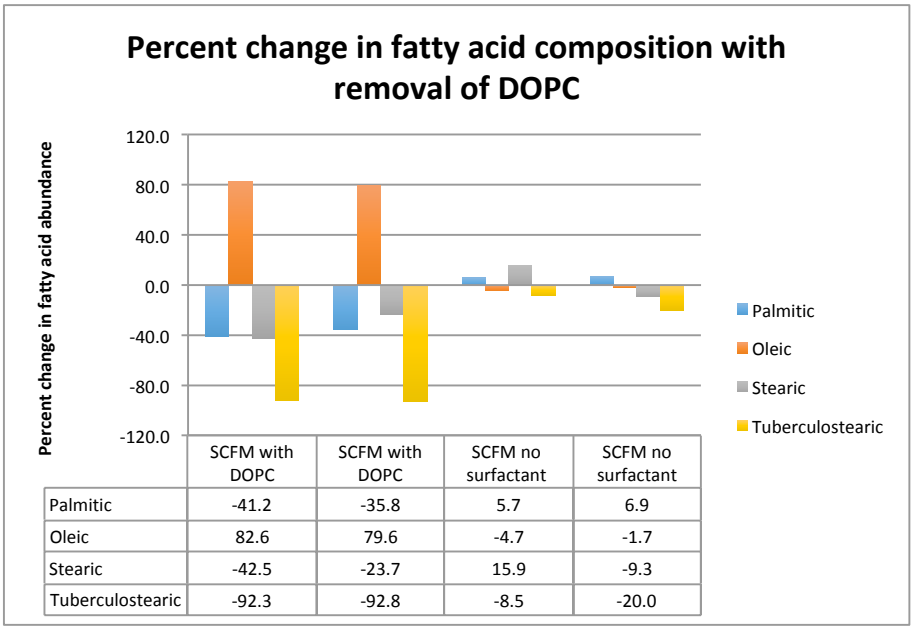

	SCFM with DOPC	SCFM with DOPC	SCFM no surfactant	SCFM no surfactant
Palmitic	-41.2	-35.8	5.7	6.9
Oleic	82.6	79.6	-4.7	-1.7
Stearic	-42.5	-23.7	15.9	-9.3
Tuberculostearic	-92.3	-92.8	-8.5	-20.0

Figure 4: Percent change in fatty acid abundance of *M. abscessus* subsp. *massiliense* 1239 grown in selected media compared to 1239 grown in 7H9-ADC-Tween 80. Duplicate samples are shown for each condition. The decrease in tuberculostearic acid is disproportional to the decrease in palmitic and stearic acid.

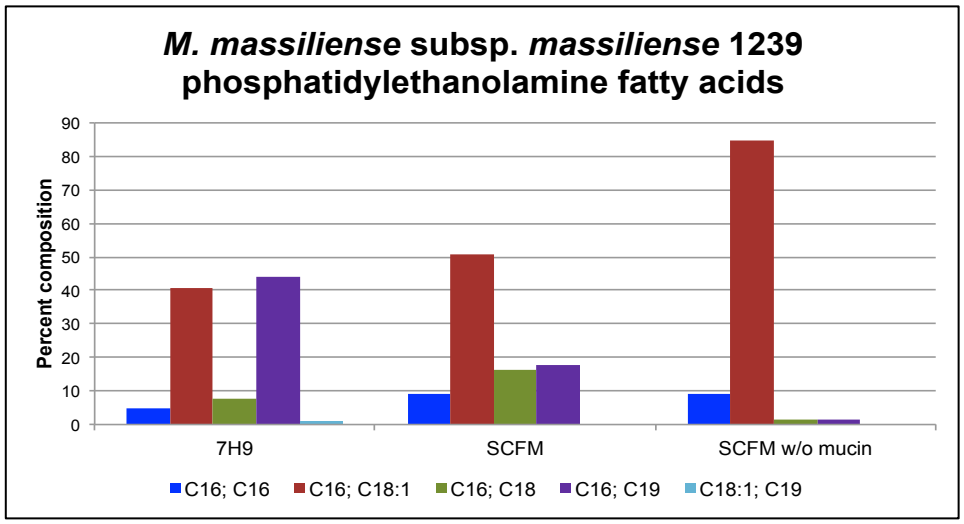

Figure 5: Fatty acid percent composition of PE as shown by the two fatty acids contained on each PE compound. Tuberculostearic acid is C19. Bacteria grown in SCFM2 with or without mucin but containing DOPC demonstrate lower abundance of PE compounds containing C19.

We also examined the LC/MS lipid profile to ensure that DOPC carryover was not skewing our results. We did find DOPC in the mass spectra from LC/MS. As a lipid, DOPC presumably associates with the cell envelope during washing steps and partitions with the lipids during extraction and thus some carries through the extraction process. Of interest, we also found small amounts of mono-methylated DOPC in the lipid profile (data not shown). This means that *Mabsc* can and is methylating the oleic acid tail of the DOPC before it is hydrolyzed from the phosphatidylcholine head group. While some amounts of DOPC is carried through the analysis, we have shown through the fatty acid levels in PE and PIM2, along with the disproportional decrease in tuberculostearic acid, that the bacteria are unable to or do not further methylate the oleic acid obtained from DOPC to tuberculostearic acid. The effect on virulence and disease of such a change is unknown.

- **Mycolic acid composition**

Mycolic acids are long chain fatty acids (C50-C90) produced by mycobacteria and closely related genera. *Mabsc* produces α-mycolates and α'-mycolates (Davidson et al. 2017). The α'-mycolates are C50-C60 fatty acids sometimes with a degree of unsaturation while α-mycolates are longer with greater than 70 carbons (Marrakchi et al. 2014). The α-mycolates often have one or two degrees of unsaturation. Both forms were present in all isolates and no significant qualitative or quantitative differences between strains or growth conditions were noted through TLC or through LC/MS (Figure 6, Figure 7).

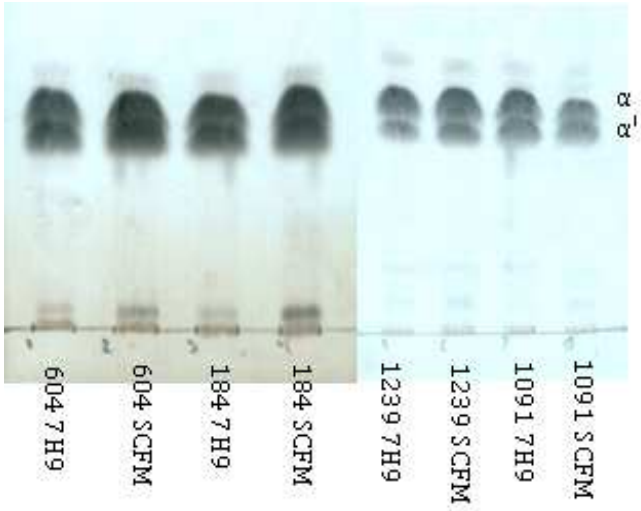

Figure 6: TLC mycolic acid patterns of mycolic acid methyl esters prepared from isolates grown in various media. All isolates in all conditions show α-mycolates and α'-mycolates

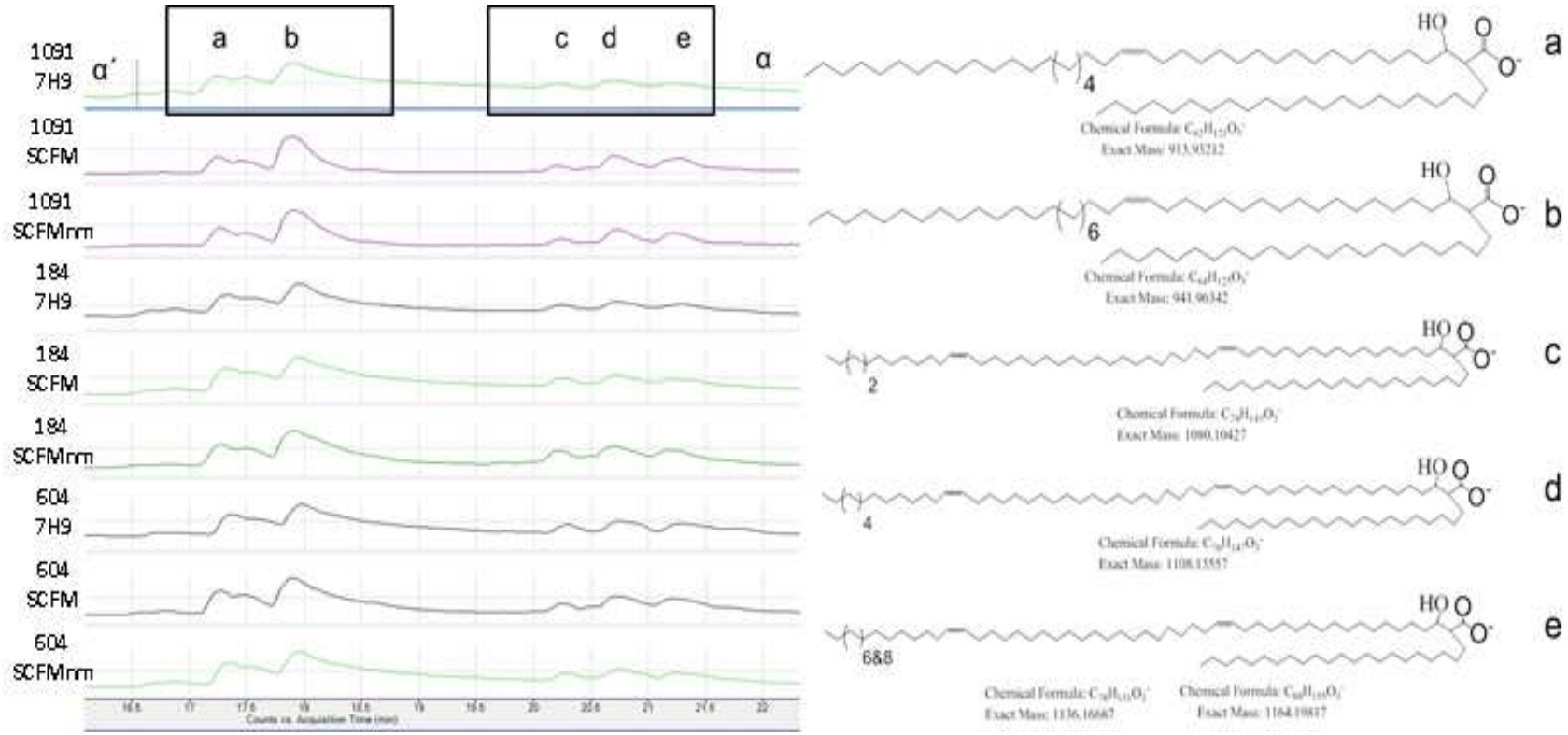

Figure 7: LC/MS TIC showing major forms of mycolic acids in *Mabsc*. This TIC shows different isolates grown in different media showing no differences in the mycolic acid profile. α-mycolates are on the right side of the TIC and α'-mycolates are the peaks on the left side. Structures and chemical formulas of the major peaks are identified are shown on the right half of the figure. SCFMnm refers to

- **Extractable lipids**

  Total extractable lipids are defined as the lipid material extractable with chloroform:methanol from intact bacilli. They populate the inner and outer membrane of mycobacteria and, in contrast to some of the mycolates, are not covalently-bound to the cell wall core. Extractable lipids were analyzed by LC/MS in positive and negative ion mode as described by Sartain et al. (2011).

  Phospholipids

  No major changes were noted, with PE, PI, and PIMs present in expected amounts. The only observed difference, as noted above, was a significant decrease in TBSA in the phospholipids prepared from the strains grown in the presence of DOPC (SCFM2 medium) (data not shown).

  Glycopeptidolipids

  M. abscessus 1091 did not produce GPLs as expected of a rough morphotype (Figure 8).

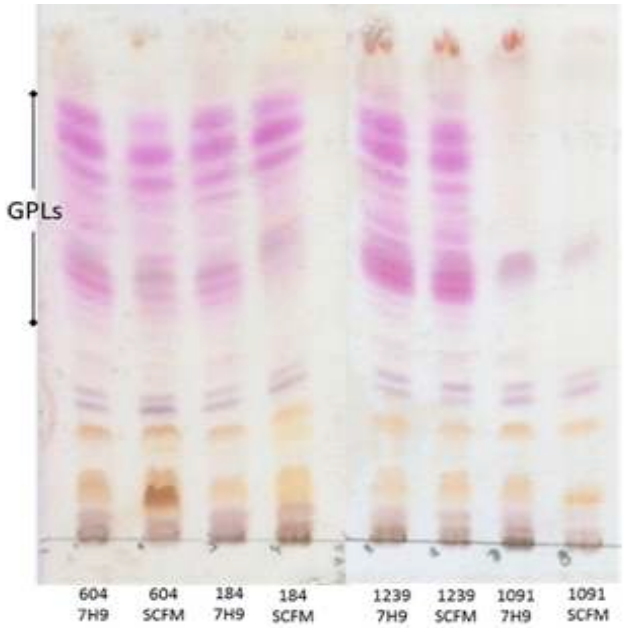

Figure 8: TLC lipid patterns of extractable lipids from isolates grown in 7H9-ADC Tween-80 (7H9) and SCFM2 (SCFM). *M. abscessus* subsp. *abscessus* 1091 (1091) showed the expected absence of GPLs characteristic of a rough morphotype. No other changes were detectable on the TLC

Detailed analysis of the GPLs produced by the three other *Mabsc* isolates revealed the expected presence of diglycosylated and triglycosylated forms of these lipids in all isolates (Figure 9). The standard diglycosylated *Mabsc* GPL is a phenylalanine-(iso)threonine-alanine-alaninol

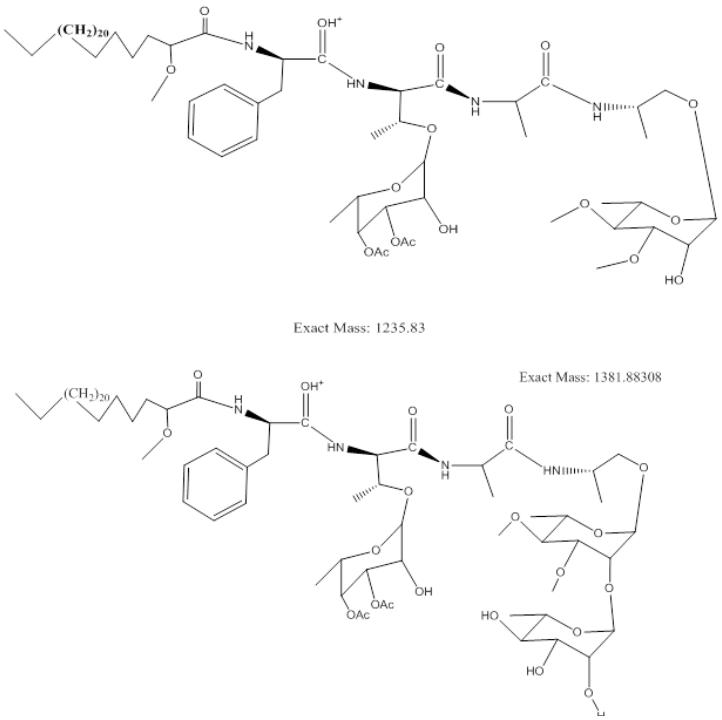

Figure 9: Chemical structure of diglycosylated GPL (top) and triglycosylated GPL (bottom) showing glycosylation positions. The structure also shows the canonical protein moiety is a phenylalanine-(iso)threonine-alanine-alaninol peptide.

peptide backbone glycosylated at the phenylalanine with a 3,4 O-di-acetyl 6 deoxytalose and at the alaninol with a 3,4 di-O methyl rhamnose (Ripoll, et al. 2007). In the standard triglycosylated form, the 3,4 di-O methyl rhamnose of diglycosylated GPL is glycosylated with an additional rhamnosyl unit at position 2. This backbone is acetylated with a C26 or C28 beta methoxy or hydroxy fatty acid. The standard di- and triglycosylated forms of GPLs comprised slightly more than half of the GPLs. An interesting observation was a change in the relative proportion of di- and triglycosylated forms of GPLs depending on the medium in which the isolates were grown. Importantly, results were consistent between SCFM2 and 10% CF sputum. When mucin was present, either artificially in SCFM2 or in the 10% CF sputum, triglycosylated GPLs increased from 13.1% of total GPLs when grown in 7H9-ADC-Tween 80 to 17.7% in SCFM2 and 21.2% when grown in M63 supplemented

with 10% CF sputum (Figure 10). M63 supplemented with glucose had 11.4% triglycosylated GPLs, similar to 7H9-ADC-Tween 80 (Figure 10).

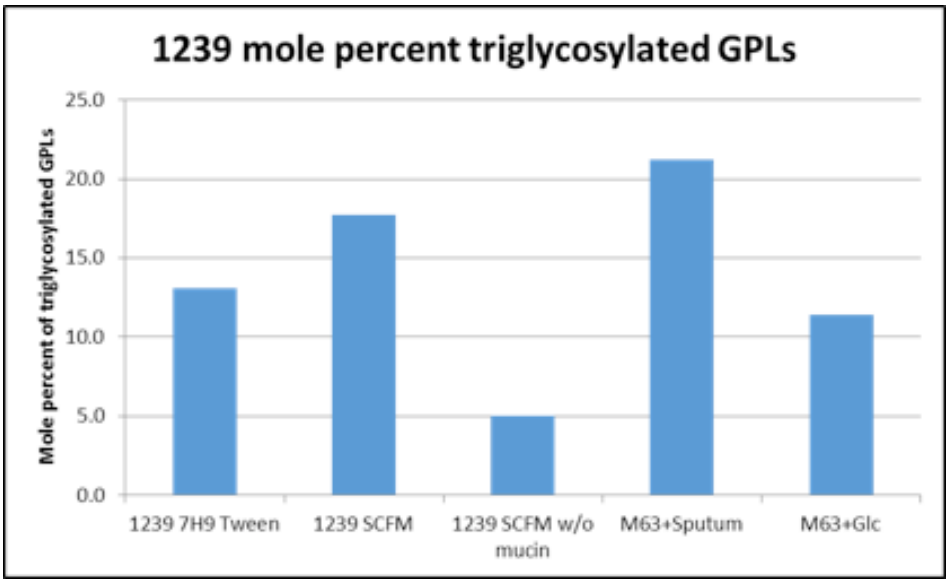

Figure 10: Mole percent of triglycosylated GPLS of *M. abscessus* subsp. *massiliense* 1239 (1239) when grown in various media 7H9-ADC-Tween-80 (7H9 Tween), SCFM2 (SCFM), SCFM2 without mucin (SCFM w/o mucin), M63 supplemented with 10% CF sputum (M63+Sputum), and M63 supplemented with glucose (M63+Glc).

There has been no previous research on the significance of tri- and diglycosylated GPLs for virulence. Triglycosylated GPLs production is known to increase at stationary growth stages in *M. smegmatis* (Mukherjee et al. 2005); but all cultures, in our case, were collected during early exponential growth. Increased quantities of triglycosylated GPLs are also thought to be produced under nutrient starvation conditions (Ojha et al. 2002). While SCFM2 and CF sputum may indeed be more nutrient limiting than 7H9-ADC-Tween 80, this does not explain why there was not an increase in the triglycosylated GPLs in SCFM2 without mucin. Physiologically, triglycosylated GPLs are slightly more polar than diglycosylated GPLs, which may affect the way the bacteria interact with their surroundings, and affect the hydrophobicity of the outer membrane.

The GPLs' pseudo-molar ions and MS/MS spectra were very complex, containing more than the standard forms of GPLs. When analyzed they revealed previously unreported unique structures of the sugars, fatty acid, and the carboxy terminus. Some sugars were acetylated or methylated

while some fatty acids had a hydroxyl group at the beta position instead of a methyl group. Of most interest, was that some GPLs had a carboxy residue possessing an extra two or three methyl groups, which we suspect is due to an altered protein moiety. At the carboxy terminus, these CH_2 could be methylating a NH to an N-methyl or inserted on the carboxy reduced amino acid, alaninol. If an N-methyl was formed, we would expect a stabilized positive charge which would reveal itself in cleavage pattern of the MS/MS spectra. We did not observe this, so we tentatively assign the group to the amino alcohol side chain. If two CH_2 groups are added, a valinol would replace the alaninol. If three CH_2 groups were added a leucinol or isoleucinol would replace the alaninol. A proposed structure is shown in Figure 11 with a GPL with a valinol residue**.** Between variations in sugars, fatty acids, and protein moiety, there are a very large number of unique GPLs in these strains – probably over 100 species.

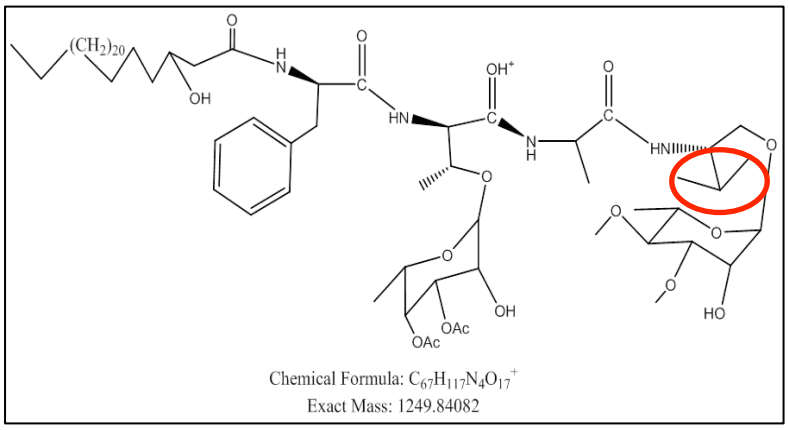

Figure 11: Structure of GPL showing unique valinol residue in the red circle. In the canonical structure (see figure 9 of di- and tri-glycosylated GPLs) this is an alaninol residue.

While not all GPLs could be examined because of the large quantity, a detailed analysis of the GPL variants produced by all the isolates in the different media identified six specific forms, 4 diglycosylated and 6 triglycosylated, which showed trends of either increasing or decreasing in abundance in SCFM2 relative to 7H9-ADC-Tween 80 and SCFM2 without mucin. This trend was confirmed in a repeat experiment with *M. abscessus* subsp. *massiliense* 1239. Of these six GPLs, only two have the typical alaninol carboxy backbone. Three contain valinol and one contains

(iso)leucinol. The results are shown in Table 4. Graphs of the species that change are shown in the supplementary materials. The significance of specific GPLs in the cell envelope has not been examined to date. However, it does appear that *Mabsc* is adapting to different media by producing more or less of very specific GPLs. What advantage this provides, if any, to *Mabsc* is unknown; however, it may be one method *Mabsc* uses to prevent the toxic build up of branch-chained amino acid intermediates, as discussed under RNAsequencing. The changes of abundance of GPLs may be due to the abundance of diverse amino acids in the SCFM2 and also known to be in CF sputum.

Table 4: Mole percent of selected GPLs produced by isolates in various media with glycosylation status, amino alcohol and direction of change noted. Some GPLs decreased and some increased in the presence of SCFM2 as detailed in the text. The trends were conserved in a repeat experiment, experiment 2.

				Experiment 1									Experiment 2					
GPL molecular mass	Di or tri glyco-sylated	Amino alchohol residue	Change	1239 7H9 ADC Tw-80	1239 SCFM	1239 SCFM without mucin	604 7H9 ADC Tw-80	604 SCFM	604 SCFM without mucin	184 7H9 ADC Tw-80	184 SCFM	184 SCFM without mucin	1239 7H9 ADC Tw-80	1239 7H9 tyloxapol	1239 SCFM	1239 SCFM without mucin	1239 M63 + CF sputum	1239 M63 + glucose
1234 B	di	alaninol	None	14.5	12.4	20.4	16.5	17.6	27.2	21.1	19.9	23.3	14.1	12.2	13.9	15.1	11.0	17.3
1220 C	di	alaninol	Increase in SCFM2	3.9	8.3	2.7	3.8	5.4	4.6	1.8	10.2	5.9	1.4	1.1	3.2	0.3	0.7	0.0
1248 B	di	valinol	Decrease in SCFM2	5.5	0.1	1.8	1.7	0.0	0.5	2.3	0.0	0.7	3.4	3.5	0.2	0.1	3.0	2.1
1276 A	di	(iso)-leucinol	Increase in SCFM2, but not SCFM2 without mucin	3.27	21.88	7.93	2.89	25.6	13.52	1.54	9.26	2.66	2.2	2.7	12	2.9	9.8	6.4
1276 B	di	valinol	Decrease in SCFM2	5.7	4.4	2.6	9.0	1.9	3.3	10.6	1.7	2.7	6.8	6.0	2.9	3.3	7.1	8.2
1380 C	tri	alaninol	Increase in SCFM2, more pronounced when mucin is present	29.6	68.9	32.9	41.1	70.3	39.6	17.2	58.8	31.1	24.1	22.9	62.8	44.4	30.9	35.1
1408	tri	valinol	Marked decrease in SCFM	3.8	0.0	0.0	13.1	0.9	1.6	10.5	0.7	1.3	16.4	18.0	7.7	1.0	22.3	16.2

- **Sugar analysis**

We found no significant difference in the total sugar (monosaccharides) profiles of samples based on media or strain. The samples were prepared from whole cells, delipidated cells and extractable lipids and analyzed as alditol acetates by GC/MS. Here, we found contamination remaining from our growth media. High levels of glucose are present in 7H9-ADC-Tween 80 which carried through analysis. Glucose is also present in lower levels in SCFM2, and it is a common

glassware contaminant. Also, mucin contains many sugar components that are not fully removed by the extraction protocols. We carried sterile SCFM2 through our alditol acetate derivatization to determine the relative abundance of sugars (See supplementary materials). We found a high abundance of N-acetylgalactosamine (47%) and N-acetylglucosamine (35%). Fucose (9%), galactose (8%) glucose (6%), ribose (4%), mannose (2%), and arabinose (1%) were present in lower abundance. After taking into consideration contamination from glucose and media derived sugars, there was overall no significant difference in sugar composition due to media choice or bacterial strain (see supplementary materials). *M. abscessus* subsp*. abscessus* 1091, a rough isolate lacking GPLs, displayed lower amounts of rhamnose and 6-deoxytalose the sugars glycosylating GPLs. This led to higher relative abundance of other sugars for 1091. We saw increased triglycosylated GPLs whenever mucin was present. This can be detected in our monosaccharide data by the increase in rhamnose whenever mucin is present. The 184 SCFM without mucin displayed an increased abundance of glucose and a decreased relative abundance of other sugars. Although we are unsure of the reason, glucose is a common contaminant in sugar analysis and could have skewed our results for this sample.

Cell infection studies

Since changes in cell surface composition caused by the different growth conditions (TBSA, GPLs) may have impacted the way *Mabsc* interacted with host cells, we next compared the uptake and intracellular replication of *Mabsc* isolates 1239 and 184 grown in different media in THP-1 bone marrow derived macrophages and A549 epithelial cells. Cell based models of *Mabsc* infections are used to assess infectivity and virulence (Bryant et al. 2016). These experiments were carried out in collaboration with Dr. Ordways' (CSU) laboratory. *Mabsc* was grown in 7H9-ADC-Tween 80, SCFM2, or SCFM2 without mucin and then THP-1 or A549 cells were infected at a MOI of 10. Overall, while no difference in cellular uptake was noticeable between growth conditions, the bacteria grown in SCFM2 (with or without mucin) displayed slightly decreased intracellular

replication compared to 7H9-ADC-Tween 80-grown cells in both A549 and THP-1 cells (Figure 12). These findings may indicate impaired virulence in the SCFM2 environment. However, the responsible factors and correlation with CF infection is unknown.

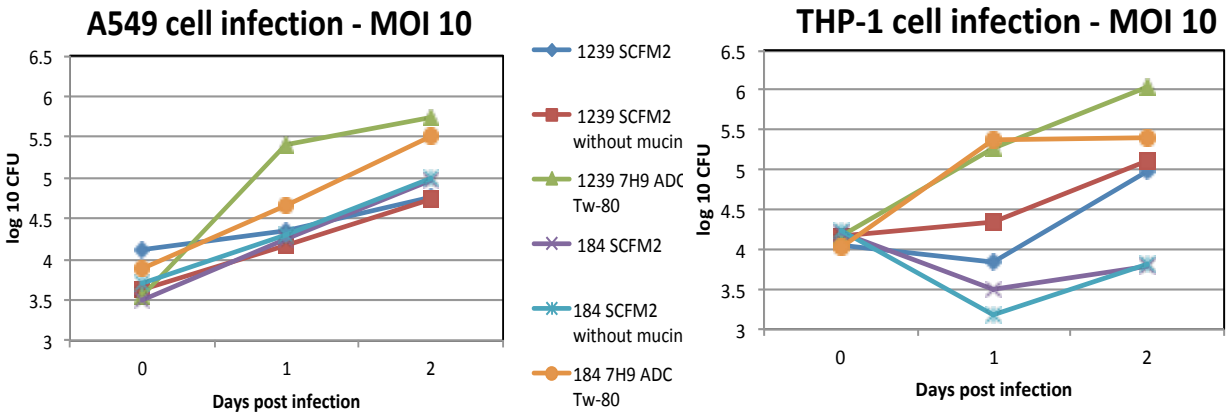

Figure 12: Intracellular replication of *Mabsc* in A549 epithelial cells (left) and THP-1 macrophages (right). Bacteria grown in SCFM2 and SCFM2 without mucin had lower rates of replication than bacteria grown in 7H9

Tuberculostearic acid biosynthetic pathway investigation

We found altered ratios of tuberculostearic to oleic acid wherever DOPC was present. We sought to identify if this was due to DOPC presence in the media or the altered expression of responsible genes. Tuberculostearic acid synthesis has been described as a two-step reaction by Akamatsu et al. (1970a, 1970b) in which oleic acid is first methylated to a methylene intermediate, 10-methylene octadecanoic acid, and subsequently reduced to tuberculostearic acid. Meena et al. have proposed two enzymes as the responsible methyltransferase in *M. tuberculosis* – Possible mycolic acid synthase (*uma1)* (2013a) and Probable cyclopropane-fatty-acyl-phospholipid synthase ufaa1 (cyclopropane fatty acid synthase) (cfa synthase) (*ufa1)* (2013b). They showed that *M. smegmatis* crude extracts overexpressing *ufa*1 synthesized tuberculostearic acid from oleic acid; however, the extract was not heat-treated and Ufa1 was never tested as a purified enzyme, so other proteins in the mixture may have accounted for this activity (Meena et al. 2013b). They also showed through radiolabeling of fatty acids that purified Uma1 in heat-treated *E. coli* extract

produced a spot with the same retention factor as TBSA (Meena et al. 2013a). However, it was never identified as TBSA by mass spectroscopy. Shuntaro et al. (2017) argue that the entirety of the Uma1 and Ufa1 proteins consists of an *S*-adenosyl methionine-dependent methyltransferase domain; and that the reductase domain expected to be necessary for biosynthesis of TBSA was not present. They characterized two enzymes in *Mycobacterium chlorophenolicum,* WP_048472120 and WP_048472121 - a methyltransferase and a reductase. When both were overexpressed in *E. coli,* and the culture supplemented with oleic acid, TBSA was produced as identified by GC/MS. When just the methyltransferase was expressed, an unknown fatty acid was produced, presumed to be a 10-methylene octadecanoic intermediate. When just the reductase was overexpressed, no product was produced.

Ufa1, Uma1, and WP_048472120 and WP_048472121 protein sequences were blasted against *M. abscessus subs. abscessus* ATCC 19977 (NCBI:txid561007) and *M. abscessus subs. massiliense* CIP 108297 *(NCBI:*txid1962118) to look for orthologous proteins using NCBI Blastp. Uma1 has two orthologs in *Mabsc*, MAB_3881 (55% identity, 100% coverage) and MAB_4088c (68% identity, 100% coverage). There are no orthologs in *Mabsc* for Ufa2. *M. chlorophenolicum* WP_048472120 ortholog is MMASJCM_0305 with 76% identity, 97% coverage and *M. chlorophenolicum* `WP_048472121 has the ortholog MMASJCM_0304 with 79% identity, 99% coverage. The expression of these genes was thus measured using qRT-PCR (and expression normalized to *sigA*) of *M. abscessus subs. massiliense* 1239 grown in SCFM2 and SCFM2 without DOPC. If the transcription level of these genes directly relates to the quantity of TBSA biosynthesized, we would expect lower expression in SCFM2 as there are lower levels of TBSA produced. However, no more than a 2-fold change in expression was detected between conditions. This indicates that the transcription of these ortholog genes is not related to the change in biosynthesis of TBSA in *Mabsc,* or if they are, they are somehow inactivated (e.g., by post-translational modifications) in *Mabsc* grown in the presence of DOPC.

RNAseq analyses

RNAseq was used to analyze changes in gene expression of the four clustered and unclustered *Mabs* and *Mmas* isolates when grown in either 7H9-ADC-Tween 80, SCFM2 complete medium or 20% CF sputum diluted in M63 medium to determine how closely SCFM2 mimic the physiological state of *Mabsc* in actual patient sputum. Using RNAseq, the differentially expressed genes from *M. abscessus* subsp. *massiliense* 1239, *M. abscessus* subsp. massiiense 604, *M. abscessus* subsp. *abscessus* 1091, and *M. abscessus* subsp. *abscessus* 184 were identified between 7H9-ADC-Tween 80 and SCFM2. In addition, the differential expression of 1239 was further identified in 20% CF sputum (diluted in M63) and glucose supplemented M63. 1239 was chosen because it is a smooth clinical isolate proficient in GPL biosynthesis and it belongs to one of the most represented clones of *Mabs* subsp*. massiliense*.globally Further, in an effort to elucidate the genes responsible for the changes in TBSA levels when DOPC is added to the culture medium, the gene expression profiles of *M. abscessus* subsp. *massiliense* 1239 grown in SCFM2 without mucin, with DOPC and grown in SCFM2 without mucin, without DOPC were analyzed and compared. A log 2 fold change of greater than the absolute value 2 and an adjusted *p*-value of less than 0.05 were considered a significant change in expression.

M63 supplemented with glucose had low mapping rates to the *M. abscessus* ATCC 19977 genome of 75%, 46%, and 46% for the triplicate samples. Unmapped reads were blasted and mapped to the *B. subtilis* genome. This led us to exclude this control from our analysis as the effect of growing in a co-culture is unknown.

First the consistency and biological relevance of the results was assessed. The up-regulated and down-regulated genes of each isolate grown in 7H9-ADC-Tween 80 and SCFM2 was determined. These gene lists were examined for consistency and randomness. We saw overlap between gene lists. There were 22 genes up-regulated in all isolates in SCFM2. In addition, the genes that were up-regulated were frequently in gene clusters, not randomly spread across the

genome as would be expected if it were not a true effect but an effect due to errors in library preparation (Figure 13, gene lists in Supplementary materials). The number of up-regulated and down-regulated genes in these conditions is shown in Table 5. The analysis showed more overlap in the up-regulated than the down-regulated genes. However, when examined for functional

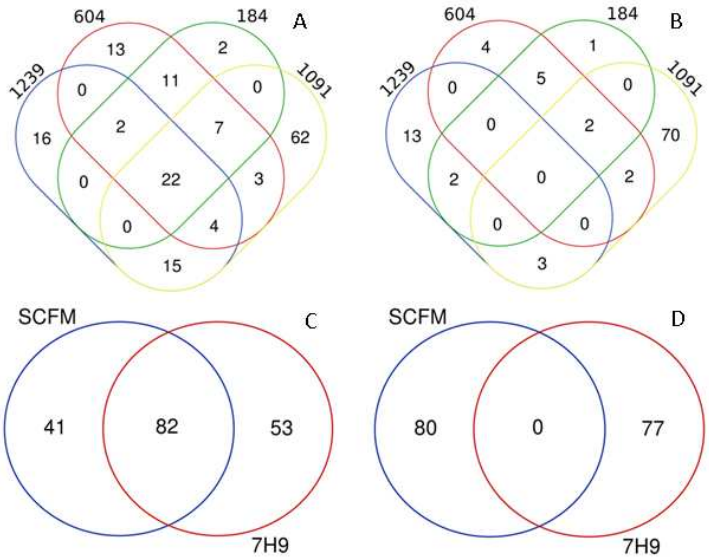

Figure 13: Venn diagrams showing overlap of genes expressed in different strains or media. A) Genes up-regulated in SCFM2 vs 7H9-ADC-Tween 80. B) Genes down-regulated in SCFM2 vs 7H9-ADC-Tween 80. C) Overlap of genes expressed higher in CF sputum than in 7H9-ADC-Tween 80 or SCFM2. D) Overlap of number of genes expressed lower in CF sputum than in SCFM2 or 7H9-ADC-Tween 80. For example in A, 11 specific genes of *M. abscessus* subsp. *massiliense* 604 and *M. abscessus* subsp. *abscessus* 184 were expressed at higher levels when grown in SCFM2 than in 7H9-ADC-Tween 80.

Table 5: Number of genes up and down-regulated in SCFM2 when compared to 7H9-ADC-Tween 80 and CF sputum. Also shows number of genes upregulated in CF sputum compared to 7H9-ADC-Tween 80

Comparison	Up-regulated	Down-regulated
1239 SCFM2 vs 7H9	59	18
1239 CF vs SCFM2	123	80
1239 CF vs 7H9	135	74
184 SCFM2 vs 7H9	44	10
604 SCFM2 vs 7H9	62	13
1091 SCFM2 vs 7H9	113	77
All four isolates SCFM2 vs All 7H9	32	3

categories no trends from the isolate, clustered or non-clustered, were apparent.

As no strain dependent trends were apparent and given the strong overlap in gene expression profiles, a strain independent response to media was calculated by pooling all SCFM2 samples and all 7H9-ADC-Tween 80samples from all four isolates for differential expression analysis. In this analysis, 32 genes had significantly higher expression in SCFM2 than 7H9-ADC-Tween 80 (Table 6) and 3 genes were expressed at significantly lower expression in SCFM2 (Table 7). This number is higher than the 22 genes overlapping in the individual isolate analyses because of the increased power of comparing 12 SCFM2 *vs* 12 7H9-ADC-Tween 80 samples, instead of 3 SCFM2 *vs* 3 7H9-ADC-Tween 80 samples.

Table 6: The 32 genes are shown that were expressed at higher levels in SCFM2 than 7H9 ADC-Tween 80, independent of strain. Colored text indicates gene clusters with changes in expression. BaseMean is the mean of the gene counts in SCFM2 and 7H9 and indicates the level of expression.

Gene_id	Gene Product	baseMean	log2Fold Change	padj
MAB_1188c	Probable acyl-CoA dehydrogenase	2952	3.69	5.18363E-05
MAB_1189c	Probable methylmalonic acid semialdehyde dehydrogenase MmsA	4478	3.19	5.88088E-05
MAB_1330	1-pyrroline-5-carboxylate dehydrogenase	32153	3.80	1.63913E-24
MAB_1331	Probable proline dehydrogenase	10679	3.81	2.15186E-38
MAB_3100	L-alanine dehydrogenase (ALD)	45451	5.37	1.67453E-15
MAB_3101c	hypothetical protein	11584	5.07	1.27271E-42
MAB_3180	hypothetical protein	103	3.09	1.2554E-08
MAB_3385	hypothetical protein	788	3.70	0.049941127
MAB_3386c	hypothetical protein	1388	4.16	7.09229E-05
MAB_3645	Putative reductase	2202	5.37	2.26262E-11
MAB_3646c	Probable aminotransferase class-III	32693	7.93	1.95825E-22
MAB_3647c	Probable transcriptional regulatory protein	3836	3.52	0.001887527
MAB_3648	hypothetical protein	6468	5.94	3.0491E-13
MAB_3649	Probable aldehyde dehydrogenase	22782	5.77	1.39365E-13
MAB_3762	hypothetical protein	959	3.14	0.021918611
MAB_3840	hypothetical protein	6816	7.18	4.34096E-81
MAB_3841	Ornithine aminotransferase RocD1	4795	5.87	9.07392E-33
MAB_4407c	Putative alkylhydroperoxidase AhpD	880	3.04	0.012667249
MAB_4538c	Putative acyl-CoA dehydrogenase FadE	2341	4.17	2.44971E-36
MAB_4539c	Putative acyl-CoA carboxylase alpha subunit AccA	2315	4.51	7.6702E-42
MAB_4540c	Putative acetyl-CoA carboxylase beta subunit AccD	1981	4.55	1.2027E-42
MAB_4742c	hypothetical protein	14035	5.13	2.96575E-29
MAB_4743c	Putative dehydrogenase/reductase	33256	7.63	4.666E-107
MAB_4744c	hypothetical protein	14307	7.99	2.0485E-104
MAB_4745	Putative membrane protein, MmpS	2277	7.83	3.78099E-79
MAB_4746	Putative membrane protein, MmpL	15104	8.05	6.48435E-54
MAB_4747	hypothetical protein	5091	4.38	5.88699E-24
MAB_4748c	Conserved hypothetical protein (pyridoxamine 5'-phosphate oxidase?)	1406	3.96	1.83699E-12
MAB_4915c	Hypothetical protein	458	3.53	9.8989E-25
MAB_4916c	Probable branched-chain keto acid dehydrogenase E2 component BkdC	8541	4.40	5.59083E-34
MAB_4917c	Probable branched-chain keto acid dehydrogenase E1 component, beta subunit BkdB	4900	4.03	0.000409761
MAB_4918c	Probable branched-chain keto acid dehydrogenase E1 component, alpha subunit BkdA	6217	3.76	0.049941127

Table 7: The 3 genes are shown that were expressed at lower levels in SCFM2 than in 7H9-ADC-Tween 80, independent of strain. BaseMean is the mean of the gene counts in SCFM2 and 7H9-ADC-Tween 80 and indicates the level of expression

Gene_ID	Gene Product	baseMean	log2Fold Change	padj
MAB_2693	Hypothetical Protein	322	-6.04	3.09E-10
MAB_4715c	Hypothetical Protein	2782	-4.44	0.009452
MAB_1031c	Probable Manganese Transport Protein MntH	2211	-3.40	0.000781

Using KEGG pathways analysis, the up-regulated genes were assigned to the pathways shown in Table 8. Genes can be assigned multiple KO numbers as noted by the greater than 32 results in the table. Metabolic pathways, particularly metabolism of amino acids, appear to be overrepresented in line with the amino acid-rich composition of the SCFM2 medium. Other pathways relate to carbon metabolism from diverse sources, fatty acid metabolism and antibiotic biosynthesis. These pathways reflect the diverse carbon sources that *Mabsc* is forced to utilize to successfully grown in SCFM.

Table 8: KEGG categories of genes up-regulated in SCFM2 independent of isolate.

KEGG category number and name
mab01100 Metabolic pathways - *Mycobacterium abscessus* ATCC 19977 (11)
mab01130 Biosynthesis of antibiotics - *Mycobacterium abscessus* ATCC 19977 (7)
mab01110 Biosynthesis of secondary metabolites - *Mycobacterium abscessus* ATCC 19977 (7)
mab01200 Carbon metabolism - *Mycobacterium abscessus* ATCC 19977 (5)
mab00620 Pyruvate metabolism - *Mycobacterium abscessus* ATCC 19977 (5)
mab01120 Microbial metabolism in diverse environments - *Mycobacterium abscessus* ATCC 19977 (5)
mab00330 Arginine and proline metabolism - *Mycobacterium abscessus* ATCC 19977 (4)
mab00280 Valine, leucine and isoleucine degradation - *Mycobacterium abscessus* ATCC 19977 (4)
mab00010 Glycolysis / Gluconeogenesis - *Mycobacterium abscessus* ATCC 19977 (4)
mab00020 Citrate cycle (TCA cycle) - *Mycobacterium abscessus* ATCC 19977 (3)
mab00640 Propanoate metabolism - *Mycobacterium abscessus* ATCC 19977 (2)
mab00250 Alanine, aspartate and glutamate metabolism - *Mycobacterium abscessus* ATCC 19977 (2)
mab00410 beta-Alanine metabolism - *Mycobacterium abscessus* ATCC 19977 (2)
mab00561 Glycerolipid metabolism - *Mycobacterium abscessus* ATCC 19977 (1)
mab00562 Inositol phosphate metabolism - *Mycobacterium abscessus* ATCC 19977 (1)
mab00053 Ascorbate and aldarate metabolism - *Mycobacterium abscessus* ATCC 19977 (1)
mab00061 Fatty acid biosynthesis - *Mycobacterium abscessus* ATCC 19977 (1)
mab00380 Tryptophan metabolism - *Mycobacterium abscessus* ATCC 19977 (1)
mab00625 Chloroalkane and chloroalkene degradation - *Mycobacterium abscessus* ATCC 19977 (1)
mab00430 Taurine and hypotaurine metabolism - *Mycobacterium abscessus* ATCC 19977 (1)
mab00630 Glyoxylate and dicarboxylate metabolism - *Mycobacterium abscessus* ATCC 19977 (1)
mab00071 Fatty acid degradation - *Mycobacterium abscessus* ATCC 19977 (1)
mab00920 Sulfur metabolism - *Mycobacterium abscessus* ATCC 19977 (1)
mab00903 Limonene and pinene degradation - *Mycobacterium abscessus* ATCC 19977 (1)
mab01212 Fatty acid metabolism - *Mycobacterium abscessus* ATCC 19977 (1)
mab00340 Histidine metabolism - *Mycobacterium abscessus* ATCC 19977 (1)
mab00310 Lysine degradation - *Mycobacterium abscessus* ATCC 19977 (1)

Comparative gene expression of *Mabsc* in SCFM2 and CF sputum

Next, we evaluated if SCFM2 more closely mimics the CF airway physiology and causes similar bacterial adaptation as activated by growth in CF sputum. To this end, we compared the genes over and under expressed in CF sputum and SCFM2 when compared to 7H9-ADC-Tween 80. There were 135 genes up-regulated in CF sputum compared to 7H9-ADC-Tween 80 and 59 genes up-regulated in SCFM2 compared to 7H9-ADC-Tween 80 (Table 5). Of these, 21 genes were in both lists. The 21 genes up-regulated in both conditions, which represent how SCFM2 is mimicking the physiology of the CF airway, are shown in table 9. The other gene lists of uniquely up-regulated genes are shown in the supplementary figures. These genes were examined to determine their functional categories. The KEGG pathways of the 21 conserved genes are shown in table 10. The

Table 9: The 21 genes that are up-regulated in both SCFM2 and CF sputum when compared to 7H9-ADC-Tween 80

Gene_id	Gene Product
MAB_0068	Putative transcriptional regulator, GntR family
MAB_0304	hypothetical protein
MAB_2122	Putative peptide synthetase MbtE
MAB_2157	Probable acyl-[acyl-carrier protein] desaturase
MAB_3467c	18 kDa antigen (HSP 16.7)
MAB_3548c	Putative fatty acid desaturase
MAB_3646c	Probable aminotransferase class-III
MAB_3762	hypothetical protein
MAB_3840	hypothetical protein
MAB_3841	Ornithine aminotransferase RocD1
MAB_4273c	Chaperone protein DnaK (Hsp 70)
MAB_4407c	Putative alkylhydroperoxidase AhpD
MAB_4532c	hypothetical protein
MAB_4538c	Putative acyl-CoA dehydrogenase FadE
MAB_4539c	Putative acyl-CoA carboxylase alpha subunit AccA
MAB_4540c	Putative acetyl-CoA carboxylase beta subunit AccD
MAB_4915c	hypothetical protein
MAB_4916c	Probable branched-chain keto acid dehydrogenase E2 component BkdC
MAB_4917c	Probable branched-chain keto acid dehydrogenase E1 component, beta subunit BkdB
MAB_4918c	Probable branched-chain keto acid dehydrogenase E1 component, alpha subunit BkdA

Table 10: The KEGG categories of the 21 genes up-regulated in both SCFM2 and CF sputum when compared to 7H9-ADC-Tween 80

KEGG category number and name
mab01100 Metabolic pathways - *Mycobacterium abscessus* ATCC 19977 (8)
mab01110 Biosynthesis of secondary metabolites - *Mycobacterium abscessus* ATCC 19977 (5)
mab01130 Biosynthesis of antibiotics - *Mycobacterium abscessus* ATCC 19977 (5)
mab01200 Carbon metabolism - *Mycobacterium abscessus* ATCC 19977 (4)
mab00620 Pyruvate metabolism - *Mycobacterium abscessus* ATCC 19977 (4)
mab01120 Microbial metabolism in diverse environments - *Mycobacterium abscessus* ATCC 19977 (4)
mab00010 Glycolysis / Gluconeogenesis - *Mycobacterium abscessus* ATCC 19977 (3)
mab01212 Fatty acid metabolism - *Mycobacterium abscessus* ATCC 19977 (3)
mab00020 Citrate cycle (TCA cycle) - *Mycobacterium abscessus* ATCC 19977 (3)
mab01040 Biosynthesis of unsaturated fatty acids - *Mycobacterium abscessus* ATCC 19977 (2)
mab00061 Fatty acid biosynthesis - *Mycobacterium abscessus* ATCC 19977 (2)
mab00280 Valine, leucine and isoleucine degradation - *Mycobacterium abscessus* ATCC 19977 (2)
mab00640 Propanoate metabolism - *Mycobacterium abscessus* ATCC 19977 (1)
mab01053 Biosynthesis of siderophore group nonribosomal peptides - *Mycobacterium abscessus* ATCC 19977 (1)
mab00630 Glyoxylate and dicarboxylate metabolism - *Mycobacterium abscessus* ATCC 19977 (1)
mab00330 Arginine and proline metabolism - *Mycobacterium abscessus* ATCC 19977 (1)
mab03018 RNA degradation - *Mycobacterium abscessus* ATCC 19977 (1)

KEGG pathways can be summarized by changes in carbon metabolism, particularly the degradation of amino acids as reflected in the increased expression of MAB_3646c, MAB_3841 and the three genes encoding the Lpd-dependent branched chain keto acid dehydrogenase (BCKADH) which was found to be required for the metabolism of branched-chain amino acids in *Mycobacterium tuberculosis* (Venugopal et al., 2011) (MAB_4916c-MAB4918c). There is also increased fatty acid metabolism (e.g., MAB_3548c; MAB_2157; MAB4538c; MAB4539c; MAB_4540c) and indications of iron deficiency (MAB_2122 involved in mycobactin synthesis), response to exposure to reactive nitrogen intermediates (MAB_4407c), and possibly other stresses triggering the expression of protein chaperones such as MAB_4273c. The amino acid metabolism and TCA cycle will produce intermediates that *Mabsc* must detoxify and utilize which, based on what is known of the metabolism of *Mycobacterium tuberculosis* in the infected host, it may do by building methyl-branched fatty acid-containing lipids. Of note, the inactivation of the BCKADH complex in *Staphylococcus aureus* and *Myxococcus xanthus* led to a decrease in quantity of branched-chain fatty acids in the cell membrane and rendered the mutants more susceptible to a variety of stresses (Singh et al., 2008; Toal et al., 1995) further highlighting the conservation of the prokaryotic

responses to the utilization of amino acids as carbon sources. Interestingly, the branched-chain amino acids that *Mabsc* must detoxify, valine, isoluecine, and leucine, are the three amino acids that we see incorporated into the identified non-canonical forms of GPLs (Figure 11). As this complex is up-regulated in both SCFM2 and CF sputum, consistent with the use of amino acids as the primary carbon source in these media, it demonstrates how SCFM2 is replicating the nutrient availability and stresses that are present in CF sputum.

When the genes uniquely up-regulated in SCFM2 (38) and CF sputum (114) compared to 7H9-ADC-Tween 80 were examined they fell into the same categories of diverse carbon metabolism, amino acid metabolism, and fatty acid metabolism. There were fewer genes down-regulated in CF sputum and SCFM2 compared to 7H9-ADC-Tween 80 than up-regulated. This may reflect that there is a need to utilize a diverse set of metabolic pathways leading to gene upregulation, not downregulation. Overall, there were 6 genes down-regulated in both SCFM2 and CF sputum. However, none of these genes had KEGG pathway annotations. There were 68 genes uniquely down-regulated in CF sputum and 12 genes uniquely down-regulated in SCFM. All gene lists are in supplementary methods. These genes fell into similar metabolic KEGG categories as the up-regulated genes.

Finally, to evaluate how SCFM2 does not mimic CF sputum, the genes differentially expressed when strain 1239 was grown in SCFM2 and CF sputum were determined. There were 123 genes expressed at higher levels in CF sputum than in SCFM2 and 80 genes expressed at lower levels in CF sputum than SCFM. The 123 up-regulated genes again largely related to different forms of metabolism including amino acid metabolism, fatty acid metabolism, and lipid metabolism. There were two probable ABC transporters up-regulated in CF sputum, MAB_0277c and MAB_1713. This could potentially reflect the presence of antibiotics due to patient treatment in the CF sputum triggering the expression of efflux pumps. The 80 genes expressed at lower levels in CF than SCFM2 again reflected the same trends in altered carbon metabolism regulation.

While functional enrichment analysis and gene network analysis is still ongoing through a collaboration with Dr. Michael Strong at National Jewish Health in Denver, CO, trends in gene expression can already be seen. Overall, SCFM2 recapitulates the type of carbon metabolism that occurs in CF sputum. There are high levels of amino acid metabolism, central carbon metabolism (TCA cycle), and fatty acid metabolism in both SCFM2 and CF sputum indicating a shift to more diverse metabolites than seen in 7H9-ADC-Tween 80. While there are different levels of expression for specific genes within these categories, these categories remain conserved. This indicates that SCFM2 is pushing *Mabsc* to a metabolic state utilizing similar carbon sources to what is observed in CF sputum**.** For further testing, this indicates that SCFM2 could be used to shift metabolism to a profile similar to what is seen in CF sputum, which will enable more physiologically relevant studies and results.

Correlating gene expression with alterations to the cell envelope

To detect genes that may be responsible for the altered levels of TBSA observed whenever DOPC was present, *M. abscessus* subsp. *abscessus* 1239 was grown in SCFM2 without mucin and SCFM2 without mucin and without DOPC. Between these two conditions, there were only four genes that were differentially expressed, all located in an apparent single gene cluster, and all showing reduced expression in the presence of DOPC (Table 10). Shuntaro et al. (2017) proposed that the biosynthesis of TBSA was a two-step reaction involving a methylation, followed by a reduction. Of note, our analysis highlights a putative dehydrogenase/reductase which could

Table 10: Genes that are differentially regulated between SCFM2 without mucin and SCFM2 without mucin and without DOPC. A negative log2 fold change indicates that the expression is higher in SCFM2 without mucin than in SCFM2 without mucin and without DOPC.

Gene_ID	Gene Product	baseMean	log2Fold Change	padj
MAB_4743c	Putative dehydrogenase/reductase	1565.64	-3.48	9.26E-12
MAB_4744c	hypothetical protein	758.39	-4.21	2.17E-28
MAB_4745	Putative membrane protein, MmpS	119.90	-4.20	3.23E-08
MAB_4746	Putative membrane protein, MmpL	313.65	-3.37	0.000147

catalyze the necessary reaction. Given that the levels of TBSA are decreased in the presence of DOPC in the medium, we would have expected to see a decrease in expression of the responsible genes in the medium containing DOPC. However, we observe the reverse with these four differentially expressed genes – they have higher expression in medium containing DOPC. If these genes are responsible for TBSA biosynthesis, it may be that they are acting on DOPC and unable to synthesize TBSA from it. MmpL proteins are involved in the transport of lipophilic macromolecules across the mycobacterial plasma membrane such as mycolic acids and (glyco)lipids, often coupling biosynthesis and export, and could be involved in the metabolism of other lipids. Also noteworthy, these four genes are among the top five most highly overexpressed in the strain independent response to complete SCFM2.

Finally, 1239 grown in SCFM2 was compared to 1239 grown in SCFM2 without mucin to identify genes responsible for the increased abundance of triglycosylated GPLs. The GPL locus is highly conserved across *M. smegmatis, M. chelonae,* and *Mabs.* In *Mabs* the majority of the genes are located in two main locuses as described by Ripoll et al (2007). No genes in the GPL locus were differentially regulated between SCFM2and SCFM2 without mucin. In fact, no genes described in the GPL locus pulled down in any of the analyses. We were unable to associate any gene with this change in triglycosylation suggesting that regulation of the responsible enzyme may not be at the transcriptional level.

Discussion

Findings

The results of this study showed that SCFM2, and the pulmonary surfactant DOPC in particular, altered the fatty acid composition of *Mabsc*. Moreover, triglycosylated GPLs were more abundant whenever mucin was present – from SCFM2 or from CF sputum. Transcriptomics showed that a conserved set of genes was up-regulated in all strains in SCFM2. *Mabsc* relies on similar metabolic pathways utilizing amino acids as main carbon sources when grown in both SCFM2 and CF sputum. The variations in expression levels give insight into the nutrient availability of the different media. Also, gene expression revealed potential genes responsible for alterations in TBSA levels. Finally, in the whole cell infection model, replication decreased when Mabsc was grown in SCFM2 compared to 7H9-ADC-Tween 80 before cell infection. This decreased replication indicates that SCFM2 may negatively affect *Mabsc* virulence or fitness in whole cells, perhaps as a consequence of amino acid catabolism/detoxification impacting fatty acid metabolism and possibly other aspects of the physiology of the bacterium.

This study is the first to compare SCFM2 to CF sputum grown bacteria in *Mabsc.* It also thoroughly characterized the cell envelope and antibiotic susceptibility of multiple clinical strains. CF sputum is a very unique nutritional environment. This was immediately evident by the long time period – 45 days - that was required to grow cultures of *M. abscessus* subsp. *massiliense* 1239 in 20% CF sputum to levels sufficient for analysis and sequencing. *M. abscessus* subsp. *massiliense* 1239 never appeared to reach a true exponential growth phase. This slow growth was repeated in M63+ glucose -grown *M. abscessus* subsp. *massiliense* 1239, where similar growth times were observed. M63 was chosen because it is a very minimal medium. A 20% dilution of CF sputum may have restricted nutrient availability to less than is in the lung. However, the cell envelope of CF sputum grown cultures is not remarkably different, only varying in percentage of triglycosylated

GPLs. In addition, RNA sequencing revealed a similar gene expression profile in CF sputum when compared to SCFM2.

Mabsc is notorious for its innate antibiotic resistance and the hope was that SCFM2 would be a medium that would finally recapitulate *in vitro* what happens during *in vivo* treatment. In our studies with SCFM2 without mucin, we found no consistent or wide-ranging differences between antibiotic susceptibility in MHII *vs* SCFM2. These preliminary *in vitro* results lead us to believe that it would not be a better model for predicting treatment success.

The genes responsible for GPLs biosynthesis have been closely studied in *Mabsc* and the GPL structure has been defined (Ripoll et al. 2007). Our RNAseq analysis showed no significant changes of expression of any of the genes in the GPL locus. However, this study revealed that the exact structure of a GPL can vary from the canonical accepted form, with types and relative amounts potentially depending on the amino acids available to *Mabsc* in the culture medium. Previously, the peptide moiety of the GPL was reported to be non-ribosomally assembled motif of Phe-Thr-Ala-alaninol by *mps1* and *mps2* (Billman-Jacobe et al. 1999). However, GC/MS analysis of the lipids revealed fragmentation patterns not consistent with alaninol leading to our conclusion that the final alaninol can also be replaced by valinol, isoleucinol, or leucinol. As we found this across all four strains, and all media, we believe that this does not reflect our culture conditions, but rather is common in *Mabsc.* Previous studies may have focused on major GPL forms, many of which do contain alaninol.

Complete SCFM2 medium effected changes in fatty acid composition never before seen with the reduction in percentage of tuberculostearic acid in all lipids examined. This effect was reversed by removing DOPC from the medium. We probed the expression of *Mabsc* orthologs of *M. tuberculosis* and *M. chlorophenolicum* genes thought to be responsible for TBSA synthesis (Meena et al. 2013a; Meena et al. 2013b; Shuntaro et al. 2017). However, through qRT-PCR, we were unable to clearly identify a responsible reductase and methyltransferase in *Mabsc*. Promisingly, RNA

sequencing results revealed only four genes differentially expressed between SCFM2 and SCFM2 without DOPC. One of these genes is a potential dehydrogenase/reductase that is worth exploring more for its role in TBSA synthesis.

Comparison to previous work in SCFM2

To validate SCFM2, Turner et al. (2015) studied the nutritionally essential genes of *Pseudomonas aeruginosa* in SCFM2. They found that less than 0.07% of *Pseudomonas aeruginosa* genes were differentially essential genes by using Tn-seq. From this, they concluded that the nutritional availability of the two media (SCFM2 and 10% CF sputum) were similar. We used RNAseq and found a large number of differentially expressed genes between these two media in *Mabsc*. However, differential expression does not indicate the essentiality of genes which was not assessed in our work. Through differential expression, we were able to show that *Mabsc* relies on similar metabolic pathways heavily utilizing amino acids along with the TCA cycle in SCFM2 and CF sputum.

In 2014, Miranda-CasoLuengo et al. published a study functionally characterizing the *Mabsc* transcriptome in various models of host adaptation and persistence. One model they choose was to grow *M. abscessus* subsp. *abscessus* ATCC 19977 in SCFM2 and compare the gene expression to 7H9-ADC-Tween 80. Their study design also significantly differed from this body of work in that they were looking at a short pulse of exposure to SCFM2 (3 hours) with no pre-adaptation to the medium. Despite these differences in study design, we were eager to compare our findings to theirs to both corroborate our findings and to detect changes that may occur when *Mabsc* is grown in SCFM2 for a longer period of time. The files from their study were retrieved from GEO and analyzed with our RNAseq analysis pipeline. However, the samples grown in SCFM2 only mapped to the *Mabsc* genome at rates of 6.7-16.85% instead of the expected mapping rates of 80-100%. Also, their SCFM2 grown samples displayed a lower GC content of 54-55% instead of 57-60% GC content of their samples grown in 7H9-ADC-Tween 80 – samples that mapped at rates of 80-100%. Taken

together these two pieces of data strongly suggested that the SCFM2 samples were contaminated with some other bacterium. Unaligned reads were blasted with NCBI BLASTn. The unaligned reads mapped to *Hydrogenaphaga.* As we struggled greatly to prepare sterile SCFM2, finally resorting to modifying the protocol for preparation of the mucin and DNA, we see this as a realistic conclusion. Despite likely contamination that may have impacted the results, we proceeded to compare our results to theirs. We saw similar upregulation of genes related to amino acid metabolism, pyruvate metabolism, and fatty acid metabolism. However, they found that aerobic respiration was increased which we did not. Also, in the Miranda-CasoLuengo study, MAB_3510c and MAB_3521c were up-regulated -genes whose homologs in *M. tuberculosis* are related to dormancy. These differences in metabolism could be due to likely being in a co-culture environment.

Future work

Although SCFM2 does not, not surprisingly, lead to the exact same bacterial physiology as CF sputum, there are many avenues to continue the study of *Mabsc* in SCFM2. *Mabsc* is a prolific biofilm producer, and likely forms biofilms during colonization of the lungs (Qvist et al. 2014). However, delayed biofilm forming ability has also been associated with increased virulence (Howard et al. 2006). Currently, our lab is characterizing *Mabsc* biofilms and testing biofilm inhibitors using SCFM2. To date, there is no reported way to alter the levels of TBSA in *Mabsc*. Within, we report that the lung surfactant DOPC decreases the relative abundance of TBSA. This could be utilized to characterize the biosynthetic pathway of TBSA in *Mabsc.* Further, our RNAseq results identified only 4 genes differentiating *Mabsc* grown in the presence or absence of DOPC in SCFM2. As one of these genes is a putative reductase, it is plausible that these are the genes or members of the operon responsible for TBSA biosynthesis. The next step is to confirm the expression with qRT-PCR and proceed to construct gene knockouts. As many effective antimycobacterial drugs target cell wall synthesis, identification of this pathway would lead to new drugs for exploration.

This study produced massive data sets on the gene expression profiles of these isolates grown in SCFM2, 7H9-ADC-Tween 80, and 20% CF sputum. Currently, functional enrichment analyses conducted in collaboration with Dr. M. Strong's laboratory at National Jewish Health are examining which, if any, gene families are overrepresented in our differentially expressed genes when compared the functional categories of the entire *Mabsc* genome. Gene network analysis, placing the differentially expressed genes in pathway and networks is also ongoing. These analyses are complicated by the annotation depth of the *Mabsc* genome. A search of a selection of genes against the KEGG database of KEGG orthology (KO) categories assigned to *M. abscessus* subsp. *abscessus* ATCC 19977 revealed that only approximately one third of the genes had been assigned KO categories. Outside of KO categories, even gene products are not fully annotated, with many gene products being annotated as hypothetical protein and unrelated to any gene networks. Work is ongoing at National Jewish Health to improve this annotation. As the annotation improves, our data can be further analyzed to reveal more about the gene networks involved in *Mabsc* adaptation to 7H9-ADC-Tween 80, SCFM2, and CF sputum.

In this study we used 4 isolates, two clustered and two non-clustered as described by Bryant et al. With only two in each group this study did not have the power to clearly typify potential clustered *vs* non-clustered specific responses to changes in growth conditions. Future work using more isolates in each group may lead to the identification of genes contributing to the increased prevalence of these clustered isolates globally.

Supplementary material

MIC testing

Supplementary Table 1: MIC values for isolates from the Bryant et al. (2016) study were tested for their MICs. Green indicates no or <2 fold difference in susceptibility. Orange indicates that the isolate was greater than 2 fold more susceptible in SCFM2 than in MHII.

	M. abscessus subsp. *abscessus ATCC 19977*		*M. abscessus* subsp. *abscessus 1334*		*M. abscessus* subsp. *abscessus OM 91*		*M. abscessus* subsp. *abscessus 1339*		*M. abscessus* subsp. *abscessus OM 200*	
	MHII	SCFM	MHII	SCFM	MHII	SCFM	MHII	SCFM	MHII	SCFM
Amikacin	16	8	64	128	64	128	64	64	8	8
Apramycin	32	32	32	16	8	8	8	8	8	8
Azithromycin	>160	>160	>160	>160	>160	>160	0.625	1.25	>160	>160
Clarithromycin	160	160	80	80	>160	>160	0.625	1.25	40	40
Erythromycin	>256	>256	>256	>256	>256	>256	32	64	>256	>256
Kanamycin	16	8	256	64	128	64	32	16	64	64
Ethambutol	160	80	160	160	80	80	160	320	80	160
Rifampicin	>320	>320	>320	>320	>320	>320	>320	320	5	2.5
Streptomycin	128	64	256	>256	256	256	256	>256	256	128
Cefoxitin	100	50	50	50	100	50	50	25	25	25
Tobramycin	64	32	256	128	256	256	Inconsistent results		64	128
Linezolid	32	64	64	64	128	128	128	128	2	1
Tetracycline	>160	>160	>160	>160	>160	>160	>160	>160	5	5
Imipinem	64	64	64	64	128	128	128	256	128	64
Ciprofloxacin	32	64	32	32	16	16	16	16	>256	>256

	M. abscessus subsp. *massiliense CIP*		*M. abscessus* subsp. *massiliense 1335*		*M. abscessus* subsp. *massiliense OM 130*		*M. abscessus* subsp. *massiliense 1337*		*M. abscessus* subsp. *massiliense OM69*		*M. abscessus* subsp. *massiliense OM 194*	
	MHII	SCFM	MHII	SCFM	MHII	SCFM	MHII	SCFM	MHII	SCFM	MHII	SCFM
Amikacin	128	64	>256	>256	>256	>256	>256	>256	>256	>256	>256	>256
Apramycin	4	4	>256	>256	>256	>256	>256	>256	>256	>256	>256	>256
Azithromycin	1.25	2.5	>160	>160	>160	>160	>160	>160	>160	>160	>160	>160
Clarithromycin	0.078	0.156	>160	>160	>160	>160	>160	>160	>160	>160	>160	>160
Erythromycin	8	8	>256	>256	>256	>256	>256	>256	>256	>256	>256	>256
Kanamycin	8	8	>256	>256	>256	>256	>256	>256	>256	>256	320	320
Ethambutol	160	160	160	160	320	320	160	320	160	160	>320	>320
Rifampicin	>320	>320	>320	>320	>320	>320	80	40	>320	>320	>320	>320
Streptomycin	8	4	>256	256	>256	>256	128	128	256	128	>256	>256
Cefoxitin	50	50	50	50	50	50	25	25	50	50	50	50
Tobramycin	16	16	>256	>256	>256	>256	>256	>256	>256	>256	>256	>256
Linezolid	8	16	64	64	64	64	1	2	32	64	64	64
Tetracycline	20	20	>160	>160	>160	>160	20	20	>160	>160	>160	>160
Imipinem	128	64	64	64	64	64	Inconsistent results		64	64	64	64
Ciprofloxacin	64	64	>256	>256	>256	>256	32	32	64	32	>256	>256

RNAseq analysis summary

Supplementary Table 2: Number of reads remaining after each step in the RNAseq analysis pipeline. The useable reads were taken into DESeq2 for analysis.

Sequence name	Reads before trimming	Sequences remaining after de-duplication levels (before trimming)	Reads after trimming	Sequences remaining after de-duplication levels (after trimming)	1 time % alignment bowtie2	Total alignment bowtie 2	No feature reads	% no feature reads	Useable reads
1239 7H91	10420357	14.74%	10419871	15.92%	82.48%	82.92%	4143217	39.8	3405507
1239 7H92	5848438	17.02%	5848286	18.23%	88.43%	88.92%	2737138	46.8	2018726
1239 7H93	8127114	16.98%	8126760	18.11%	94.90%	95.48%	4204421	51.7	3400945
1239 SCFM 1	13635819	20.46%	13629144	22.69%	93.58%	94.09%	5695829	41.8	7598350
1239 SCFM 2	13158583	21.02%	13151394	23.22%	93.71%	94.21%	5505511	41.9	7324278
1239 SCFM 3	13570241	20.62%	13564905	22.99%	93.76%	94.26%	5534673	40.8	7699359
1239 M63 1	1983948	16.36%	1982988	18.12%	74.69%	75.49%	966072	48.7	816374
1239 M63 2	7020168	8.93%	7015895	10.50%	46.13%	46.33%	1305848	18.6	4260104
1239 M63 3	10060677	6.87%	10060012	8.22%	45.94%	46.07%	1440398	14.3	6007125
1239 CF 2a	14713600	11.17%	14710513	12.47%	97.23%	97.45%	11515407	78.3	3013047
1239 CF 2b	14089311	11.42%	14085943	12.72%	97.38%	97.59%	10931549	77.6	2977554
1239 CF 3	14195420	10.80%	14192694	11.99%	97.33%	97.56%	11336013	79.9	2673399
1239 SCFM no mucin 1	10904140	16.64%	10903738	17.94%	86.79%	87.33%	3659451	33.6	4780239
1239 SCFM no mucin 2	17098154	7.58%	17097894	8.55%	81.23%	81.46%	3988985	23.3	2850361
1239 SCFM no mucin 3	10114096	9.18%	10113954	10.38%	76.54%	76.78%	1772568	17.5	1735789
1239 SCFMno mucin no DOPC1	9971674	15.69%	9970823	16.99%	81.40%	81.95%	2664777	26.7	4290091
1239 SCFMno mucin no DOPC 2	9699677	16.23%	9699052	17.61%	85.76%	86.21%	2922610	30.1	4014957
1239 SCFM no mucin no DOPC 3	9508732	12.89%	9507486	14.12%	87.20%	87.58%	2523980	26.5	2965354
184 7H9 1	20342067	65.05%	20341113	68.79%	95.38%	95.97%	5534060	27.2	13561699
184 7H9 2	22721496	65.87%	22720743	68.12%	95.38%	95.98%	6157414	27.1	15177149
184 7H9 3	20647004	64.19%	20645553	68.20%	95.60%	96.17%	6293043	30.5	13155530
184 SCFM 1	26699941	65.63%	26698916	67.62%	94.57%	95.26%	3670804	13.7	21059312
184 SCFM 2	23981274	65.29%	23979879	67.48%	94.67%	95.33%	3850904	16.1	18402158
184 SCFM 3	21552016	65.40%	21551023	67.74%	94.68%	95.33%	3382708	15.7	16637436
604 7H9 1	21658303	64.73%	21657465	67.90%	95.64%	96.37%	7096178	32.8	13138578
604 7H9 2	22522575	64.81%	22521759	67.45%	95.63%	96.41%	7412219	32.9	13577702
604 7H9 3	22767949	64.10%	22765846	67.49%	95.73%	96.46%	7901539	34.7	13465690
604 SCFM 1	23878370	63.58%	23877559	66.14%	94.35%	95.55%	3876741	16.2	18180586
604 SCFM 2	23312983	64.14%	23312236	66.44%	94.48%	95.62%	3958619	17.0	17568145
604 SCFM 3	22869816	62.89%	22868874	65.54%	94.58%	95.71%	4310007	18.8	16940185
1091 7H9 1	10212861	69.79%	10212843	72.96%	97.14%	99.22%	2458572	24.1	7492184
1091 7H9 2	4728034	63.25%	4727986	75.29%	97.13%	99.15%	1146657	24.3	3418854
1091 7H9 3	9279660	68.81%	9279646	71.14%	97.05%	99.17%	2027942	21.9	7006548
1239 M63 1	1983948	16.36%	1982988	18.12%	74.69%	75.49%	966072	48.7	816374
1239 M63 2	7020168	8.93%	7015895	10.50%	46.13%	46.33%	1305848	18.6	4260104
1239 M63 3	10060677	6.87%	10060012	8.22%	45.94%	46.07%	1440398	14.3	6007125
1091 SCFM 1	13330549	20.27%	13346000	22.52%	98.26%	98.89%	5846090	43.8	7413249
1091 SCFM 2	12772707	20.28%	12764259	22.61%	98.26%	98.89%	5756639	45.1	6908028
1091 SCFM 3	13360213	20.57%	13355672	22.82%	98.01%	98.65%	5657347	42.4	7604907

Structures of GPLs that change based on media

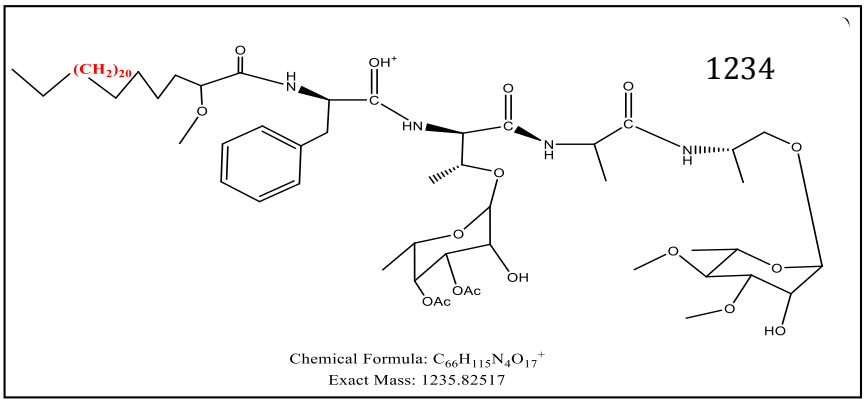

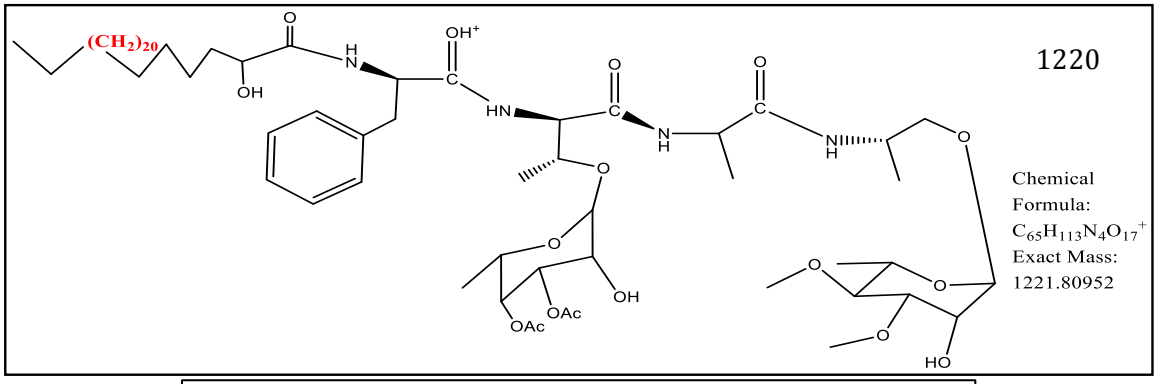

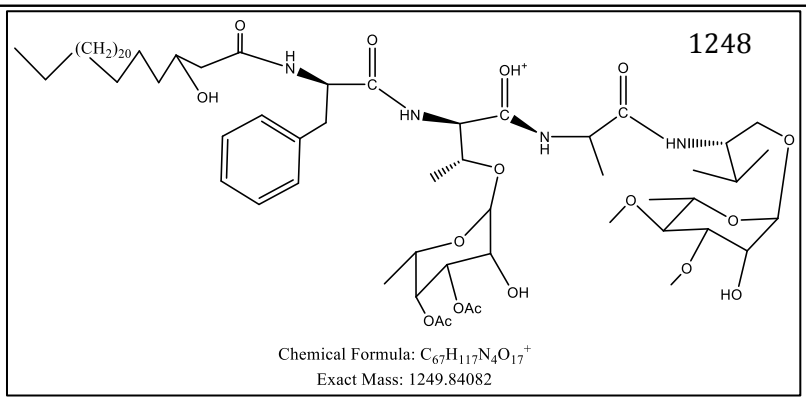

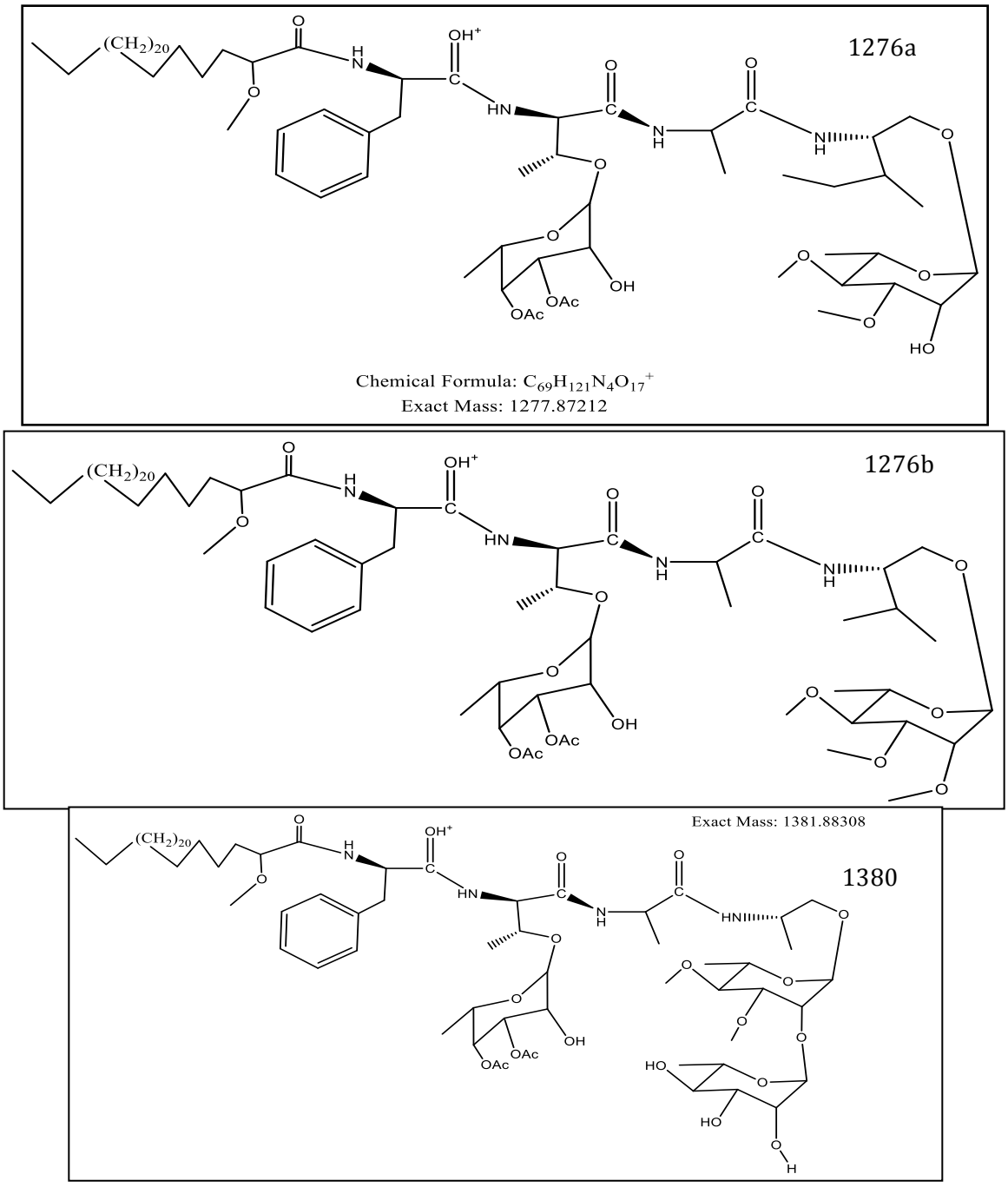

Supplementary Figure 1: The structures of the GPLs that change based on media are shown below by molecular weight. The number they are referred to by in the text is shown in the upper right. 1276b and 1276a have the same exact mass and chemical formula.

Sugar analysis figures

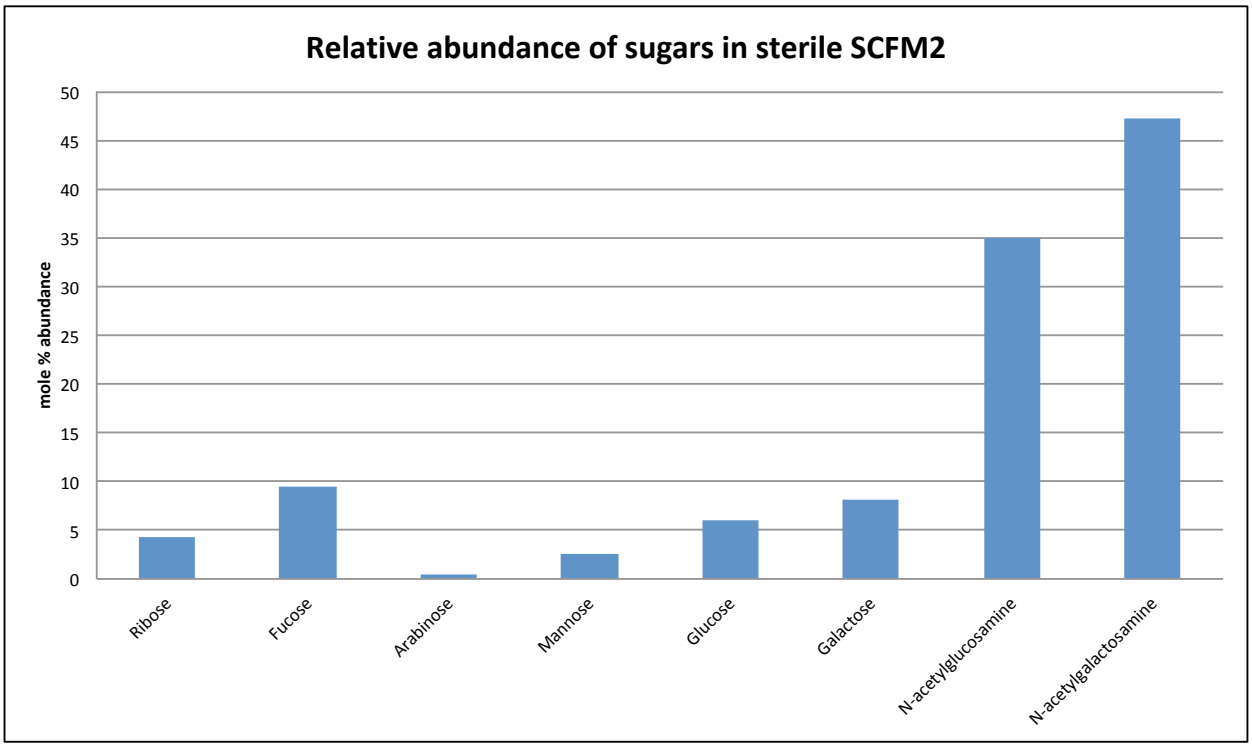

Supplementary Figure 2: Relative abundance of sugars extracted from sterile SCFM2

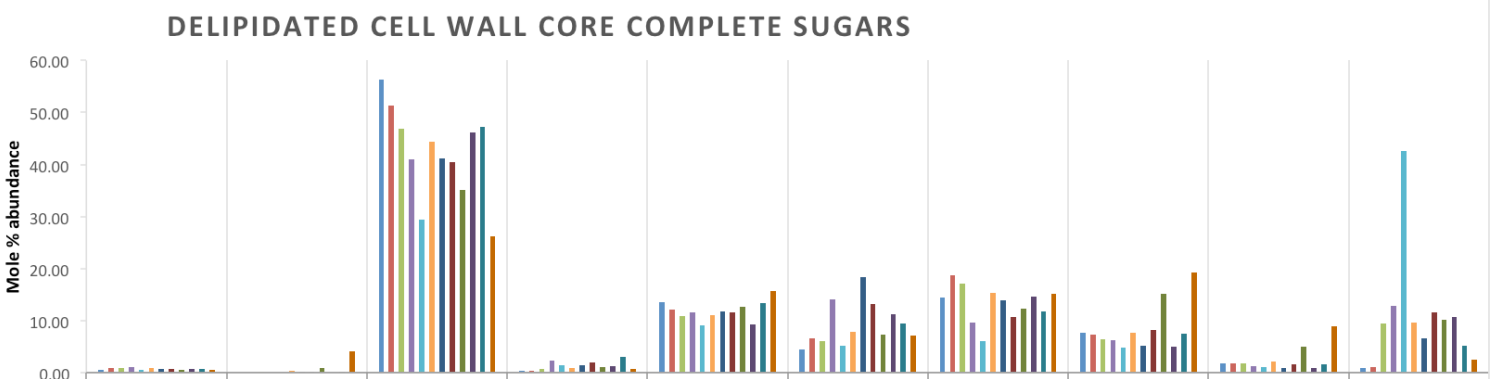

	Rhamnose	Fucose	Arabinose	Myo Insoitol	Mannose	Glucose	Galactose	N-acetylglucosamine	N-acetylgalactosamine	Muramic acid glucosamine
1239 cell wall 7H9	0.49	0.00	56.33	0.39	13.52	4.50	14.51	7.57	1.85	0.83
1239 cell wall SCFM2 without mucin	0.80	0.00	51.41	0.34	12.03	6.60	18.71	7.30	1.74	1.08
1239 cell wall SCFM2	0.87	0.01	46.81	0.63	10.92	6.07	17.07	6.43	1.69	9.50
184 cell wall 7H9	1.12	0.00	40.96	2.31	11.64	14.07	9.64	6.29	1.20	12.77
184 cell wall SCFM2 without mucin	0.44	0.00	29.40	1.38	9.07	5.12	6.07	4.83	1.03	42.67
184 cell wall SCFM2	0.84	0.29	44.38	0.83	11.09	7.84	15.32	7.69	2.16	9.56
604 cell wall 7H9	0.64	0.04	41.15	1.49	11.76	18.39	13.95	5.20	0.83	6.56
604 cell wall SCFM2 without mucin	0.63	0.00	40.54	1.93	11.59	13.24	10.71	8.13	1.64	11.59
604 cell wall SCFM2	0.60	0.84	35.17	1.10	12.61	7.22	12.36	15.09	4.94	10.06
1091 cell wall 7H9	0.77	0.00	46.11	1.32	9.23	11.17	14.68	5.03	0.92	10.77
1091 cell wall SCFM2 without mucin	0.73	0.03	47.17	2.98	13.43	9.51	11.79	7.53	1.63	5.21
1091 cell wall SCFM2	0.54	4.04	26.19	0.77	15.65	7.04	15.13	19.25	8.82	2.57

Supplementary Figure 3: Monosaccharides derived from the cell wall core.
Isolate number and medium it was grown in is shown.

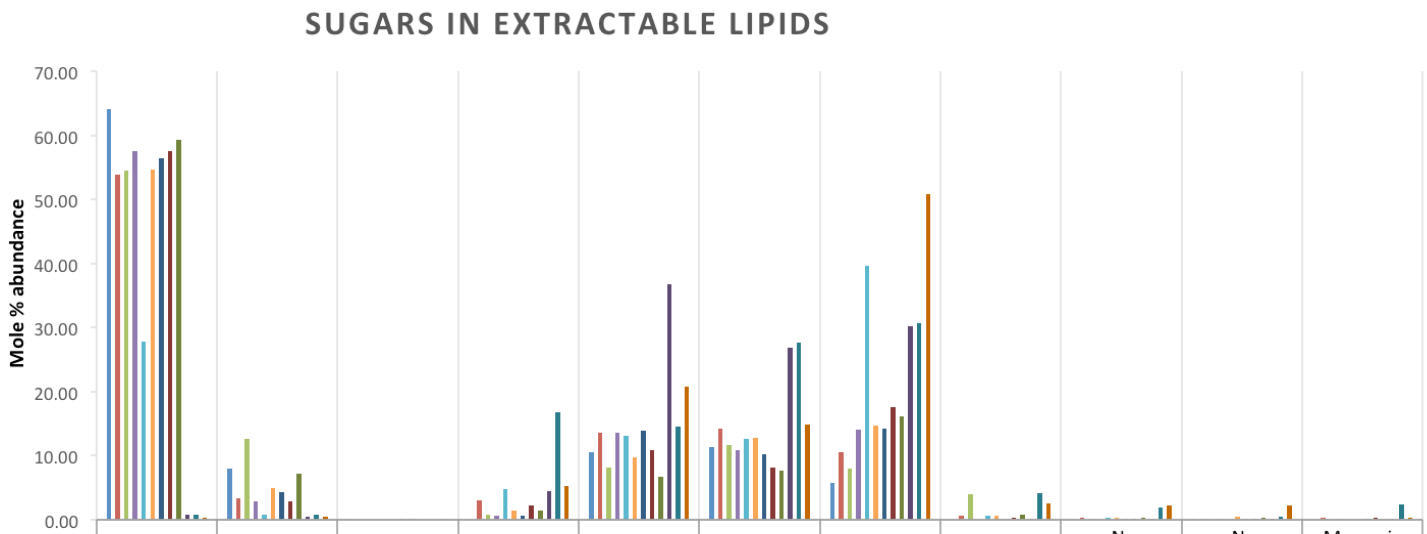

	6-d Tal	Rhamnose	Fucose	Arabinose	Myo Insoitol	Mannose	Glucose	Galactose	N-acetylglucosamine	N-acetylgalactosamine	Muramic acid glucosamine
1239 extractable lipids 7H9	64.16	7.96	0.01	0.03	10.62	11.37	5.70	0.05	0.04	0.03	0.04
1239 extractable lipids SCFM no mucin	53.84	3.41	0.02	3.03	13.57	14.28	10.49	0.67	0.26	0.12	0.31
1239 extractable lipids SCFM + mucin	54.56	12.66	0.03	0.82	8.18	11.62	7.92	3.96	0.13	0.09	0.03
184 extractable lipids 7H9	57.58	2.86	0.01	0.70	13.55	10.91	14.02	0.15	0.09	0.02	0.10
184 extractable lipids SCFM no mucin	27.85	0.85	0.03	4.79	13.08	12.57	39.66	0.68	0.25	0.03	0.20
184 extractable lipids SCFM + mucin	54.66	4.97	0.05	1.47	9.69	12.86	14.77	0.66	0.31	0.40	0.16
604 extractable lipids 7H9	56.45	4.33	0.01	0.62	13.82	10.22	14.24	0.12	0.08	0.04	0.07
604 extractable lipids SCFM no mucin	57.47	2.82	0.03	2.28	10.85	8.14	17.55	0.37	0.21	0.05	0.25
604 extractable lipids SCFM + mucin	59.30	7.14	0.07	1.42	6.78	7.65	16.13	0.71	0.36	0.32	0.12
1091 extractable lipids 7H9	0.76	0.40	0.00	4.51	36.74	26.81	30.18	0.16	0.19	0.05	0.18
1091 extractable lipids SCFM no mucin	0.85	0.74	0.00	16.73	14.48	27.57	30.69	4.12	1.96	0.39	2.46
1091 extractable lipids SCFM + mucin	0.31	0.42	0.15	5.29	20.77	14.85	50.88	2.49	2.27	2.22	0.36

Supplementary Figure 3: Monosaccharides derived from the extractable lipids. Isolate number and medium it was grown in is shown.

Gene expression lists

The following pages contain lists of differentially expressed genes. The first row of every list indicates the isolate and the media that were compared. Some lists are continued on two or three pages. 7H9 refers to 7H9-ADC-Tween 80, SCFM refers to complete SCFM2 unless a component is noted removed i.e. SCFM without mucin is SCFM2 prepared without mucin.

Supplementary Table 3: Genes up-regulated in *M. abscessus* subsp. *massiliense* 1239 in SCFM2 *vs* 7H9-ADC-Tween 80.

M. abscessus subsp. *massiliense 1239* genes upregulated in SCFM *vs* 7H9				
	Gene name	baseMean	log2Fold Change	padj
MAB_0068	Putative transcriptional regulator, GntR family	1302	4.81	4.17E-92
MAB_0069	Major facilitator family transporter	598	4.61	2.532E-47
MAB_0304	Hypothetical protein	94	3.93	0.02893293
MAB_0650	60 kDa chaperonin 2 (Protein Cpn60 2) (GroEL)	93122	3.55	1.6071E-07
MAB_0677c	Conserved hypothetical protein (amino acid metabolite efflux pump?)	166	3.63	7.5237E-10
MAB_0766	Hypothetical conserved integral membrane protein	389	2.73	5.3201E-06
MAB_1125c	Hypothetical acetyltransferase, GNAT family	406	2.98	4.3253E-09
MAB_1184c	Putative transcriptional regulator, MarR family	784	3.75	1.0911E-41
MAB_1185c	Probable enoyl-CoA hydratase	2646	3.98	1.2073E-74
MAB_1186c	3-hydroxyisobutyrate dehydrogenase	1734	3.80	2.1031E-47
MAB_1187c	Probable enoyl-CoA hydratase	2836	3.71	2.7898E-78
MAB_1188c	Probable acyl-CoA dehydrogenase	3497	4.99	3.955E-211
MAB_1189c	Probable methylmalonic acid semialdehyde dehydrogenase MmsA	4268	4.14	4.678E-150
MAB_1274	Putative ABC transporter, permease protein	332	2.75	1.1732E-05
MAB_1296	hypothetical protein	353	2.64	0.00285476
MAB_1330	1-pyrroline-5-carboxylate dehydrogenase	12945	2.71	8.2043E-30
MAB_1331	Probable proline dehydrogenase	4506	3.00	5.1112E-30
MAB_1409c	Putative drug antiporter protein precursor	346	2.45	0.03394732
MAB_2122	Putative peptide synthetase MbtE	283	2.78	3.8298E-05
MAB_2157	Probable acyl-[acyl-carrier protein] desaturase	954	3.69	1.5737E-47
MAB_2233c	hypothetical protein	319	2.64	0.00046853
MAB_2234c	Conserved hypothetical protein (AAA ATPase?)	492	2.74	9.5378E-08
MAB_2273	Putative MFS transporter	674	3.16	3.6955E-21
MAB_2355c	Putative ABC transporter ATP-binding protein	1256	2.97	1.2413E-23
MAB_2886c	Hypothetical protein	185	2.66	0.04260873
MAB_2989	Probable chloramphenicol acetyltransferase	352	2.54	0.00741598
MAB_3100	L-alanine dehydrogenase (ALD)	17390	3.53	8.3938E-55
MAB_3101c	hypothetical protein	5112	4.07	1.091E-103
MAB_3385	hypothetical protein	401	4.05	2.2266E-29
MAB_3386c	hypothetical protein	1375	4.93	3.378E-111
MAB_3387	Putative GntR-family regulatory protein	648	2.44	0.00164149
MAB_3467c	18 kDa antigen (HSP 16.7)	4148	3.53	2.4879E-85
MAB_3548c	Putative fatty acid desaturase	1503	4.12	8.5259E-90
MAB_3646c	Probable aminotransferase class-III	827	3.59	3.4906E-40
MAB_3731c	60 kDa chaperonin 1 (GroEL protein 1)	4517	3.47	2.7395E-63
MAB_3732c	10 kDa chaperonin (GroES)	54549	2.90	8.2625E-33
MAB_3762	hypothetical protein	651	4.61	4.1809E-54
MAB_3840	hypothetical protein	1620	6.05	1.505E-136
MAB_3841	Ornithine aminotransferase RocD1	799	5.17	5.8878E-74
MAB_4272c	Protein GrpE (HSP-70 cofactor)	1415	2.75	8.7767E-09
MAB_4273c	Chaperone protein DnaK (Hsp 70)	4616	2.66	0.00038702
MAB_4324c	Putative acetyltransferase, GNAT	1635	2.68	5.2401E-13
MAB_4407c	Putative alkylhydroperoxidase AhpD	343	2.75	4.4815E-06
MAB_4532c	hypothetical protein	5221	2.32	9.1743E-06
MAB_4538c	Putative acyl-CoA dehydrogenase FadE	1697	4.70	1.68E-125
MAB_4539c	Putative acyl-CoA carboxylase alpha subunit AccA	1916	5.14	4.27E-153
MAB_4540c	Putative acetyl-CoA carboxylase beta subunit AccD	1452	4.84	2.623E-114
MAB_4742c	hypothetical protein	7567	4.11	3.755E-194
MAB_4743c	Putative dehydrogenase/reductase	15696	6.78	0
MAB_4744c	hypothetical protein	4881	7.33	7.227E-292
MAB_4745	Putative membrane protein, MmpS	1098	7.05	1.9056E-80
MAB_4746	Putative membrane protein, MmpL	3190	6.61	4.974E-226
MAB_4747	hypothetical protein	1681	3.98	4.5398E-70
MAB_4748c	Conserved hypothetical protein (pyridoxamine 5'-phosphate oxidase?)	661	3.19	8.303E-18
MAB_4915c	hypothetical protein	208	3.13	7.7977E-07
MAB_4916c	Probable branched-chain keto acid dehydrogenase E2 component BkdC	4282	3.77	3.646E-116
MAB_4917c	Probable branched-chain keto acid dehydrogenase E1 component, beta subunit BkdB	4077	3.66	3.949E-101
MAB_4918c	Probable branched-chain keto acid dehydrogenase E1 component, alpha subunit BkdA	6343	3.31	5.1407E-81
MAB_4919	Putative transcriptional regulator, AsnC family	215	2.61	0.01520853

Supplementary Table 4: Genes down-regulated in *M. abscessus* subsp. *massiliense* 1239 in SCFM2 *vs* 7H9-ADC-Tween 80.

M. abscessus subsp. *massiliense 1239* genes downregulated in SCFM *vs* 7H9				
	Gene_name	baseMean	log2Fold Change	padj
MAB_0262	Probable amino acid ABC transporter, ATP-binding	1289	-2.34	0.0008693
MAB_1314	Hypothetical protein	576	-2.87	4.4614E-06
MAB_1427c	Putative cytochrome P450	2838	-2.74	3.5398E-23
MAB_1627	Conserved hypothetical protein (ComEC/Rec2-related protein?)	142	-3.80	5.233E-17
MAB_1628c	hypothetical protein	638	-3.69	1.1573E-55
MAB_1925	hypothetical protein	3065	-4.23	1.0132E-45
MAB_1926	Putative transcriptional regulatory protein PrrA	661	-3.42	0.00024412
MAB_2047c	Probable ferredoxin reductase	4535	-2.67	3.6729E-21
MAB_2048c	Probable cytochrome P450	10333	-3.12	5.6789E-55
MAB_2049c	Probable ferredoxin	2218	-2.93	1.3507E-31
MAB_2512	Conserved hypothetical protein (sulfate transporter/antisigma-factor antagonist STAS?)	4539	-3.58	7.0487E-94
MAB_2601	Hypothetical protein	154	-3.12	8.3429E-09
MAB_2792c	Probable aldehyde dehydrogenase	914	-2.52	5.605E-08
MAB_3370	Putative branched-chain amino acid transport protein	888	-2.96	8.2298E-20
MAB_3371c	hypothetical protein	2593	-3.21	3.856E-25
MAB_4114	hypothetical protein	13049	-2.51	6.7257E-09
MAB_4456	Putative cytochrome P450	692	-3.16	1.1178E-28
MAB_4683c	Hypothetical protein	4826	-2.48	4.9665E-05

Supplementary Table 5: Genes up-regulated in *M. abscessus* subsp. *massiliense* 604 in SCFM2 *vs* 7H9-ADC-Tween 80.

M. abscessus subsp. *massiliense 604* genes upregulated in SCFM *vs* 7H9				
	gene_function	baseMean	log2Fold Change	padj
MAB_0068	Putative transcriptional regulator, GntR family	983	3.13	9.32E-37
MAB_0069	Major facilitator family transporter	818	3.46	1.34E-51
MAB_0547c	Putative iron compound ABC transporter, substrate-binding protein	560	2.81	5.48E-14
MAB_0551	hypothetical protein	11355	2.62	1.18E-60
MAB_1041	hypothetical protein	2535	3.40	4.06E-135
MAB_1174c	Probable acyl-CoA synthase FadD	1169	2.60	5.53E-16
MAB_1187c	Probable enoyl-CoA hydratase	5836	2.13	0.0203627
MAB_1188c	Probable acyl-CoA dehydrogenase	2130	2.84	2.05E-45
MAB_1189c	Probable methylmalonic acid semialdehyde dehydrogenase	6405	2.89	9.64E-110
MAB_1330	1-pyrroline-5-carboxylate dehydrogenase	57677	4.19	0
MAB_1331	Probable proline dehydrogenase	18769	4.23	3.23E-141
MAB_2264c	Probable hydroxylase/dioxygenase	769	2.37	0.00050365
MAB_2489	hypothetical protein	37633	2.63	2.45E-79
MAB_2490	hypothetical protein	5068	2.54	9.82E-38
MAB_2958	Putative transmembrate-transport protein	5421	3.53	7.14E-62
MAB_2959	putative acetyltransferase	1242	3.18	1.10E-54
MAB_3100	L-alanine dehydrogenase (ALD)	112426	6.46	1.36E-38
MAB_3101c	hypothetical protein	23950	5.58	3.01E-61
MAB_3132c	hypothetical protein	18212	3.73	0
MAB_3133c	Putative flavohemoprotein	225608	3.31	0
MAB_3153c	hypothetical protein	100	2.91	0.00956248
MAB_3154c	hypothetical protein	232	3.00	3.09E-08
MAB_3180	hypothetical protein	184	3.45	7.11E-12
MAB_3354	Probable acyl-[acyl-carrier protein] desaturase DesA1	51194	3.42	2.52E-97
MAB_3369	Putative integral membane amino acid transport protein	695	4.76	8.34E-86
MAB_3486	Probable acyl-CoA dehydrogenase	16794	2.78	5.38E-82
MAB_3487	Probable acyl-CoA dehydrogenase	35913	3.04	7.60E-175
MAB_3645	Putative reductase	5745	5.74	3.08E-29
MAB_3646c	Probable aminotransferase class-III	111101	7.93	6.87E-08
MAB_3647c	Probable transcriptional regulatory protein	10335	3.98	0
MAB_3648	hypothetical protein	22189	6.44	7.65E-67
MAB_3649	Probable aldehyde dehydrogenase	77549	6.49	5.86E-48
MAB_3650	Putative TetR-family transcriptional regulator	5443	3.76	0
MAB_3762	hypothetical protein	615	2.39	0.00090684
MAB_3834c	Possible L-lactate dehydrogenase (cytochrome) LldD1	9009	2.15	0.00012894
MAB_3840	hypothetical protein	15865	7.04	2.26E-23
MAB_3841	Ornithine animotransferase RocD1	8575	5.40	2.39E-297
MAB_3842	Probable cationic amino acid transport integral membrane protein	7182	2.15	0.00159434
MAB_3902c	hypothetical protein	4179	2.51	1.02E-27
MAB_3903	hypothetical protein	5419	2.89	5.20E-102
MAB_3904	hypothetical protein	1609	3.21	1.87E-70
MAB_3937	hypothetical protein	7481	3.61	0
MAB_3938	Putative Clp protease subunit	4337	3.51	1.84E-209
MAB_4407c	Putative alkylhydroperoxidase AhpD	1170	2.60	2.42E-13
MAB_4408c	Putative alkylhydroperoxidase C	3165	2.47	1.44E-21
MAB_4538c	Putative acyl-CoA dehydrogenase FadE	2260	3.41	5.87E-105
MAB_4539c	Putative acyl-CoA carboxylase alpha subunit AccA	2563	3.67	3.65E-157
MAB_4540c	Putative acetyl-CoA carboxylase beta subunit AccD	3070	4.02	2.87E-258
MAB_4623c	5-methyltetrahydropteroyltriglutamate--homocysteine S-methyltransferase	3182	2.93	1.87E-72
MAB_4724	Sodium/calcium exchanger family protein	444	2.94	6.83E-14
MAB_4741c	Putative terminal quinol oxidase, subunit 1	1298	2.43	1.10E-07
MAB_4742c	hypothetical protein	22159	5.30	3.21E-74
MAB_4743c	Putative dehydrogenase/reductase	43903	7.25	1.13E-10
MAB_4744c	hypothetical protein	30041	7.64	8.41E-11
MAB_4745	Putative membrane protein, MmpS	5033	7.96	2.46E-08
MAB_4746	Putative membrane protein, MmpL	42220	7.97	2.57E-09
MAB_4747	hypothetical protein	6329	4.79	0
MAB_4748c	Conserved hypothetical protein (pyridoxamine 5'phosphate oxidase?)	1111	3.16	3.97E-49
MAB_4915c	hypothetical protein	589	2.78	1.43E-13
MAB_4916c	Probable branched-chain keto acid dehydrogenase E2 component BkdC	14908	5.02	1.80E-43
MAB_4917c	Probable branched-chain keto acid dehydrogenase E1 component, beta subunit BkdB	3540	4.97	5.64E-34
MAB_4918c	Probable branched-chain keto acid dehydrogenase E1 component, alpha subunit BkdA	4340	5.06	6.06E-94

Supplementary Table 6: Genes down-regulated in *M. abscessus* subsp. *massiliense* 604 in SCFM2 *vs* 7H9-ADC-Tween 80.

M. abscessus subsp. massiliense 604 genes downregulated in SCFM *vs* 7H9				
	gene_function	baseMean	log2Fold Change	padj
MAB_0741c	hypothetical protein	1712	-3.22	4.02E-78
MAB_1031c	Probable manganese transport protein MntH	4507	-4.38	0
MAB_1662c	Probable sulfite reductase [ferredoxin]	3792	-2.26	1.88E-08
MAB_2165	Probable acetolactate synthase, large subunit	247	-2.62	0.00083494
MAB_2166	hypothetical protein	740	-2.40	4.70E-05
MAB_2167	Putative 2-oxoacyl-ACP synthase III	767	-2.42	1.65E-05
MAB_2599	Hypothetical protein	331	-2.96	1.48E-11
MAB_2693	hypothetical protein	416	-6.39	4.14E-56
MAB_3689	Putative methyltransferase	724	-2.32	0.00495888
MAB_3881	Cyclopropane-fatty-acyl-phospholipid synthase 1	3389	-2.27	6.05E-06
MAB_4714c	Probable fatty-acid-coa ligase FadD	11948	-3.21	7.91E-299
MAB_4715c	hypothetical protein	13747	-7.16	0
MAB_4716c	Possible membrane transport protein	817	-3.89	2.09E-77

Supplementary Table 7: Genes up-regulated in *M. abscessus* subsp. *abscessus* 1091 in SCFM2 *vs* 7H9-ADC-Tween 80. (Continued on two pages)

M. abscessus subsp. *abscessus* 1091 genes upregulated in SCFM *vs* 7H9				
Gene_id	Gene Product	baseMean	log2Fold Change	padj
MAB_0325c	Hypothetical protein	190	3.11	2.7511E-08
MAB_0899c	Possible ethyl tert-butyl ether degradation protein EthD	2409	2.24	0.0059103
MAB_0902	Probable beta-ketoadipyl-CoA thiolase	1425	2.60	7.5472E-14
MAB_0903	Putative enoyl-CoA hydratase/isomerase	522	2.37	0.00995192
MAB_0905	Putative enoyl-CoA hydratase/isomerase	1219	2.36	0.00030396
MAB_0906	Putative phenylacetic acid degradation protein PaaA/phenylacetate-CoA oxygenase, PaaG subunit	1548	2.76	9.5405E-22
MAB_0907	Putative phenylacetic acid degradation protein PaaB/phenylacetate-CoA oxygenase, PaaH subunit	501	2.44	0.00113906
MAB_0908	Putative phenylacetic acid degradation protein PaaC/phenylacetate-CoA oxygenase, PaaI subunit	1087	2.44	2.8666E-06
MAB_0911	Putative phenylacetate-CoA ligase	922	2.39	5.4228E-05
MAB_0964	hypothetical protein	574	2.49	3.9794E-05
MAB_0968c	Luciferase-like hypothetical protein	2936	2.77	1.0688E-29
MAB_1029c	Putative transcriptional regulator, MarR family	644	2.45	6.2981E-05
MAB_1030	hypothetical protein	6442	2.36	8.0256E-10
MAB_1184c	Putative transcriptional regulator, MarR family	412	2.70	1.4937E-07
MAB_1185c	Probable enoyl-CoA hydratase	1603	2.25	0.00651268
MAB_1186c	3-hydroxyisobutyrate dehydrogenase	998	2.28	0.03538566
MAB_1187c	Probable enoyl-CoA hydratase	1505	2.32	0.00012211
MAB_1188c	Probable acyl-CoA dehydrogenase	1560	3.35	4.462E-60
MAB_1189c	Probable methylmalonic acid semialdehyde dehydrogenase MmsA	2211	2.84	7.4426E-31
MAB_1271c	Probable oxidase (copper-binding protein)	275	2.80	1.9651E-06
MAB_1330	1-pyrroline-5-carboxylate dehydrogenase	24682	4.62	0
MAB_1331	Probable proline dehydrogenase	8597	4.24	2.664E-305
MAB_1332	Probable fatty-acid-CoA ligase FadD	2477	2.68	6.6988E-27
MAB_1528c	Probable oxidoreductase	504	2.60	1.3622E-06
MAB_1766	Hypothetical protein	198	3.37	1.588E-10
MAB_1767	Hypothetical protein	468	2.71	4.5291E-08
MAB_1769	Hypothetical protein	379	2.77	3.6103E-08
MAB_1913	Conserved hypothetical protein (ribonuclease?)	195281	3.22	3.1311E-17
MAB_1916c	3-methyl-2-oxobutanoate hydroxymethyltransferase	2971	2.73	8.7319E-31
MAB_1923c	hypothetical protein	760	2.77	3.6102E-15
MAB_2122	Putative peptide synthetase MbtE	505	2.83	1.8781E-11
MAB_2157	Probable acyl-[acyl-carrier protein] desaturase	4926	2.38	6.1943E-09
MAB_2232c	Putative FtsK/SpoIIIE family protein	1776	2.57	1.4058E-14
MAB_2233c	hypothetical protein	412	3.43	2.07E-24
MAB_2234c	Conserved hypothetical protein (AAA ATPase?)	536	3.64	2.8332E-36
MAB_2248	Probable peptide synthetase MbtE	253	3.08	8.6369E-10
MAB_2249	Probable lysine-N-oxygenase MbtG	180	3.45	3.5381E-11
MAB_2273	Putative MFS transporter	676	2.47	2.1144E-05
MAB_2379	Hypothetical lipoprotein LpqH precursor	2301	2.47	3.1849E-09
MAB_2605c	hypothetical protein	230	2.62	0.00116008
MAB_2606c	Putative transcriptional regulator, TetR family	75	3.01	0.0090611
MAB_2886c	Hypothetical protein	413	3.03	8.2234E-13
MAB_3016c	hypothetical protein	128	3.17	4.3911E-06
MAB_3099c	Putative transcriptional regulator, AsnC family	215	2.61	0.00207069
MAB_3100	L-alanine dehydrogenase (ALD)	15505	6.11	0
MAB_3101c	hypothetical protein	4379	4.66	3.101E-278
MAB_3151	Putative TetR-family transcriptional regulator	63	3.38	0.00066117
MAB_3369	Putative integral membrane amino acid transport protein	297	3.27	3.6102E-15
MAB_3370	Putative branched-chain amino acid transport protein	49	3.54	0.00159357
MAB_3371c	hypothetical protein	133	2.94	0.00018408
MAB_3385	hypothetical protein	1265	5.54	2.534E-140
MAB_3386c	hypothetical protein	1362	5.78	1.665E-148
MAB_3438	Putative short-chain dehydrogenase/reductase	246	3.30	2.0086E-11
MAB_3464	Hypothetical protein	104	2.81	0.00925031
MAB_3465	Putative sulfate transporter/antisigma-factor	1090	3.76	1.7721E-68

M. abscessus subsp. *abscessus* 1091 genes upregulated in SCFM *vs* 7H9 continued				
MAB_3466c	Hypothetical protein	746	5.49	2.4586E-85
MAB_3467c	18 kDa antigen (HSP 16.7)	6797	4.67	5.97E-298
MAB_3509c	Hypothetical protein	2983	2.79	8.3708E-07
MAB_3548c	Putative fatty acid desaturase	6570	2.49	2.5931E-19
MAB_3617	hypothetical protein	425	2.48	0.00082441
MAB_3645	Putative reductase	654	4.10	1.3791E-56
MAB_3646c	Probable aminotransferase class-III	8316	8.42	0
MAB_3647c	Probable transcriptional regulatory protein	2147	4.22	1.14E-148
MAB_3648	hypothetical protein	1997	5.55	2.402E-207
MAB_3649	Probable aldehyde dehydrogenase	8952	5.60	0
MAB_3650	Putative TetR-family transcriptional regulator	1115	3.19	3.1341E-41
MAB_3730c	Hypothetical protein	85	3.02	0.00227179
MAB_3731c	60 kDa chaperonin 1 (GroEL protein 1)	6447	2.39	9.8398E-10
MAB_3732c	10 kDa chaperonin (GroES)	27656	2.56	1.5776E-19
MAB_3762	hypothetical protein	790	2.36	0.00094118
MAB_3840	hypothetical protein	4596	8.32	2.153E-268
MAB_3841	Ornithine aminotransferase RocD1	5682	7.07	0
MAB_3842	Probable cationic amino acid transport integral membrane protein	2171	3.45	1.1621E-89
MAB_3843	hypothetical protein	1229	2.73	2.8367E-19
MAB_4357c	Putative monooxygenase	210	2.97	7.7642E-07
MAB_4402	Heat shock protein Hsp20	1295	4.99	6.3749E-21
MAB_4407c	Putative alkylhydroperoxidase AhpD	1102	3.91	1.619E-76
MAB_4408c	Putative alkylhydroperoxidase C	1338	3.49	8.7704E-59
MAB_4412c	Putative decarboxylase	328	2.46	0.00613853
MAB_4415	Probable amidase	597	2.69	2.8446E-10
MAB_4416c	hypothetical protein	501	3.02	1.5317E-16
MAB_4417c	Probable aminotransferase	1106	2.91	3.5002E-26
MAB_4418	Succinate-semialdehyde dehydrogenase	539	2.74	8.4601E-10
MAB_4419	Tartrate dehydrogenase	685	3.32	3.7933E-31
MAB_4538c	Putative acyl-CoA dehydrogenase FadE	1771	4.57	3.881E-145
MAB_4539c	Putative acyl-CoA carboxylase alpha subunit AccA	1406	4.82	4.34E-140
MAB_4540c	Putative acetyl-CoA carboxylase beta subunit AccD	1037	5.17	5.691E-114
MAB_4621c	Putative acetyltransferase	204	2.60	0.0047042
MAB_4622c	hypothetical protein	1048	2.77	6.162E-19
MAB_4623c	5-methyltetrahydropteroyltriglutamate--homocysteine S-methyltransferase	4028	2.73	1.2795E-28
MAB_4663	Hypothetical protein	69	4.43	2.7303E-07
MAB_4664	Hypothetical protein	116	2.75	0.01316889
MAB_4682c	Hypothetical protein	120	4.53	1.2838E-13
MAB_4683c	Hypothetical protein	83	3.07	0.00169549
MAB_4694c	Glycosyltransferase	1089	2.58	1.5231E-10
MAB_4695c	Putative glycosyltransferase/rhamnosyltransferase	1576	2.44	4.0714E-09
MAB_4699c	hypothetical protein	823	2.35	0.00169421
MAB_4735	Putative starvation-induced DNA protecting protein/Ferritin and Dps	274	3.61	0.00279754
MAB_4736	Conserved hypothetical protein (serine/threonine-protein kinase PknE?)	584	2.47	0.00058039
MAB_4737	Putative citrate lyase/aldolase	628	2.38	0.00169549
MAB_4741c	Putative terminal quinol oxidase, subunit I	641	2.60	2.2138E-08
MAB_4742c	hypothetical protein	11014	6.42	0
MAB_4743c	Putative dehydrogenase/reductase	29311	8.57	0
MAB_4744c	hypothetical protein	10058	8.71	1.9911E-66
MAB_4745	Putative membrane protein, MmpS	1477	9.11	3.9997E-67
MAB_4746	Putative membrane protein, MmpL	9058	9.87	2.49E-289
MAB_4747	hypothetical protein	4463	3.99	4.878E-185
MAB_4748c	Conserved hypothetical protein (pyridoxamine 5'-phosphate oxidase?)	1570	5.52	3.395E-167
MAB_4806c	hypothetical protein	2105	3.05	2.0748E-47
MAB_4915c	hypothetical protein	333	4.10	1.1261E-31
MAB_4916c	Probable branched-chain keto acid dehydrogenase E2 component BkdC	5817	4.08	4.889E-266
MAB_4917c	Probable branched-chain keto acid dehydrogenase E1 component, beta subunit BkdB	4324	3.89	2.561E-187
MAB_4918c	Probable branched-chain keto acid dehydrogenase E1 component, alpha subunit BkdA	4329	3.87	1.969E-195

Supplementary Table 8: Genes down-regulated in *M. abscessus* subsp. *abscessus* 1091 in SCFM2 *vs* 7H9-ADC-Tween 80. (Continued on two pages)

M. abscessus subsp. *abscessus* 1091 genes downregulated in SCFM *vs* 7H9				
	Gene name	baseMean	log2Fold Change	padj
MAB_0103	Probable monooxygenase EthA	9797	-2.90	1.0519E-51
MAB_0125c	hypothetical protein	2107	-3.03	9.7992E-55
MAB_0126c	Possible bacterioferritin BfrB	72404	-2.45	7.5679E-26
MAB_0331c	30S ribosomal protein S18	57	-2.86	0.03954531
MAB_0332c	30s ribosomal protein S14.2	51	-3.75	0.04442752
MAB_0334c	50S ribosomal protein L28	29	-4.25	0.00038096
MAB_0335	Probable cobalamin synthesis protein	115	-2.82	0.00056742
MAB_0694	hypothetical protein	1733	-2.62	2.0738E-19
MAB_0741c	hypothetical protein	379	-3.27	1.1355E-23
MAB_0746	Putative phosphate ABC transporter, phosphate-binding protein	3561	-2.37	2.1678E-07
MAB_0753c	Probable tRNA-dihydrouridine synthase	5073	-2.39	5.1275E-13
MAB_0754c	Probable fatty acid desaturase	12941	-2.51	1.6913E-26
MAB_0894c	Putative dihydrolipoamide dehydrogenase (LpdA)	784	-3.53	1.3019E-58
MAB_0895c	Putative dihydrolipoamide s-acetyltransferase component of pyruvate dehydrogenase complex E2	848	-2.58	9.4657E-12
MAB_0896c	Putative pyruvate dehydrogenase E1 component, beta subunit	648	-2.63	8.2782E-10
MAB_0978	Hypothetical protein	996	-2.25	0.0198992
MAB_1005c	Putative MCE family protein	4275	-2.36	2.8654E-10
MAB_1031c	Probable manganese transport protein MntH	1349	-3.26	1.8118E-64
MAB_1237	Possible acyl-[acyl-carrier protein] desaturase DesA2	14400	-2.24	0.00012575
MAB_1368	hypothetical protein	490	-2.54	5.9008E-06
MAB_1567	Probable HNH endonuclease precursor	1710	-2.67	2.4208E-16
MAB_1628c	hypothetical protein	2292	-3.42	4.439E-101
MAB_1659c	CysN/CysC bifunctional enzyme	1337	-2.24	0.01042775
MAB_1661c	Phosphoadenosine phosphosulfate reductase (CysH)	777	-2.80	1.17E-19
MAB_1662c	Probable sulfite reductase [ferredoxin]	1878	-2.93	2.2878E-37
MAB_1876c	Probable propionyl-CoA carboxylase beta chain 6	34018	-2.31	1.1394E-08
MAB_1877c	3-oxoacyl-[acyl-carrier-protein] synthase 1 KasA	94458	-2.56	2.7647E-31
MAB_1878c	acyl carrier protein	40763	-2.70	3.122E-39
MAB_1967c	Probable ubiquinol-cytochrome c reductase iron-sulfur subunit (Rieske iron-sulfur protein)	13751	-2.14	0.04323538
MAB_2322	50S ribosomal protein L35	4433	-2.78	4.6505E-25
MAB_2324	Possible tRNA/rRNA methyltransferase	1019	-2.37	0.00026292
MAB_2489	hypothetical protein	117815	-3.23	2.072E-143
MAB_2490	hypothetical protein	27134	-3.22	3.148E-151
MAB_2491c	hypothetical protein	2428	-3.20	1.7191E-72
MAB_2550c	Probable fatty acid desaturase	1064	-2.76	4.7755E-20
MAB_2551	Hypothetical protein	225	-2.61	0.00041898
MAB_2601	Hypothetical protein	120	-2.66	0.01465118
MAB_2673c	Probable L-aspartate oxidase NadB	3691	-2.31	5.3285E-07
MAB_2675	Conserved hypothetical protein (NUDIX hydrolase?)	1901	-2.63	8.6792E-21
MAB_2693	Hypothetical protein	496	-7.41	1.0845E-63
MAB_2754	hypothetical protein	1325	-2.62	7.2977E-13
MAB_2790c	Probable ethanolamine ammonia-lyase, heavy subunit	300	-3.33	9.125E-21
MAB_2791c	Putative ethanolamine permease	606	-3.63	1.372E-51
MAB_2792c	Probable aldehyde dehydrogenase	1280	-4.96	4.619E-176
MAB_3105c	Hypothetical protease	4005	-2.23	0.00054741
MAB_3132c	hypothetical protein	7136	-3.66	1.095E-187
MAB_3133c	Putative flavohemoprotein	50784	-2.84	8.6184E-33
MAB_3134c	hypothetical protein	5260	-2.76	2.1373E-37
MAB_3294c	3-isopropylmalate dehydratase large subunit	2865	-2.64	1.8343E-27
MAB_3353c	Putative xanthine/uracil/vitamin C permease family protein	375	-2.39	0.01230247
MAB_3354	Probable acyl-[acyl-carrier protein] desaturase DesA1	92855	-4.02	0
MAB_3355	Putative secreted hydrolase	13479	-3.72	6.929E-171

M. abscessus subsp. *abscessus* 1091 genes downregulated in SCFM *vs* 7H9 cont.				
MAB_3358c	Putative acyltransferase	682	-3.75	1.023E-61
MAB_3359c	hypothetical protein	804	-3.15	1.4993E-37
MAB_3483	Putative oxygenase	976	-2.30	0.00427808
MAB_3486	Probable acyl-CoA dehydrogenase	9889	-3.37	1.2097E-81
MAB_3487	Probable acyl-CoA dehydrogenase	14839	-4.61	0
MAB_3531	Probable ATP-dependent DEAD-box RNA helicase	6799	-2.42	7.1113E-11
MAB_3598c	Putative alkane-1-monooxygenase AlkB (fatty acid omega-hydroxylase)	2785	-3.40	2.616E-103
MAB_3687	Probable o-acetylhomoserine sulfhydrylase MetC (homocysteine synthase)	931	-2.94	3.7057E-25
MAB_3688	Homoserine O-acetyltransferase	844	-2.71	6.6882E-17
MAB_3769c	50S ribosomal proein L17	16302	-2.29	0.00034883
MAB_3774c	Translation initiation factor IF-1	5757	-2.30	2.1862E-07
MAB_3820c	50S ribosomal protein L3	14784	-2.22	0.00077067
MAB_3822	Hypothetical protein	311	-2.71	1.2327E-06
MAB_3834c	Possible L-lactate dehydrogenase (cytochrome) LldD1	9481	-2.67	2.234E-39
MAB_3835c	Probable coenzyme PQQ synthesis protein E PqqE	15278	-2.46	8.9982E-19
MAB_3890c	Probable histidine kinase response regulator	15246	-2.63	2.7825E-43
MAB_3891c	Probable transcriptional regulator, LuxR family	31696	-2.91	3.9096E-71
MAB_3903	hypothetical protein	17050	-3.67	6.099E-181
MAB_3904	hypothetical protein	8272	-3.06	8.1221E-48
MAB_3905	Hypothetical protein	394	-3.04	1.057E-15
MAB_3931c	Probable glycosyl transferase	781	-2.79	1.1173E-17
MAB_4437	Probable acyl-CoA dehydrogenase FadE	23287	-2.42	1.1093E-18
MAB_4906	Putative transcriptional regulator, PadR family	1727	-2.92	5.1719E-43
MAB_r5052	23S ribosomal RNA	68161	-3.38	0.03658997
MAB_t5044c	tRNA-Met(CAT)	122	-2.60	0.04422492

Supplementary Table 9: Genes up-regulated in *M. abscessus* subsp. *abscessus* 184 in SCFM2 *vs* 7H9-ADC-Tween 80.

M. abscessus subsp. *abscessus 184* genes upregulated in SCFM *vs* 7H9				
Gene_id	Gene Product	baseMean	log2Fold Change	padj
MAB_0068	Putative transcriptional regulator, GntR family	1473	2.92	2.215E-49
MAB_0069	Major facilitator family transporter	922	3.02	1.589E-37
MAB_0547c	Putative iron compound ABC transporter, substrate-binding protein	876	3.35	2.102E-55
MAB_0548c	Putative iron compound ABC transporter, ATP-binding protein	152	3.66	9.865E-13
MAB_0549c	Putative heme/hemin ABC transporter, permease protein	733	3.58	2.102E-55
MAB_0551	hypothetical protein	10781	2.90	2.69E-187
MAB_1330	1-pyrroline-5-carboxylate dehydrogenase	53026	3.81	0
MAB_1331	Probable proline dehydrogenase	16167	3.74	0
MAB_2958	Putative transmembrate-transport protein	5391	3.00	5.04E-155
MAB_2959	putative acetyltransferase	949	2.87	6.596E-30
MAB_3100	L-alanine dehydrogenase (ALD)	99143	6.88	0
MAB_3101c	hypothetical protein	26988	6.05	0
MAB_3132c	hypothetical protein	5963	3.75	0
MAB_3133c	Putative flavohemoprotein	81924	3.61	1.34E-106
MAB_3153c	hypothetical protein	226	3.17	8.645E-12
MAB_3154c	hypothetical protein	502	3.23	6.559E-28
MAB_3180	hypothetical protein	233	3.31	2.075E-14
MAB_3369	Putative integral membane amino acid transport protein	597	3.61	4.032E-46
MAB_3645	Putative reductase	7416	6.67	0
MAB_3646c	Probable aminotransferase class-III	86753	9.03	0
MAB_3647c	Probable transcriptional regulatory protein	8625	3.61	0
MAB_3648	hypothetical protein	15820	6.35	0
MAB_3649	Probable aldehyde dehydrogenase	50115	6.40	0
MAB_3650	Putative TetR-family transcriptional regulator	6299	4.17	0
MAB_3762	hypothetical protein	1754	3.41	7.77E-113
MAB_3840	hypothetical protein	12943	7.39	0
MAB_3841	Ornithine animotransferase RocD1	6164	5.15	0
MAB_3842	Probable cationic amino acid transport integral membrane protein	6813	2.37	3.446E-30
MAB_3937	hypothetical protein	2417	3.46	5.98E-156
MAB_3938	Putative Clp protease subunit	1471	2.65	1.261E-26
MAB_4538c	Putative acyl-CoA dehydrogenase FadE	3457	3.65	3.88E-254
MAB_4539c	Putative acyl-CoA carboxylase alpha subunit AccA	3194	4.08	0
MAB_4540c	Putative acetyl-CoA carboxylase beta subunit AccD	2882	4.41	0
MAB_4742c	hypothetical protein	19038	5.58	0
MAB_4743c	Putative dehydrogenase/reductase	53606	8.25	0
MAB_4744c	hypothetical protein	24408	8.53	0
MAB_4745	Putative membrane protein, MmpS	2808	7.73	2.77E-235
MAB_4746	Putative membrane protein, MmpL	25301	8.33	0
MAB_4747	hypothetical protein	11325	4.96	0
MAB_4748c	Conserved hypothetical protein (pyridoxamine 5'phosphate oxidase?)	2167	3.56	5.67E-150
MAB_4915c	hypothetical protein	996	4.10	1.19E-104
MAB_4916c	Probable branched-chain keto acid dehydrogenase E2 component BkdC	13709	5.19	0
MAB_4917c	Probable branched-chain keto acid dehydrogenase E1 component, beta subunit BkdB	4942	5.26	0
MAB_4918c	Probable branched-chain keto acid dehydrogenase E1 component, alpha subunit BkdA	5609	5.23	0

Supplementary Table 10: Genes down-regulated in *M. abscessus* subsp. *abscessus* 184 in SCFM2 *vs* 7H9-ADC-Tween 80.

M. abscessus subsp. a*bscessus* 184 genes downregulated in SCFM *vs* 7H9				
Gene_id	Gene product	baseMean	log2Fold Change	padj
MAB_1031c	Probable manganese transport protein MntH	6198	-3.80	0
MAB_2048c	Probable cytochrome P450	11859	-2.27	4E-13
MAB_2049c	Probable ferredoxin	1619	-2.64	8.79E-28
MAB_2165	Probable acetolactate synthase, large subunit	520	-3.24	5.06E-33
MAB_2166	hypothetical protein	814	-2.87	2.91E-27
MAB_2167	Putative 2-oxoacyl-ACP synthase III	994	-2.82	1.53E-29
MAB_2168	Putative aminotransferase	808	-2.55	9.48E-12
MAB_2693	hypothetical protein	486	-5.60	1.5E-79
MAB_3689	Putative methyltransferase	669	-2.31	0.00348071
MAB_4715c	hypothetical protein	2535	-4.63	0

Gene expression comparison lists

The following pages show the gene comparison lists referenced in the text and the corresponding KEGG categories assigned by KEGG mapper. The first row shows the condition and medium being compared.

Supplementary Table 11: Genes up-regulated by *M. abscessus* subsp. *massiliense* 1239 when grown in SCFM2 but not CF sputum when compared to 7H9-ADC-Tween-80.

M. abscessus subsp. *massiliense 1239* genes upregulated in SCFM but not CF sputum compared to 7H9	
Gene_id	Gene Product
MAB_0069	Major facilitator family transporter
MAB_0650	60 kDa chaperonin 2 (Protein Cpn60 2) (GroEL)
MAB_0677c	Conserved hypothetical protein (amino acid metabolite efflux pump?)
MAB_0766	Hypothetical conserved integral membrane protein
MAB_1125c	Hypothetical acetyltransferase, GNAT family
MAB_1184c	Putative transcriptional regulator, MarR family
MAB_1185c	Probable enoyl-CoA hydratase
MAB_1186c	3-hydroxyisobutyrate dehydrogenase
MAB_1187c	Probable enoyl-CoA hydratase
MAB_1188c	Probable acyl-CoA dehydrogenase
MAB_1189c	Probable methylmalonic acid semialdehyde dehydrogenase MmsA
MAB_1274	Putative ABC transporter, permease protein
MAB_1296	hypothetical protein
MAB_1330	1-pyrroline-5-carboxylate dehydrogenase
MAB_1331	Probable proline dehydrogenase
MAB_1409c	Putative drug antiporter protein precursor
MAB_2233c	hypothetical protein
MAB_2234c	Conserved hypothetical protein (AAA ATPase?)
MAB_2273	Putative MFS transporter
MAB_2355c	Putative ABC transporter ATP-binding protein
MAB_2886c	Hypothetical protein
MAB_2989	Probable chloramphenicol acetyltransferase
MAB_3100	L-alanine dehydrogenase (ALD)
MAB_3101c	hypothetical protein
MAB_3385	hypothetical protein
MAB_3386c	hypothetical protein
MAB_3387	Putative GntR-family regulatory protein
MAB_3731c	60 kDa chaperonin 1 (GroEL protein 1)
MAB_3732c	10 kDa chaperonin (GroES)
MAB_4272c	Protein GrpE (HSP-70 cofactor)
MAB_4324c	Putative acetyltransferase, GNAT
MAB_4742c	hypothetical protein
MAB_4743c	Putative dehydrogenase/reductase
MAB_4744c	hypothetical protein
MAB_4745	Putative membrane protein, MmpS
MAB_4746	Putative membrane protein, MmpL
MAB_4747	hypothetical protein
MAB_4748c	Conserved hypothetical protein (pyridoxamine 5'-phosphate oxidase?)
MAB_4919	Putative transcriptional regulator, AsnC family

Supplementary Table 12: KEGG categories of genes up-regulated by *M. abscessus* subsp. *massiliense* 1239 when grown in SCFM2 but not CF sputum when compared to 7H9-ADC-Tween-80.

M. abscessus subsp. *massiliense 1239* KEGG categories of genes upregulated in SCFM, but not in CF sputum.
KEGG category number and name
mab01100 Metabolic pathways - *Mycobacterium abscessus* ATCC 19977 (7)
mab00280 Valine, leucine and isoleucine degradation - *Mycobacterium abscessus* ATCC 19977 (4)
mab01110 Biosynthesis of secondary metabolites - Mycobacterium abscessus ATCC 19977 (3)
mab00410 beta-Alanine metabolism - *Mycobacterium abscessus* ATCC 19977 (3)
mab00640 Propanoate metabolism - *Mycobacterium abscessus* ATCC 19977 (3)
mab01130 Biosynthesis of antibiotics - *Mycobacterium abscessus* ATCC 19977 (3)
mab00627 Aminobenzoate degradation - *Mycobacterium abscessus* ATCC 19977 (2)
mab00250 Alanine, aspartate and glutamate metabolism - *Mycobacterium abscessus* ATCC 19977 (2)
mab03018 RNA degradation - *Mycobacterium abscessus* ATCC 19977 (2)
mab00071 Fatty acid degradation - *Mycobacterium abscessus* ATCC 19977 (2)
mab00650 Butanoate metabolism - *Mycobacterium abscessus* ATCC 19977 (2)
mab00360 Phenylalanine metabolism - *Mycobacterium abscessus* ATCC 19977 (2)
mab00362 Benzoate degradation - *Mycobacterium abscessus* ATCC 19977 (2)
mab00380 Tryptophan metabolism - *Mycobacterium abscessus* ATCC 19977 (2)
mab00903 Limonene and pinene degradation - *Mycobacterium abscessus* ATCC 19977 (2)
mab01120 Microbial metabolism in diverse environments - *Mycobacterium abscessus* ATCC 19977 (2)
mab01212 Fatty acid metabolism - *Mycobacterium abscessus* ATCC 19977 (2)
mab00930 Caprolactam degradation - *Mycobacterium abscessus* ATCC 19977 (2)
mab00310 Lysine degradation - *Mycobacterium abscessus* ATCC 19977 (2)
mab00281 Geraniol degradation - *Mycobacterium abscessus* ATCC 19977 (2)
mab00330 Arginine and proline metabolism - *Mycobacterium abscessus* ATCC 19977 (2)
mab00920 Sulfur metabolism - *Mycobacterium abscessus* ATCC 19977 (1)
mab01200 Carbon metabolism - *Mycobacterium abscessus* ATCC 19977 (1)
mab00430 Taurine and hypotaurine metabolism - *Mycobacterium abscessus* ATCC 19977 (1)
mab00562 Inositol phosphate metabolism - *Mycobacterium abscessus* ATCC 19977 (1)

Supplementary Table 13: Genes up-regulated by *M. abscessus* subsp. *massiliense* 1239 when grown in CF sputum but not SCFM2 when compared to 7H9-ADC-Tween-80. (Continued on three pages)

M. abscessus subsp. *massiliense 1239* genes upregulated in CF sputum but not in SCFM compared to 7H9	
Gene_id	Gene Product
MAB_0121	Rhodanese-like protein
MAB_0145c	Probable transcriptional regulator, TetR family
MAB_0213c	hypothetical protein
MAB_0249	hypothetical protein
MAB_0270c	Hypothetical protein
MAB_0276	Probable cytochrome P450
MAB_0601	Hypothetical protein
MAB_0602c	Hypothetical protein
MAB_0673	Putative DNA-binding response regulator PhoP
MAB_0750	Putative oxidoreductase
MAB_0926	Probable glycosyltransferase
MAB_0927	Probable glycosyltransferase
MAB_0969	Putative transcriptional regulator, TetR
MAB_1030	hypothetical protein
MAB_1031c	Probable manganese transport protein MntH
MAB_1043c	Putative oxidoreductase
MAB_1077	Probable two component sensor kinase MprB
MAB_1138c	Putative transcriptional regulator, MarR family
MAB_1169	Putative hydrolase, alpha/beta fold
MAB_1246c	Hypothetical protein
MAB_1247c	hypothetical protein
MAB_1261	Hypothetical protein
MAB_1262	hypothetical protein
MAB_1263	Hypothetical protein
MAB_1362	Probable alternative RNA polymerase sigma factor
MAB_1363	hypothetical protein
MAB_1394c	hypothetical protein
MAB_1411	Putative mechanosensitive ion channel
MAB_1412	Hypothetical protein
MAB_1457	Probable UDP-N-acetylglucosamine 1-carboxyvinyltransferase MurA
MAB_1489	Probable acyl-CoA ligase FadD
MAB_1539c	hypothetical protein
MAB_1713	Hypothetical ABC transporter ATP-binding protein
MAB_1846	Putative ABC transporter ATP-binding protein
MAB_1850c	Hypothetical protein
MAB_1855c	Putative zinc-binding alcohol dehydrogenase
MAB_1871	hypothetical protein
MAB_1872c	hypothetical protein
MAB_1873c	Putative TetR family transcriptional regulator
MAB_1874	Putative oxidoreductase
MAB_2043	Putative transcriptional regulator, TetR
MAB_2050	Putative HTH-type transcriptional regulator AraC
MAB_2123	Putative peptide synthetase MbtF

M. abscessus subsp. *massiliense 1239* genes upregulated in CF sputum but not in SCFM compared to 7H9 continued	
MAB_2148	Putative linoleoyl-CoA desaturase
MAB_2158c	Probable ATP-dependent RNA helicase
MAB_2163	Probable RNA polymerase sigma-70 factor, ECF subfamily
MAB_2202	hypothetical protein
MAB_2204	Conserved hypothetical protein (FxsA cytoplasmic membrane protein?)
MAB_2235	Possible siderophore-interacting protein
MAB_2236c	Putative short-chain dehydrogenase/reductase
MAB_2248	Probable peptide synthetase MbtE
MAB_2262c	Hypothetical ABC transporter ATP-binding protein
MAB_2451c	Conserved hypothetical protein (esterase?)
MAB_2603c	Probable conserved integral membrane protein
MAB_2693	Hypothetical protein
MAB_2717c	hypothetical protein
MAB_2745c	Possible SUF system FeS assembly protein
MAB_2750c	Probable transcriptional regulatory protein
MAB_2847c	hypothetical protein
MAB_3028	RNA polymerase sigma factor
MAB_3030c	hypothetical protein
MAB_3065c	hypothetical protein
MAB_3177	Putative FAD-dependent pyridine nucleotide-disulphide oxidoreductase
MAB_3178	Conserved hypothetical protein (putative methyltransferase)
MAB_3179c	Putative transcriptional regulator, LysR family
MAB_3330	Putative salicylate hydroxylase
MAB_3357c	Putative aminotransferase/cysteine desulfurase
MAB_3455c	Putative acyl-CoA thiolase
MAB_3502	hypothetical protein
MAB_3509c	Hypothetical protein
MAB_3549c	Putative oxidoreductase
MAB_3645	Putative reductase
MAB_3647c	Probable transcriptional regulatory protein
MAB_3648	hypothetical protein
MAB_3649	Probable aldehyde dehydrogenase
MAB_3650	Putative TetR-family transcriptional regulator
MAB_3716	hypothetical protein
MAB_3761c	hypothetical protein
MAB_3878	Probable lipase/esterase LipG
MAB_3885	hypothetical protein
MAB_3886c	hypothetical protein
MAB_3902c	hypothetical protein
MAB_3926	hypothetical protein
MAB_3971	hypothetical protein
MAB_3985c	hypothetical protein
MAB_4132	Hypothetical protein
MAB_4139	Putative transcription regulator, ArsR family

M. abscessus subsp. *massiliense 1239* genes upregulated in CF sputum but not in SCFM compared to 7H9 continued

MAB_4270c	Probable heat shock protein transcriptional regulator HspR
MAB_4298c	hypothetical protein
MAB_4308c	Hypothetical protein
MAB_4309c	Putative serine protease
MAB_4402	Heat shock protein Hsp20
MAB_4408c	Putative alkylhydroperoxidase C
MAB_4426	Putative transcription regulator, ArsR family
MAB_4427c	Putative transcriptional regulator
MAB_4531	Hypothetical protein
MAB_4584c	hypothetical protein
MAB_4586c	hypothetical protein
MAB_4587c	hypothetical protein
MAB_4612	hypothetical protein
MAB_4616c	Probable transcriptional regulator protein
MAB_4617	Methylcitrate dehydratase family (MmgE/PrpD)
MAB_4618	Probable carboxyvinyl-carboxyphosphonate phosphorylmutase, possible methylisocitrate lyase (PrpB)
MAB_4619	Probable citrate synthase
MAB_4620c	Hypothetical protein
MAB_4621c	Putative acetyltransferase
MAB_4622c	hypothetical protein
MAB_4623c	5-methyltetrahydropteroyltriglutamate--homocysteine S-methyltransferase
MAB_4681c	hypothetical protein
MAB_4713	Similarity with Glyoxalase/Bleomycin resistance protein
MAB_4714c	Probable fatty-acid-coa ligase FadD
MAB_4715c	hypothetical protein
MAB_4716c	Possible membrane transport protein
MAB_4798	hypothetical protein
MAB_t5013	tRNA-Glu(TTC)

Supplementary Table 14: KEGG categories of genes up-regulated by *M. abscessus* subsp. *massiliense* 1239 when grown in CF sputum but not SCFM2 when compared to 7H9-ADC-Tween-80.

M. abscessus subsp. *massiliense 1239* KEGG categories of genes upregulated in CF sputum, but not in SCFM.
KEGG category number and name
mab01100 Metabolic pathways - *Mycobacterium abscessus* ATCC 19977 (12)
mab01110 Biosynthesis of secondary metabolites - *Mycobacterium abscessus* ATCC 19977 (5)
mab01120 Microbial metabolism in diverse environments - *Mycobacterium abscessus* ATCC 19977 (4)
mab01212 Fatty acid metabolism - *Mycobacterium abscessus* ATCC 19977 (3)
mab01130 Biosynthesis of antibiotics - *Mycobacterium abscessus* ATCC 19977 (3)
mab00071 Fatty acid degradation - *Mycobacterium abscessus* ATCC 19977 (2)
mab02010 ABC transporters - *Mycobacterium abscessus* ATCC 19977 (2)
mab01230 Biosynthesis of amino acids - *Mycobacterium abscessus* ATCC 19977 (2)
mab00561 Glycerolipid metabolism - *Mycobacterium abscessus* ATCC 19977 (2)
mab00640 Propanoate metabolism - *Mycobacterium abscessus* ATCC 19977 (2)
mab00280 Valine, leucine and isoleucine degradation - *Mycobacterium abscessus* ATCC 19977 (2)
mab01040 Biosynthesis of unsaturated fatty acids - *Mycobacterium abscessus* ATCC 19977 (2)
mab00550 Peptidoglycan biosynthesis - *Mycobacterium abscessus* ATCC 19977 (1)
mab01200 Carbon metabolism - *Mycobacterium abscessus* ATCC 19977 (1)
mab00630 Glyoxylate and dicarboxylate metabolism - *Mycobacterium abscessus* ATCC 19977 (1)
mab00564 Glycerophospholipid metabolism - *Mycobacterium abscessus* ATCC 19977 (1)
mab00903 Limonene and pinene degradation - *Mycobacterium abscessus* ATCC 19977 (1)
mab00010 Glycolysis / Gluconeogenesis - *Mycobacterium abscessus* ATCC 19977 (1)
mab00730 Thiamine metabolism - *Mycobacterium abscessus* ATCC 19977 (1)
mab00626 Naphthalene degradation - *Mycobacterium abscessus* ATCC 19977 (1)
mab00330 Arginine and proline metabolism - *Mycobacterium abscessus* ATCC 19977 (1)
mab01210 2-Oxocarboxylic acid metabolism - *Mycobacterium abscessus* ATCC 19977 (1)
mab01053 Biosynthesis of siderophore group nonribosomal peptides - *Mycobacterium abscessus* ATCC 19977 (1)
mab00620 Pyruvate metabolism - *Mycobacterium abscessus* ATCC 19977 (1)
mab02020 Two-component system - *Mycobacterium abscessus* ATCC 19977 (1)
mab00270 Cysteine and methionine metabolism - *Mycobacterium abscessus* ATCC 19977 (1)
mab00380 Tryptophan metabolism - *Mycobacterium abscessus* ATCC 19977 (1)
mab00970 Aminoacyl-tRNA biosynthesis - *Mycobacterium abscessus* ATCC 19977 (1)
mab00592 alpha-Linolenic acid metabolism - *Mycobacterium abscessus* ATCC 19977 (1)
mab00340 Histidine metabolism - *Mycobacterium abscessus* ATCC 19977 (1)
mab00053 Ascorbate and aldarate metabolism - *Mycobacterium abscessus* ATCC 19977 (1)
mab00410 beta-Alanine metabolism - *Mycobacterium abscessus* ATCC 19977 (1)
mab04122 Sulfur relay system - *Mycobacterium abscessus* ATCC 19977 (1)
mab00281 Geraniol degradation - *Mycobacterium abscessus* ATCC 19977 (1)
mab00625 Chloroalkane and chloroalkene degradation - *Mycobacterium abscessus* ATCC 19977 (1)
mab00310 Lysine degradation - *Mycobacterium abscessus* ATCC 19977 (1)
mab00362 Benzoate degradation - *Mycobacterium abscessus* ATCC 19977 (1)
mab00450 Selenocompound metabolism - *Mycobacterium abscessus* ATCC 19977 (1)
mab00624 Polycyclic aromatic hydrocarbon degradation - *Mycobacterium abscessus* ATCC 19977 (1)
mab00621 Dioxin degradation - *Mycobacterium abscessus* ATCC 19977 (1)
mab00520 Amino sugar and nucleotide sugar metabolism - *Mycobacterium abscessus* ATCC 19977 (1)
mab00020 Citrate cycle (TCA cycle) - *Mycobacterium abscessus* ATCC 19977 (1)
mab01220 Degradation of aromatic compounds - *Mycobacterium abscessus* ATCC 19977 (1)

Supplementary Figure 15: Genes down-regulated by *M. abscessus* subsp. *massiliense* 1239 when grown in SCFM2 and CF sputum when compared to 7H9-ADC-Tween-80. No KEGG categories are assigned for the genes down-regulated in both SCFM2 and CF sputum.

M. abscessus subsp. *massiliense* 1239 genes downregulated in both SCFM and CF sputum	
Gene_id	Gene Product
MAB_1314	Hypothetical protein
MAB_1925	hypothetical protein
MAB_1926	Putative transcriptional regulatory protein PrrA
MAB_2601	Hypothetical protein
MAB_3371c	hypothetical protein
MAB_4114	hypothetical protein

Supplementary Table 16: Genes down-regulated by *M. abscessus* subsp. *massiliense* 1239 when grown in CF sputum but not SCFM2 when compared to 7H9-ADC-Tween-80. (Continued on two pages)

M. abscessus subsp. *massiliense* 1239 genes downregulated in CF sputum but not SCFM when compared to 7H9	
MAB_0126c	Possible bacterioferritin BfrB
MAB_0183c	Putative cation transporter
MAB_0184c	Hypothetical protein
MAB_0315	hypothetical protein
MAB_0389c	Putative regulatory protein
MAB_0405c	Hypothetical protein
MAB_0487	Probable cold shock protein A (CspA)
MAB_0545	Protein lsr2 precursor
MAB_0587	Probable acetamidase/formamidase
MAB_0611	Putative cytochrome P450
MAB_0740c	Probable thiosulfate sulfurtransferase (CysA)
MAB_0852	Possible conserved polyketide synthase associated protein PapA2
MAB_0853	Probable esterase/lipase LipP
MAB_0884c	Hypothetical protein
MAB_0885c	Hypothetical lipoprotein lpqH precursor
MAB_0938c	Probable conserved polyketide synthase associated protein PapA3
MAB_1005c	Putative MCE family protein
MAB_1013	Hypothetical protein
MAB_1020	Probable undecaprenyl-phosphate galactosephosphotransferase
MAB_1026c	hypothetical protein
MAB_1196	Proline-rich antigen (36 kDa antigen)
MAB_1271c	Probable oxidase (copper-binding protein)
MAB_1447	ATP synthase A chain AtpB
MAB_1506c	Conserved hypothetical protein (MaoC-like dehydratase)
MAB_1630c	hypothetical protein
MAB_1655	Probable sulfate ABC transporter, ATP-binding protein SysA
MAB_1657c	hypothetical protein
MAB_2113	Hypothetical protein
MAB_2329c	hypothetical protein
MAB_2373	Putative mannose-specific lectin precursor
MAB_2421c	hypothetical protein
MAB_2422c	Hypothetical protein
MAB_2728c	Hypothetical invasion protein Inv1
MAB_2785	Hypothetical protein
MAB_2786	Hypothetical protein
MAB_2791c	Putative ethanolamine permease
MAB_3230c	hypothetical protein
MAB_3245	hypothetical protein
MAB_3359c	hypothetical protein
MAB_3413c	Ribonucleoside-diphosphate reductase alpha subunit
MAB_3414c	Protein NrdI
MAB_3415c	Glutaredoxin-like protein NrdH
MAB_3493	Hypothetical protein
MAB_3753c	hypothetical protein

M. abscessus subsp. *massiliense* 1239 genes downregulated in CF sputum but not SCFM when compared to 7H9 continued	
MAB_3998	hypothetical protein
MAB_3999	hypothetical protein
MAB_4004c	Conserved hypothetical protein (excisionase?)
MAB_4080c	hypothetical protein
MAB_4098c	Probable peptide synthetase NRP
MAB_4103c	Probable methyltransferase
MAB_4105c	Methyltransferase MtfD
MAB_4106c	acyltransferase
MAB_4107c	Glycosyltransferase GtfA
MAB_4108c	Methyltransferase MtfB
MAB_4111c	Putative epimerase/dehydratase
MAB_4112c	Putative glycosyltransferase GtfA
MAB_4421	Putative succinate dehydrogenase
MAB_4422	Putative succinate dehydrogenase, flavoprotein subunit
MAB_4666c	hypothetical protein
MAB_4694c	Glycosyltransferase
MAB_4695c	Putative glycosyltransferase/rhamnosyltransferase
MAB_4696c	Possible methyltransferase
MAB_4698	hypothetical protein
MAB_4699c	hypothetical protein
MAB_4700c	hypothetical protein
MAB_4701	hypothetical protein
MAB_4702c	hypothetical protein
MAB_4724	Sodium/calcium exchanger family protein

Supplementary Table 17: KEGG categories of genes down-regulated by *M. abscessus* subsp. *massiliense* 1239 when grown in CF sputum but not SCFM2 when compared to 7H9-ADC-Tween-80

M. abscessus subsp. *massiliense 1239* KEGG categories of genes downregulated in CF sputum, but not in SCFM.
KEGG category number and name
mab01100 Metabolic pathways - *Mycobacterium abscessus* ATCC 19977 (5)
mab01120 Microbial metabolism in diverse environments - *Mycobacterium abscessus* ATCC 19977 (3)
mab00920 Sulfur metabolism - *Mycobacterium abscessus* ATCC 19977 (2)
mab01130 Biosynthesis of antibiotics - *Mycobacterium abscessus* ATCC 19977 (2)
mab01200 Carbon metabolism - *Mycobacterium abscessus* ATCC 19977 (2)
mab00190 Oxidative phosphorylation - *Mycobacterium abscessus* ATCC 19977 (2)
mab00860 Porphyrin and chlorophyll metabolism - *Mycobacterium abscessus* ATCC 19977 (2)
mab04122 Sulfur relay system - *Mycobacterium abscessus* ATCC 19977 (1)
mab00650 Butanoate metabolism - *Mycobacterium abscessus* ATCC 19977 (1)
mab01110 Biosynthesis of secondary metabolites - *Mycobacterium abscessus* ATCC 19977 (1)
mab00523 Polyketide sugar unit biosynthesis - *Mycobacterium abscessus* ATCC 19977 (1)
mab00910 Nitrogen metabolism - *Mycobacterium abscessus* ATCC 19977 (1)
mab00270 Cysteine and methionine metabolism - *Mycobacterium abscessus* ATCC 19977 (1)
mab00020 Citrate cycle (TCA cycle) - *Mycobacterium abscessus* ATCC 19977 (1)
mab00630 Glyoxylate and dicarboxylate metabolism - *Mycobacterium abscessus* ATCC 19977 (1)
mab00984 Steroid degradation - *Mycobacterium abscessus* ATCC 19977 (1)
mab00230 Purine metabolism - *Mycobacterium abscessus* ATCC 19977 (1)
mab00460 Cyanoamino acid metabolism - *Mycobacterium abscessus* ATCC 19977 (1)
mab00240 Pyrimidine metabolism - *Mycobacterium abscessus* ATCC 19977 (1)
mab02010 ABC transporters - *Mycobacterium abscessus* ATCC 19977 (1)

Supplementary Table 18: Genes down-regulated by *M. abscessus* subsp. *massiliense* 1239 when grown in SCFM2 but not CF sputum when compared to 7H9-ADC-Tween-80

M. abscessus subsp. *massiliense* 1239 genes downregulated in SCFM but not CF sputum when compared to 7H9	
MAB_0262	Probable amino acid ABC transporter, ATP-binding
MAB_1427c	Putative cytochrome P450
MAB_1627	Conserved hypothetical protein (ComEC/Rec2-related protein?)
MAB_1628c	hypothetical protein
MAB_2047c	Probable ferredoxin reductase
MAB_2048c	Probable cytochrome P450
MAB_2049c	Probable ferredoxin
MAB_2512	Conserved hypothetical protein (sulfate transporter/antisigma-factor antagonist STAS?)
MAB_2792c	Probable aldehyde dehydrogenase
MAB_3370	Putative branched-chain amino acid transport protein
MAB_4456	Putative cytochrome P450
MAB_4683c	Hypothetical protein

Supplementary Table 19: KEGG categories of genes down-regulated by *M. abscessus* subsp. *massiliense* 1239 when grown in SCFM2 but not CF sputum when compared to 7H9-ADC-Tween-80

M. abscessus subsp. *massiliense 1239* KEGG categories of genes downregulated in SCFM, but not in CF sputum when compared to 7H9.
KEGG category number and name
mab01120 Microbial metabolism in diverse environments - *Mycobacterium abscessus* ATCC 19977 (2)
mab01100 Metabolic pathways - *Mycobacterium abscessus* ATCC 19977 (2)
mab01220 Degradation of aromatic compounds - *Mycobacterium abscessus* ATCC 19977 (1)
mab02010 ABC transporters - *Mycobacterium abscessus* ATCC 19977 (1)
mab01110 Biosynthesis of secondary metabolites - *Mycobacterium abscessus* ATCC 19977 (1)
mab00360 Phenylalanine metabolism - *Mycobacterium abscessus* ATCC 19977 (1)
mab00071 Fatty acid degradation - *Mycobacterium abscessus* ATCC 19977 (1)
mab00620 Pyruvate metabolism - *Mycobacterium abscessus* ATCC 19977 (1)
mab00010 Glycolysis / Gluconeogenesis - *Mycobacterium abscessus* ATCC 19977 (1)

Bibliography

Akamatsu, Y., and J. H. Law. 1970a. "Enzymatic alkylenation of phospholipid fatty acid chains by extracts of *Mycobacterium phlei*." *The Journal of Biological Chemistry* 245 (4):701.

Akamatsu, Y., and J. H. Law. 1970b. "The enzymatic synthesis of fatty acid methyl esters by carboxyl group alkylation." *The Journal of Biological Chemistry* 245 (4):709.

Barrett, Tanya, Stephen E. Wilhite, Pierre Ledoux, Carlos Evangelista, Irene F. Kim, Maxim Tomashevsky, Kimberly A. Marshall, Katherine H. Phillippy, Patti M. Sherman, Michelle Holko, Andrey Yefanov, Hyeseung Lee, Naigong Zhang, Cynthia L. Robertson, Nadezhda Serova, Sean Davis, and Alexandra Soboleva. 2013. "NCBI GEO: archive for functional genomics data sets--update." *Nucleic Acids Research* 41 (Database issue):D991. doi: 10.1093/nar/gks1193.

Bhamidi, Suresh, Libin Shi, Delphi Chatterjee, John T. Belisle, Dean C. Crick, and Michael R. McNeil. 2012. "A bioanalytical method to determine the cell wall composition of *Mycobacterium tuberculosis* grown in vivo." *Analytical Biochemistry* 421 (1):240-249. doi: 10.1016/j.ab.2011.10.046.

Billman-Jacobe, Helen, Malcolm J. McConville, Ruth E. Haites, Svetozar Kovacevic, and Ross L. Coppel. 1999. "Identification of a peptide synthetase involved in the biosynthesis of glycopeptidolipids of *Mycobacterium smegmatis*." *Molecular Microbiology* 33 (6):1244-1253. doi: 10.1046/j.1365-2958.1999.01572.x.

Bryant, Josephine M., Dorothy M. Grogono, Daniel Greaves, Juliet Foweraker, Iain Roddick, Thomas Inns, Mark Reacher, Charles S. Haworth, Martin D. Curran, Simon R. Harris, Sharon J. Peacock, Julian Parkhill, and R. Andres Floto. 2013. "Whole-genome sequencing to identify transmission of *Mycobacterium abscessus* between patients with cystic fibrosis: a retrospective cohort study." *The Lancet.* 381 (9877):1551-1560. doi: 10.1016/S0140-6736(13)60632-7.

Bryant, Josephine M., Dorothy M. Grogono, Daniela Rodriguez-Rincon, Isobel Everall, Karen P. Brown, Pablo Moreno, Deepshikha Verma, Emily Hill, Judith Drijkoningen, Peter Gilligan, Charles R. Esther, Peadar G. Noone, Olivia Giddings, Scott C. Bell, Rachel Thomson, Claire E. Wainwright, Chris Coulter, Sushil Pandey, Michelle E. Wood, Rebecca E. Stockwell, Kay A. Ramsay, Laura J. Sherrard, Timothy J. Kidd, Nassib Jabbour, Graham R. Johnson, Luke D. Knibbs, Lidia Morawska, Peter D. Sly, Andrew Jones, Diana Bilton, Ian Laurenson, Michael Ruddy, Stephen Bourke, Ian Cjw Bowler, Stephen J. Chapman, Andrew Clayton, Mairi Cullen, Thomas Daniels, Owen Dempsey, Miles Denton, Maya Desai, Richard J. Drew, Frank Edenborough, Jason Evans, Jonathan Folb, Helen Humphrey, Barbara Isalska, Søren Jensen-Fangel, Bodil Jönsson, Andrew M. Jones, Terese L. Katzenstein, Troels Lillebaek, Gordon Macgregor, Sarah Mayell, Michael Millar, Deborah Modha, Edward F. Nash, Christopher O'Brien, Deirdre O'Brien, Chandra Ohri, Caroline S. Pao, Daniel Peckham, Felicity Perrin, Audrey Perry, Tania Pressler, Laura Prtak, Tavs Qvist, Ali Robb, Helen Rodgers, Kirsten Schaffer, Nadia Shafi, Jakko van Ingen, Martin Walshaw, Danie Watson, Noreen West, Joanna Whitehouse, Charles S. Haworth, Simon R. Harris, Diane Ordway, Julian Parkhill,

and R. Andres Floto. 2016. "Emergence and spread of a human-transmissible multidrug-resistant nontuberculous mycobacterium." *Science (New York, N.Y.)* 354 (6313):751. doi: 10.1126/science.aaf8156.

Choi, Ge, S. J. Shin, C. J. Won, Kn Min, T. Oh, My Hahn, K. Lee, Sh Lee, Cl Daley, S. Kim, Bh Jeong, K. Jeon, and Wj Koh. 2012. "Macrolide Treatment for Mycobacterium abscessus and *Mycobacterium massiliense* Infection and Inducible Resistance." *American Journal Of Respiratory And Critical Care Medicine* 186 (9):917-925. doi: 10.1164/rccm.201111-2005OC.

Claeys, T. A., and Rt Robinson. 2018. "The Many Lives of Nontuberculous Mycobacteria." *Journal Of Bacteriology* 200 (11). doi: 10.1128/JB.00739-17.

Covert, Terry C., Mark R. Rodgers, Antolin L. Reyes, and Gerard N. Stelma, Jr. 1999. "Occurrence of Nontuberculous Mycobacteria in Environmental Samples." *Applied and Environmental Microbiology* 65 (6):2492.

Daffe, Mamadou, Dean Crick, and Mary Jackson. 2014. "Genetics of Capsular Polysaccharides and Cell Envelope (Glyco)lipids." *Microbiology Spectrum* 2 (4).

Davidson, Rebecca M., Mary Ann Degroote, Jamie L. Marola, Sarah Buss, Victoria Jones, Michael R. McNeil, Alison G. Freifeld, L. Elaine Epperson, Nabeeh A. Hasan, Mary Jackson, Peter C. Iwen, Max Salfinger, and Michael Strong. 2017. "*Mycobacterium talmoniae* sp. nov., a slowly growing mycobacterium isolated from human respiratory samples." *International Journal of Systematic and Evolutionary Microbiology* 67 (8):2640. doi: 10.1099/ijsem.0.001998.

Falkinham, Joseph, O. 2018. "Challenges of NTM Drug Development." *Frontiers in Microbiology* 9. doi: 10.3389/fmicb.2018.01613.

Floto, R. Andres, Kenneth N. Olivier, Lisa Saiman, Charles L. Daley, Jean-Louis Herrmann, Jerry A. Nick, Peadar G. Noone, Diana Bilton, Paul Corris, Ronald L. Gibson, Sarah E. Hempstead, Karsten Koetz, Kathryn A. Sabadosa, Isabelle Sermet-Gaudelus, Alan R. Smyth, Jakko van Ingen, Richard J. Wallace, Kevin L. Winthrop, Bruce C. Marshall, and Charles S. Haworth. 2016. "US Cystic Fibrosis Foundation and European Cystic Fibrosis Society consensus recommendations for the management of non-tuberculous mycobacteria in individuals with cystic fibrosis: executive summary." *Thorax* 71 (1):88. doi: 10.1136/thoraxjnl-2015-207983.

Griffith, David E., and SpringerLink. 2019. *Nontuberculous Mycobacterial Disease : A Comprehensive Approach to Diagnosis and Management*. Cham, Switzerland: Cham, Switzerland : Springer.

Grzegorzewicz, Anna E., Jana Korduláková, Victoria Jones, Sarah E. M. Born, Juan M. Belardinelli, Adrien Vaquié, Vijay A. K. B. Gundi, Jan Madacki, Nawel Slama, Françoise Laval, Julien Vaubourgeix, Rebecca M. Crew, Brigitte Gicquel, Mamadou Daffé, Hector R. Morbidoni, Patrick J. Brennan, Annaik Quémard, Michael R. McNeil, and Mary Jackson. 2012. "A common mechanism of inhibition of the *Mycobacterium tuberculosis* mycolic acid biosynthetic pathway by isoxyl and thiacetazone." *The Journal of Biological Chemistry* 287 (46):38434. doi: 10.1074/jbc.M112.400994.

Grzegorzewicz, Anna E., Pham Ha, A. K. B. Gundi Vijay, S. Scherman Michael, J. North Elton, Hess Tamara, Jones Victoria, Gruppo Veronica, E. M. Born Sarah, Korduláková Jana, Chavadi Sivagami Sundaram, Morisseau Christophe, J. Lenaerts Anne, E. Lee Richard, R. Mcneil Michael, and Jackson Mary. 2012. "Inhibition of mycolic acid transport across the *Mycobacterium tuberculosis* plasma membrane." *Nature Chemical Biology* 8 (4):334. doi: 10.1038/nchembio.794.

Hasan, Nabeeh A., Rebecca M. Davidson, L. Elaine Epperson, Sara M. Kammlade, Rachael R. Rodger, Adrah R. Levin, Alyssa Sherwood, Scott D. Sagel, Stacey L.Martiniano, Charles L. Daley, Max Salfinger, Jerry A. Nick, and Michael Strong. 2019. "Population Genomics of Nontuberculous Mycobacteria Recovered from United States Cystic Fibrosis Patients." bioRxiv 663559. doi: 10.1101/663559

Howard, Susan T., Elizabeth Rhoades, Judith Recht, Xiuhua Pang, Anny Alsup, Roberto Kolter, C. Rick Lyons, and Thomas F. Byrd. 2006. "Spontaneous reversion of *Mycobacterium abscessus* from a smooth to a rough morphotype is associated with reduced expression of glycopeptidolipid and reacquisition of an invasive phenotype." *Microbiology (Reading, England)* 152 (Pt 6):1581. doi: 10.1099/mic.0.28625-0.

Jiang, Hongshan, Rong Lei, Shou-Wei Ding, and Shuifang Zhu. 2014. "Skewer: a fast and accurate adapter trimmer for next-generation sequencing paired-end reads." *BMC Bioinformatics* 15 (1):182. doi: 10.1186/1471-2105-15-182.

Kim, Hee-Youn, Byoung Jun Kim, Yoonwon Kook, Yeo-Jun Yun, Jeong Hwan Shin, Bum-Joon Kim, and Yoon-Hoh Kook. 2010. "*Mycobacterium massiliense* is differentiated from *Mycobacterium abscessus* and *Mycobacterium bolletii* by erythromycin ribosome methyltransferase gene (erm) and clarithromycin susceptibility patterns." *Microbiology and Immunology* 54 (6):347-353. doi: 10.1111/j.1348-0421.2010.00221.x.

Langmead, Ben, and L. Salzberg Steven. 2012. "Fast gapped-read alignment with Bowtie 2." *Nature Methods* 9 (4):357. doi: 10.1038/nmeth.1923.

Maksymiuk, Christina, Anand Balakrishnan, Ruslana Bryk, Kyu Rhee, and Carl Nathan. 2015. "E1 of [alpha]-ketoglutarate dehydrogenase defends *Mycobacterium tuberculosis* against glutamate anaplerosis and nitroxidative stress." *Proceedings of the National Academy of Sciences of the United States of America* 112 (43):E5834.

Marrakchi, Hedia, Marie-Antoinette Lanéelle, and Mamadou Daffé. 2014. "Mycolic Acids: Structures, Biosynthesis, and Beyond." *Chemistry & Biology* 21 (1):67-85. doi: 10.1016/j.chembiol.2013.11.011.

Maurer, Florian P., Vera L. Bruderer, Claudia Ritter, Claudio Castelberg, Guido V. Bloemberg, and Erik C. Böttger. 2014. "Lack of Antimicrobial Bactericidal Activity in *Mycobacterium abscessus*." *Antimicrobial Agents and Chemotherapy* 58 (7):3828. doi: 10.1128/AAC.02448-14.

Meena, Laxman S., Puneet Chopra, Ram A. Vishwakarma, and Yogendra Singh. 2013. "Biochemical characterization of an S-adenosyl-l-methionine-dependent methyltransferase (Rv0469) of *Mycobacterium tuberculosis*." *Biological Chemistry* 394 (7):871. doi: 10.1515/hsz-2013-0126.

Meena, Laxman S., and Pappachan E. Kolattukudy. 2013. "Expression and characterization of Rv0447c product, potentially the methyltransferase involved in tuberculostearic acid biosynthesis in *Mycobacterium tuberculosis*." *Biotechnology and Applied Biochemistry* 60 (4):412-6. doi: 10.1002/bab.1112.

Miranda-CasoLuengo, Aleksandra A., Patrick M. Staunton, Adam M. Dinan, Amanda J. Lohan, and Brendan J. Loftus. 2016. "Functional characterization of the *Mycobacterium abscessus* genome coupled with condition specific transcriptomics reveals conserved molecular strategies for host adaptation and persistence." *BMC Genomics* 17 (1). doi: 10.1186/s12864-016-2868-y.

Mukherjee, Raju, Manuel Gomez, Narayanaswamy Jayaraman, Issar Smith, and Dipankar Chatterji. 2005. "Hyperglycosylation of glycopeptidolipid of *Mycobacterium smegmatis* under nutrient starvation: structural studies." *Microbiology (Reading, England)* 151 (7):2385. doi: 10.1099/mic.0.27908-0.

Nessar, Rachid, Emmanuelle Cambau, Jean Reyrat, Alan Murray, and Brigitte Gicquel. 2012. "*Mycobacterium abscessus*: a new antibiotic nightmare." *The Journal of Antimicrobial Chemotherapy* 67 (4):810. doi: 10.1093/jac/dkr578.

Ojha, A., S. Varma, and D. Chatterji. 2002. "Synthesis of an unusual polar glycopeptidolipid in glucose-limited culture of *Mycobacterium smegmatis*." *Microbiology* 148 (10):3039-3048. doi: 10.1099/00221287-148-10-3039.

Palmer, Kelli L., Lindsay M. Aye, and Marvin Whiteley. 2007. "Nutritional Cues Control *Pseudomonas aeruginosa* Multicellular Behavior in Cystic Fibrosis Sputum." *The Journal of Bacteriology* 189 (22):8079. doi: 10.1128/JB.01138-07.

Palmer, Kelli L., Lauren M. Mashburn, Pradeep K. Singh, and Marvin Whiteley. 2005. "Cystic Fibrosis Sputum Supports Growth and Cues Key Aspects of *Pseudomonas aeruginosa* Physiology." *The Journal of Bacteriology* 187 (15):5267. doi: 10.1128/JB.187.15.5267-5277.2005.

Palčeková, Zuzana, Shiva Kumar Angala, Juan M. Belardinelli, Haig A. Eskandarian, Maju Joe, Richard Brunton, Christopher Rithner, Victoria Jones, Jérôme Nigou, Todd L. Lowary, Martine Gilleron, Michael McNeil, and Mary Jackson. 2019. "Disruption of the SucT acyltransferase in *Mycobacterium smegmatis* abrogates succinylation of cell envelope polysaccharides." *Journal of Biological Chemistry* 294 (26):jbc.RA119.008585. doi: 10.1074/jbc.RA119.008585.

Pawlik, Alexandre, Guillaume Garnier, Mickael Orgeur, Pin Tong, Amanda Lohan, Fabien Le Chevalier, Guillaume Sapriel, Anne-Laure Roux, Kevin Conlon, Nadine Honoré, Marie-Agnès Dillies, Laurence Ma, Christiane Bouchier, Jean-Yves Coppée, Jean-Louis Gaillard, Stephen V. Gordon, Brendan Loftus, Roland Brosch, and Jean Louis Herrmann. 2013. "Identification and characterization of the genetic changes responsible for the characteristic smooth-to-rough morphotype alterations of clinically persistent *Mycobacterium abscessus*." *Molecular Microbiology* 90 (3):612-629. doi: 10.1111/mmi.12387.

Pierre-Audigier, Catherine, Agnes Ferroni, Isabelle Sermet-Gaudelus, Muriel Le Bourgeois, Catherine Offredo, Hoang Vu-Thien, Brigitte Fauroux, Patricia Mariani, Anne Munck,

Edouard Bingen, Didier Guillemot, Gilles Quesne, Veronique Vincent, Patrick Berche, and Jean-Louis Gaillard. 2005. "Age-Related Prevalence and Distribution of Nontuberculous Mycobacterial Species among Patients with Cystic Fibrosis." *Journal of Clinical Microbiology* 43 (7):3467-3470. doi: 10.1128/JCM.43.7.3467-3470.2005.

Prevots, D. Rebecca, and Theodore K Marras. 2016. "Epidemiology of Human Pulmonary Infection with Non-Tuberculous Mycobacteria: A Review." *Clinical Chest Medicine* 36 (1):13-34.

Prevots, D. Rebecca, Pamela A. Shaw, Daniel Strickland, Lisa A. Jackson, Marsha A. Raebel, Mary Ann Blosky, Ruben Montes de Oca, Yvonne R. Shea, Amy E. Seitz, Steven M. Holland, and Kenneth N. Olivier. 2010. "Nontuberculous mycobacterial lung disease prevalence at four integrated health care delivery systems." *American Journal of Respiratory and Critical Care Medicine* 182 (7):970. doi: 10.1164/rccm.201002-0310OC.

Prinzis, S., D. Chatterjee, and P. J. Brennan. 1993. "Structure and antigenicity of lipoarabinomannan from *Mycobacterium bovis* BCG." *Journal of General Microbiology* 139 (11):2649. doi: 10.1099/00221287-139-11-2649.

Qvist, Tavs, Steffen Eickhardt, Kasper N. Kragh, Claus B. Andersen, Martin Iversen, Niels Høiby, and Thomas Bjarnsholt. 2015. "Chronic pulmonary disease with *Mycobacterium abscessus* complex is a biofilm infection." *The European Respiratory Journal* 46 (6):1823. doi: 10.1183/13993003.01102-2015.

Ripoll, Fabienne, Caroline Deshayes, Sophie Pasek, Françoise Laval, Jean-Luc Beretti, Franck Biet, Jean-Loup Risler, Mamadou Daffé, Gilles Etienne, Jean-Louis Gaillard, and Jean-Marc Reyrat. 2007. "Genomics of glycopeptidolipid biosynthesis in *Mycobacterium abscessus* and *M. chelonae*." *BMC Genomics* 8 (1):114. doi: 10.1186/1471-2164-8-114.

Sartain, Mark, Donald Dick, Christopher Rithner, Dean Crick, and John Belisle. 2011. "Lipidomic analyses of *Mycobacterium tuberculosis* based on accurate mass measurements and the novel "Mtb LipidDB"." *Journal of Lipid Research* 52 (5):861-872. doi: 10.1194/jlr.M010363.

Shuntaro, Machida, K. Bakku Ranjith, and Suzuki Iwane. 2017. "Expression of Genes for a Flavin Adenine Dinucleotide-Binding Oxidoreductase and a Methyltransferase from *Mycobacterium chlorophenolicum* Is Necessary for Biosynthesis of 10-Methyl Stearic Acid from Oleic Acid in Escherichia coli." *Frontiers in Microbiology* 8. doi: 10.3389/fmicb.2017.02061.

Singh, Vineet K., Dipti S. Hattangady, Efstathios S. Giotis, Atul K. Singh, Neal R. Chamberlain, Melissa K. Stuart, and Brian J. Wilkinson. 2008. "Insertional Inactivation of Branched-Chain {alpha}-Keto Acid Dehydrogenase in *Staphylococcus aureus* Leads to Decreased Branched-Chain Membrane Fatty Acid Content and Increased Susceptibility to Certain Stresses." *Applied and Environmental Microbiology* 74 (19):5882. doi: 10.1128/AEM.00882-08.

Suutari, Merja, and Simo Laakso. 1993. "Effect of growth temperature on the fatty acid composition of *Mycobacterium phlei*." *Archives of Microbiology* 159 (2):119-123. doi: 10.1007/BF00250270.

Taneja, R., U. Malik, and G. K. Khuller. 1979. "Effect of growth temperature on the lipid composition of *Mycobacterium smegmatis* ATCC 607." *Journal of General Microbiology*113 (2):413. doi: 10.1099/00221287-113-2-413.

Taylor Sitarik, Cohen, and Prince Alice. 2012. "Cystic fibrosis: a mucosal immunodeficiency syndrome." *Nature Medicine* 18 (4):509. doi: 10.1038/nm.2715.

Thomson, Rachel M. 2010. "Changing epidemiology of pulmonary nontuberculous mycobacteria infections." *Emerging Infectious Diseases* 16 (10):1576. doi: 10.3201/eid1610.091201.

Thomson, Rachel, Carla Tolson, Robyn Carter, Chris Coulter, Flavia Huygens, and Megan Hargreaves. 2013. "Isolation of Nontuberculous Mycobacteria (NTM) from Household Water and Shower Aerosols in Patients with Pulmonary Disease Caused by NTM." *Journal of Clinical Microbiology* 51 (9):3006. doi: 10.1128/JCM.00899-13.

Thomson, Rachel, Carla Tolson, Hanna Sidjabat, Flavia Huygens, and Megan Hargreaves. 2013. "*Mycobacterium abscessus* isolated from municipal water - a potential source of human infection." *BMC Infectious Diseases* 13 (1):241. doi: 10.1186/1471-2334-13-241.

Tian, Jing, Ruslana Bryk, Shuangping Shi, Hediye Erdjument-Bromage, Paul Tempst, and Carl Nathan. 2005. "*Mycobacterium tuberculosis* appears to lack α-ketoglutarate dehydrogenase and encodes pyruvate dehydrogenase in widely separated genes." *Molecular Microbiology* 57 (3):859-868. doi: 10.1111/j.1365-2958.2005.04741.x.

Toal DR, Clifton SW, Roe BA, Downard J. 1995. "The esg locus of *Myxococcus xanthus* encodes the E1 alpha and E1 beta subunits of a branched-chain keto acid dehydrogenase." *Molecular Microbiology* 16:177-189. doi: 10.1111/j.1365-2958.1995.tb02291.x10.1111/j.

Turner, Keith, K. Wessel Aimee, C. Palmer Gregory, L. Murray Justine, and Whiteley Marvin. 2015. "Essential genome of *Pseudomonas aeruginosa* in cystic fibrosis sputum." *Proceedings of the National Academy of Sciences* 112 (13):4110. doi: 10.1073/pnas.1419677112.

van Ingen, J., and Ej Kuijper. 2014. "Drug susceptibility testing of nontuberculous mycobacteria." *Future Microbiology* 9 (9):1095-1110. doi: 10.2217/FMB.14.60.

Venugopal, Aditya, Ruslana Bryk, Shuangping Shi, Kyu Rhee, Poonam Rath, Dirk Schnappinger, Sabine Ehrt, and Carl Nathan. 2011. "Virulence of *Mycobacterium tuberculosis* Depends on Lipoamide Dehydrogenase, a Member of Three Multienzyme Complexes." *Cell Host & Microbe* 9 (1):21-31. doi: 10.1016/j.chom.2010.12.004.